Dissertation
submitted to the
Combined Faculties for the Natural Sciences and for Mathematics
of the Ruperto-Carola University of Heidelberg, Germany
for the degree of
Doctor of Natural Sciences

presented by

Master of Science
Dario Pedronel Arcos Díaz
born in
Pasto, Colombia

Oral examination .....

Genetic analysis of emotional memory in AMPA and NMDA receptor mutant mice

Referees

Prof. Dr. Peter H. Seeburg

Dr. Rolf Sprengel

Max Planck Institute for Medical Research

Heidelberg

Erklärung gemäß § 7 (3) b) und c) der Promotionsordnung:
Ich erkläre hiermit, dass ich die vorgelegte Dissertation selbst verfaßt und mich dabei keiner anderen als der von mir ausdrücklich bezeichneten Quellen und Hilfen bedient habe. Desweiteren erkläre ich hiermit, dass ich an keiner anderen Stelle ein Prüfungsverfahren beantragt bzw. die Dissertation in dieser oder anderer Form bereits anderweitig als Prüfungsarbeit verwendet oder einer anderen Fakultät als Dissertation vorgelegt habe.

Heidelberg, den 30. August 2011 Dario Arcos-Díaz

A mi madre, mi padre y mi hermana

Table of Contents

Figures

Tables

Acknowledgements

I want to express my gratitude to Prof. Dr. Peter H. Seeburg for his insightful input and thorough revision of my thesis, and for the financial support of my work at his department. I am deeply thankful to Dr. Rolf Sprengel for his constant guidance, for fostering critical thinking and independence, and for having helped me become a better scientist. I also appreciate the participation of Prof. Dr. Stephan Frings and Prof. Dr. Andreas Draguhn in the evaluation of this thesis.

I thank Dr. Wannan Tang, Godwin Dogbevia, Yiwei Chen, Ling Zhang, Dr. Ilaria Bertocchi, Horst Obenhaus, as well as former members of the Sprengel Lab, Dr. Simone Schievink, and Liliana Layer, for the friendly working atmosphere and for helping me uncountable times in the everyday challenges. To Dr. Verena Bosch, special thanks for introducing me to the different techniques and aiding me at the beginning of the project.

Many thanks to Dr. Soojin Ryu, Dr. Mazahir Hasan, Dr. Georg Köhr, and Dr. Miyoko Higuchi for their many productive discussions and advice. In particular to Dr. Ryu, for taking part in my advisory committee, and to Miya, for her assistance with the organization of the mouse lines and the genotyping team. I also want to acknowledge Simone Hundemeer, Sabine Grünewald, Martina Lang and Gwenaëlle Matthies for their technical and administrative work, and, very specially, Annette Herold for her valuable help with the slicing of brains and anything one could need in the lab.

I thank Ilona Pfeffer and Lili Hocke for their assistance in performing some of the behavioral experiments. Additionally, I thank Dr. Evgeny Resnik for helping me so many times with MatLab, and Dr. Mario Treviño for his assistance with the visual-association swimming task. I also thank Tina Miucci, Jessica Birn, and Rita Pfeffer for their constant labor in taking care of the many mice. To the rest of the scientists and technicians of the Molecular Neurobiology Department, many thanks for having contributed with a friendly smile and a useful tip to the development of this thesis.

This work would have been much harder without Ann-Marie Michalski and Areej Albariri. I am deeply thankful for their friendship and support, when I most needed them. I also want to thank Sabina and Alexander for being always there with delicious meals and kind words.

Many thanks to my dear Göttingen friends Ahmed, Ramya, Chao-Hua, and Shahaf, for being my early companions in this German adventure. And to my Colombian friends Támara, María, Pilar, Liliana, Fabio, Sergio, and all those who supported me from the distance, for always listening and making me laugh. Also, many thanks to the amazing people I have met in Heidelberg, who have made this little town so entertaining.

I am especially thankful to Sven and his family for their motivation and constant support, which helped me through the rough times and made these years much happier.

And most importantly, I am grateful to my parents and my sister, whom I cannot thank enough with words, for their unconditional love, and so I dedicate to them this thesis.

Summary

My goal was to study the role of AMPA and NMDA receptors in fear memory using genetic tools. In particular, I aimed to unravel the function of these glutamate receptors in the long-term retrieval of passive avoidance and fear conditioning, both in the brain in general and in the Basolateral Amygdala (BLA).

Through the analysis of GluA3 knockout mice, I could show that the AMPA receptor subunit GluA3 is not necessary for the initial phases of cued fear learning, but is required for the normal attenuation of fear to a remote negative event, both in the passive-avoidance and fear-conditioning paradigms.

In contrast, GluA1 is essential for the acquisition and short-term retrieval of cue- and context-induced fear. Two gene-targeted mouse lines were used, one with a global GluA1 knockout, and a ”loss of function“ mutant GluA1 (Q586R). Both lines showed impaired acquisition and reduced cue- and context-induced retrieval 24 h and 48 h after fear conditioning, supporting the hypothesis of involvement of GluA1-containing AMPA receptors in learning of emotional associations. Moreover, in a similar way as for GluA3, GluA1 is also required for the normal decrease of fear to remote events in the passive avoidance test, suggesting that both subunits play an important role in the normal destabilization of older memories such as those that no longer provide an advantage in survival.

To study AMPA and NMDA receptor function specifically in the retrieval phase of fear conditioning, I used inducible recombinant adeno-associated virus (rAAV)-mediated gene manipulations in the amygdala. The efforts to generate a BLA-specific promoter for rAAV failed. Therefore a doxycycline-inducible neuron-specific system was used for synaptic silencing of neurons in the amygdala, and to inactivate NMDA and GluA1-containing AMPA receptors in the BLA. Altogether, the analysis of rAAV-injected mice provided strong evidence that retrieval of cued fear memory is dependent on the chronic expression of NMDA receptors in the BLA, whereas the contribution of the GluA1-containing AMPA receptors remains to be confirmed.

In the second part of this thesis, I generated and analyzed a new rAAV vector for tissue-specific gene delivery. A new endogenous promoter was cloned from the murine *lynx2* gene, a member of the Ly-6/neurotoxin superfamily, for overexpression of genes in dentate gyrus granule cells. This virus can be used to further restrict rAAV-mediated targeting to certain groups of cells.

Zusammenfassung

Die vorliegende Arbeit beschreibt neue gentechnisch unterstützte Untersuchungen zur Funktion von AMPA- und NMDA-Rezeptoren im Gehirn und insbesondere der basolateralen Amygdala (BLA) von Mäusen beim Erlernen und bei der Ausprägung emotionaler Erinnerungen.

In Verhaltensstudien an GluA3-Knockout Mäusen konnte ich zeigen, dass AMPA-Rezeptoren, welche die Untereinheit GluA3 tragen, für eine Angstkonditionierung nicht benötigt werden. Allerdings sind diese Rezeptoren für eine allmähliche Attenuierung der Angstreaktion bezüglich einer ursprünglich erworbenen negativen Erfahrung notwendig, wie Messungen des passiven Vermeidungsreflexes als auch der Angstreaktion auf den negativ assoziierten Reiz einige Wochen nach der Konditionierung belegen können.

Im Gegensatz dazu sind die GluA1-haltigen AMPA-Rezeptoren für das Erlernen und Memorieren reiz- und kontext-konditionierter Angst essentiell. Dies zeigen Verhaltensstudien mit globalen GluA1-Knockout- Mäusen als auch mit den „Loss of Function" GluA1 (Q586R)-Mutanten. In beiden Mauslinien ist eine verminderte Lernfähigkeit und eine deutlich reduzierte reiz- bzw. kontext-induzierte Angstreaktion 24 und 48 Stunden nach der Konditionierung nachweisbar, was auf eine Beteiligung von GluA1(Q) haltigen AMPA-Rezeptoren beim effektiven Erlernen emotionaler Assoziationen hinweist. Außerdem werden die GluA1 als auch GluA3 im AMPA-Rezeptorkomplex für die normale Abschwächung traumatisierter Angst, die im passiven Vermeidungstest quantifiziert wurde, benötigt. Dies deutet darauf hin, dass beide Untereinheiten bei der Destabilisierung älterer Erinnerungen, wie z. B. solcher, die keine Überlebensvorteile mehr verleihen, eine wichtige Rolle spielen.

Um die Funktion von AMPA- und NMDA-Rezeptoren bei der Reaktion auf einen konditionierten Reiz zu untersuchen, wurden induzierbare Genmanipulationen in der Amygdala mit Hilfe von rekombinanten adeno-assoziierten Viren (rAAV) durchgeführt. Da es nicht möglich war einen BLA-spezifischen Promotor für rAAV zu generieren, wurde ein Doxycyclin induzierbares System benutzt, um die synaptische Aktivität von Neuronen in der Amygdala auszuschalten und um NMDA- und GluA1-enthaltende Rezeptoren in der BLA zu inaktivieren. Die Analyse der rAAV-infizierten Mäuse lieferte erste starke Hinweise für eine Beteiligung der NMDA-Rezeptoren bei der Erinnerung an einen lange zurückliegenden konditionierten Stimulus und somit einen Beweis, dass chronische NMDA-Rezeptorexpression für den langfristigen Erhalt einer negativen emotionalen Erfahrung notwendig ist. Die Mitwirkung von GluA1-enthaltenden AMPA-Rezeptoren konnte nicht eindeutig gezeigt werden.

Im zweiten Teil meiner Dissertation generierte und analysierte ich einen neuen rAAV-Vektor für gewebespezifische Genexpression. Genfragmente aus der Promotorregion des *lynx2*-Gens wurden isoliert, um mit deren Hilfe die Überexpression von rAAV-transduzierten Genen in den Körnerzellen des Gyrus dentatus zu ermöglichen. Ein aus diesen Studien resultierendes neues Virus ermöglicht die Eingrenzung eines rAAV-vermittelten Gentransfers auf bestimmte neuronale Zellpopulationen.

Abbreviations

ACh	Acetylcholine
AMPA	α-amino-3-hydroxy-5-methyl-4-isoxazolepropionic acid
AMPAR	AMPA receptor
ANOVA	Analysis of variance
APV	2-amino-5-phosphonopentanoic acid
BA	Basal amygdala
BCA	Bicinchoninic acid
BLA	Basolateral amygdala
bp	Base pairs
CA1,3	Cornu Ammonis area 1,3
CeA	Central amygdala
CMV	Cytomegalovirus
CNQX	6-cyano-7-nitroquinoxaline-2,3-dione
CR	Conditioned response
Cre	Cause of recombination
CS	Conditioned stimulus
DAB	3,3'-Diaminobenzidine
DAPI	4',6-diamidino-2-phenylindole
DG	Dentate gyrus
DNA	Deoxyribonucleic acid
Dox	Doxycycline
E1–5	Extinction trial 1–5
EGFP	Enhanced green fluorescent protein
GFAP	Glial fibrillary acidic protein
GFP	Green fluorescent protein
HEK293	Human embryonic kidney 293 cells
HEPES	4-(2-hydroxyethyl)-1-piperazineethanesulfonic acid
kb	Kilobases
LA	Lateral amygdala
LTP	Long-term potentiation
nAChR	Nicotinic acetylcholine receptor

NBQX	2,3-dihydroxy-6-nitro-7-sulfamoyl-benzo[f]quinoxaline-2,3-dione
NMDA	N-methyl-D-aspartate
NMDAR	NMDA receptor
P0	Postnatal day 0
PBS	Phosphate buffer solution
PCR	Polymerase chain reaction
P_{tetbi}	Bidirectional tetracycline-activated promoter
rAAV	Recombinant adeno-associated virus
RNA	Ribonucleic acid
rtTA	Reverse tetracycline-controlled transcriptional trans-activator
SDS-PAGE	Sodium dodecyl sulfate polyacrylamide gel electrophoresis
SOP	Standard operating procedures in Memory/ Sometimes-oponent process
SRR	Synaptic reentry reinforcement
syn	Human synapsin I promoter
tdTomato	Tandem-dimer tomato
TEMED	Tetramethylethylenediamine
tTA	Tetracycline-controlled transcriptional trans-activator
TTLC	Tetanus toxin light chain
US	Unconditioned stimulus

Part I:
AMPA and NMDA receptors in emotional learning

1. Introduction

We are who we are thanks to the things we remember: from our names to the events in our lives, our memories shape our identity. The general curiosity about the mechanisms behind learning date back to the ancient civilizations, but the systematic study of learning only began with the development of simplified models for analysis (Ebbinghaus, 1885; Pavlov, 1927). The conditioning paradigm established by Pavlov (Pavlov, 1927) provided strong insights into the principles of learning and memory. In brief, the basic principle consists in exposing an animal to a harmless stimulus (the conditioned stimulus; CS), which is paired with a naturally aversive stimulus (the unconditioned stimulus; US), usually an electric shock. Subsequently the animal will display a conditioned fear response (CR) when re-exposed to the initially harmless CS.

Several variants of this basic paradigm have been developed and different brain structures have been found to be involved in each of them. For example, when the CS consists of a tone—termed auditory or cued conditioning—the amygdaloid complex is required but not the hippocampus (LeDoux, 2003), whereas both regions are necessary if the CS is in the form of a context—as in contextual fear conditioning (Phillips and LeDoux, 1994). The CR can be measured in several ways, such as the startle reflex (Brown et al., 1951; Davis et al., 1993), or, most commonly in the form of 'freezing', an inborn behavior shown by rodents in response to a frightening stimulus, consisting in the total absence of movements except for those necessary for respiration (Blanchard and Blanchard, 1969a, b), and is widely used as an index of learned fear (Kandel, 2001). The simplicity of the fear-conditioning paradigm allowed the systematic study of learning and memory.

1.1.A primer on memory formation

The first proposal that memory undergoes maturation over time was made more than a century ago (Lechner and Squire, 1999). Since then, a great amount

of evidence has been obtained, supporting the general view that memories first undergo a phase of lability after they have been learned and become stable over time (Kandel, 2001; McGaugh, 2000). However, consolidation can be analyzed at different levels.

At the level of 'cellular consolidation', there is a time window lasting 1–2 days after initial learning during which memories can be disrupted by a number of manipulations ranging from inhibition of protein or RNA synthesis to head concussions, hypothermia or electroconvulsive shock. After this vulnerability period, these amnesic treatments do not exert the same effect and memories become stable (Kandel, 2001; McGaugh, 2000).

Memories also undergo 'systems consolidation', which refers to a change in their requirement of certain brain regions with the passage of time. Scoville and Milner first reported that the medial temporal lobe, a region which contains the hippocampus, is required for the recall of recent but not remote memories in humans (1957). Several models have proposed that certain types of memories, for example, contextual memories, initially depend on the hippocampus but later become hippocampus-independent and are 'transferred' to the neocortex (Frankland and Bontempi, 2005).

More recently, attention rose around the long-reported observation that memories that had already undergone consolidation and were thought to be stable, can again become labile after reactivation (Misanin et al., 1968; Nader et al., 2000). This process, termed 'reconsolidation', challenged the view that the important molecular mechanisms of learning occurred only after initial learning. Reconsolidation has been proposed to be a mechanism for updating old memories by linking them to, or adding, new information (Sara, 2000a), but also as a way of strengthening memories by reactivation (Alberini, 2011; Sara, 2000b).

Another important memory process is 'extinction', which consists in the formation of a new association between a CS and the absence of a US, where the CS had been previously coupled with a US to produce a CR. This process leads to the decrease of the CR, e.g. in the form of decreased fear, and can have important clinical applications. In practice, whether reactivation of a memory

leads to extinction or to reconsolidation depends on many factors like the duration of the reactivation trial (Pedreira and Maldonado, 2003) and the strength of the memory (Suzuki et al., 2004). Moreover, there are 'boundary' situations in which subtle changes in the behavioral protocol can lead to either strengthening or overwriting of the memory: for example, triggering reconsolidation can facilitate the subsequent extinction of a fear memory (Monfils et al., 2009).

Finally, there is evidence that the passage of time alone can change the susceptibility of memories to reconsolidate or extinguish (Inda et al., 2011) (Dudai and Eisenberg, 2004). This implies that there are ongoing 'lingering' processes that continue after a memory has been consolidated or reconsolidated, but the molecular nature of these phenomena remains unclear.

1.2. The amygdaloid complex

The amygdaloid complex is a key player in the emotional modulation of learning. Lesion studies in different organisms have shown that ablation of the basolateral amygdala (BLA) by mechanical (Weiskrantz, 1956; Zola-Morgan et al., 1991), pharmacological (Maren et al., 1996a), or electrical methods (Armony et al., 1998) leads to the inability to form associations between noxious (US) and non-noxious (CS) events. It is also accepted that synaptic plasticity in the BLA plays an important role in the formation of these associations. The firing rate of BLA neurons changes during fear conditioning and increases when the CS is presented (Collins and Paré, 2000; Quirk et al., 1997; Quirk et al., 1995; Repa et al., 2001). Moreover, induction of long-term potentiation (LTP) in the BLA has also been correlated with fear learning (Huang and Kandel, 1998; Maren and Fanselow, 1995; McKernan and Shinnick-Gallagher, 1997; Rogan et al., 1997). Therefore, the analysis of the mechanisms mediating plasticity changes in the amygdala became of utmost importance to understand the underpinnings of emotional learning.

Anatomically, the amygdala consists of more than ten different highly interconnected nuclei in the medial temporal lobe (Davis and Whalen, 2001). The BLA receives afferents from subcortical and cortical sensory systems,

among which those from the thalamus and the auditory cortex are critical for auditory fear conditioning (Campeau and Davis, 1995; LeDoux et al., 1986). The BLA connects with the central amygdala (CeA), which has outputs to the brainstem and the hypothalamus, enabling the association of sensory information from CS and US with the physiological fear responses (Pare et al., 2004). Lesion studies showed that the amygdala is necessary for the acquisition of fear conditioning and expression of the fear response (Kim and Davis, 1993a; Roozendaal et al., 1991) and for the long-term storage of the fear memory (Kim and Davis, 1993b; Maren et al., 1996a).

The mechanisms involved in emotional learning are related to synaptic strength changes in the input projections to the lateral amygdala (Maren and Quirk, 2004). An example of such changes is LTP, an activity-dependent increase of synaptic transmission that lasts for hours or days (Bliss and Lomo, 1973) and is believed to underlie learning and memory (Malenka and Nicoll, 1999). LTP has been demonstrated to occur at the input synapses to the lateral amygdala (Huang and Kandel, 1998; Maren and Fanselow, 1995; Rogan et al., 1997) and to be driven by different mechanisms at its thalamic and cortical afferents (Sigurdsson et al., 2007). Intensive research efforts have been dedicated to study these mechanisms in the hope of improving our understanding of memory and learning, but the details of the molecular underpinnings are not yet fully understood.

1.3.AMPA receptors in emotional memory

1.3.1. AMPA receptors

Alpha-amino-3-hydroxy-5-methyl-4-isoxazolepropionic acid receptors (AMPARs) are glutamate-gated tetrameric ion channels formed by four types of subunits: GluA1 through GluA4 (Collingridge et al., 2008; Keinänen et al., 1990). Each subunit has an extracellular N-terminus and an intracellular C-tail (Hollmann et al., 1989). The ion-permeable pore of the channel is formed by the second hydrophobic domain of each subunit and allows the flow of Na^+ and K^+. Ca^{2+}-impermeability is given by the presence of the GluA2 subunit in the receptor complex (Hume et al., 1991; Verdoorn et al., 1991). In neurons,

AMPARs are dimers of heterodimers, consisting of one GluA2 subunit and either one GluA1 or one GluA3 subunit. The crystal structure for a homo-oligomeric AMPAR has already been determined (Sobolevsky et al., 2009). AMPARs have been shown to be involved in synaptic transmission and LTP in the lateral amygdala (LA) by pharmacological methods. For example, blockade of AMPARs, or the related kainate receptors, by 6-cyano-7-nitroquinoxaline-2,3-dione (CNQX) or 2,3-dihydroxy-6-nitro-7-sulfamoyl-benzo[f]quinoxaline-2,3-dione (NBQX) indicates that AMPAR activation in the amygdala is important for the formation of fear memories and also for the expression of fear responses (Kim et al., 1993; Walker and Davis, 2002), but not for reconsolidation of cued fear (Ben Mamou et al., 2006). But pharmacological studies present several important drawbacks, e.g. toxicity of the drugs, unspecificity of activity, inability to distinguish between affected cell-types. For this reason, it is necessary to use a genetic approach to help to elucidate the role of AMPARs in the amygdala, including that of its different subunits.

1.3.2. GluA1 knockout mice

Genetic targeting revealed a great deal of information about the role of AMPAR subunits in behavioral responses. Mice with a global knockout of the GluA1 subunit (*GluA1*$^{-/-}$) are viable and exhibit normal gross behavior (Bannerman et al., 2004), they have impaired CA1-to-CA3 LTP in the hippocampus, but their spatial reference memory is normal, for example, in the Morris water maze (Reisel et al., 2002; Zamanillo et al., 1999) or in the Y-maze (Reisel et al., 2002). However, these mice exhibit a memory dissociation, in which the spatial working memory is impaired, for example, in the T-maze (Reisel et al., 2002). A rescue of GluA1 expression in pyramidal neurons of the hippocampus by transgenic methods showed that the T-maze performance could be restored in *GluA1*$^{-/-}$ mice (Mack et al., 2001; Schmitt et al., 2005).

Regarding GluA1 function in the amygdala, through the analysis of global GluA1 and GluA3 knockout mice, it was shown that GluA1-containing AMPARs are essential for LTP in the thalamo-LA pathway, whereas both GluA1 and GluA3 subunits contribute to LTP at the cortico-LA synapses

(Humeau et al., 2007). Moreover, the same study showed that *GluA1*$^{-/-}$ mice exhibit impaired acquisition and retrieval of cued and contextual fear conditioning, but since these animals express no GluA1 in any tissue, this approach does not allow distinguishing the degree of participation of the AMPA receptors in the amygdala specifically. Nonetheless, these data are in line with a key involvement of the GluA1 subunit in learning processes in regions of the brain other than the hippocampus.

Further evidence for the role of GluA1 in learning mechanisms in the amygdala comes from a virus-mediated approach for disrupting GluA1 trafficking in LA neurons, which blocked thalamo-LA LTP and impaired the acquisition of auditory fear conditioning (Rumpel et al., 2005). However, it is not clear from this study whether the observed impairment is solely due to the interference with GluA1 trafficking or to unspecific effects of the over-expression of the C-tail of the GluA1 subunit.

1.3.3. GluA3 knockout mice

GluA3 is expressed in high levels only in the cerebellum, and in low levels in pyramidal neurons (Keinänen et al., 1990), in contrast to another subunit, GluA2, which is expressed in most of the receptors in the adult (Wenthold et al., 1992). The GluA3 subunit, like GluA2, has a short intracellular C-terminal tail and interacts with a subset of PDZ proteins (Song and Huganir, 2002). The exact function of GluA2/3-containing AMPARs remains unclear. These receptors are thought to be part of a constitutive pathway for constant renewal of the AMPAR pool in the membrane and not to be necessary for activity-dependent endocytosis of AMPARs (Biou et al., 2008), contrasting with GluA1-containing receptors, which are critical for plasticity-related processes, in which synaptic strength changes due to experience (Shi et al., 2001).

The analysis of mice with global GluA3 knockout (*GluA3*$^{-/-}$) has only revealed subtle abnormalities. Studies *in vitro* have shown that the synaptic properties of the neurons are only weakly affected by GluA3 knockout (Biou et al., 2008). Moreover, only a small percentage (~16%) of synaptic AMPARs contain GluA3 in CA1 pyramidal neurons (Lu et al., 2009), which would

explain the minor effects in fast glutamatergic synaptic transmission. In the cerebellum, deletion of GluA3 is correlated with a reduction in the levels of GluA1, -2, and -4. This fact might be related to the slight motor coordination impairment seen in the rotarod and beam balance tests, as well as the reduced locomotor activity shown in the open-field test (Sanchis-Segura et al., 2006). However, in areas where there are low constitutive amounts of GluA3, e.g. the hippocampus, deletion of the GluA3 gene does not affect the expression of the other AMPAR subunits, and the spatial reference memory in the Morris water maze is not impaired (Sanchis-Segura et al., 2006).

Overall, *GluA3*$^{-/-}$ mouse behavior is largely normal compared with wild-type littermates, and differences have only been found in very specific tests and observations. For example, sleep-related abnormalities have been reported, with an absence of non-Rapid Eye Movement sleep phases in *GluA3*$^{-/-}$ mice and abnormal breathing during periods of inactivity (Steenland et al., 2008). Additionally, higher locomotor activity was reported in the forced-swim test, a test for depression-like behavior. A role in alcohol addiction has also been reported: although *GluA3*$^{-/-}$ mice have a normal alcohol-seeking phenotype, they exhibit reduced reinstatement after extinction (Sanchis-Segura et al., 2006).

1.4.NMDA receptors in emotional memory

1.4.1. NMDA Receptors

N-methyl-D-aspartate receptors (NMDARs) are unique tetrameric ion channels that require simultaneous binding of glutamate and glycine, as well as depolarization of the membrane, in order to be fully activated (Johnson and Ascher, 1987). This is due to the blockade of the ion pore by Mg^{2+} at resting membrane potential (Nowak et al., 1984). Hence, NMDARs are thought of as coincidence detectors of pre- and postsynaptic neuronal activation. NMDARs are formed by different subunits, the most important being GluN1, GluN2A and GluN2B. Functional channels require two GluN1 and two GluN2 subunits, and the receptor assembly can occur only when GluN1 subunits are available (Schüler et al., 2008).

1.4.2. Pharmacological blockade of NMDARs

Among the first attempts to study the molecular processes mediating memory formation in the amygdala, pharmacological studies targeting NMDA and AMPA receptors were performed. It is now generally accepted that NMDARs are essential for the acquisition of fear memories (Bauer et al., 2002; Campeau et al., 1992; Fanselow and Kim, 1994; Miserendino et al., 1990).

The role of NMDARs in the expression of fear, that is, in the performance on the actual retrieval test has been less clear and was intensely disputed for several years. Two decades ago, Miserendino and colleagues (1990) showed that the NMDAR antagonist 2-amino-5-phosphonopentanoic acid (APV) did not impair the expression of fear in a potentiated startle reflex paradigm—which is different from the fear conditioning paradigm. Later on, Maren and colleagues (1996b) found that APV did impair the expression of fear in a contextual fear-conditioning paradigm. This observation was again debated by Gewirtz and Davis (1997) by showing that APV once again did not impair fear potentiated startle. Shortly afterwards, Lee and Kim (Lee and Kim, 1998) claimed that APV did impair the expression of fear both in contextual and cued fear conditioning and proposed that the role of NMDARs is different for the startle and the conditioning paradigms. The controversy remained unresolved until a growing amount of evidence supported the notion that NMDARs are only required for acquisition but not for expression of fear. More recently, Matus-Amat and colleagues (2007) proposed that the reason for the conflicting results could be due to the use of different enantiomers in the different studies: D-APV was shown not to impair expression of fear, whereas DL-APV and L-APV did reduce fear expression.

In the last decade, experiments assessing the effect of intra-BLA APV injection in fear extinction have shown that NMDAR blockade does not impair expression of fear but does impair the extinction of fear both in avoidance learning (Myskiw et al., 2010) and in fear conditioning (Zimmerman and Maren, 2010), whereas the NMDAR partial agonist D-cycloserine facilitates extinction (Walker et al., 2002). Similarly, injection of APV or ifenprodil, a selective blocker of GluN1/GluN2B receptors, into the BLA prior to cued fear

reactivation did not have an effect on expression of fear, but did impair reconsolidation from occurring afterwards (Ben Mamou et al., 2006). Also, fear-conditioning reconsolidation can be potentiated by intra-BLA injection of D-cycloserine (Lee et al., 2006). A requirement of NMDARs for reconsolidation has also been reported in rewarded memory paradigms (Torras-Garcia et al., 2005) and in avoidance memory in invertebrates (Pedreira et al., 2002). Therefore, it is currently accepted that NMDARs are essential for the acquisition phase, are not required for the expression of memory, and are necessary for memory extinction and reconsolidation.

Regarding the subunit composition of NMDARs, an important role for GluN2B receptors on reconsolidation has been proposed (Wang et al., 2009).

1.4.3. Transgenic models of NMDAR-deficient mice

Global knockout of NMDARs in *GluN1*$^{-/-}$ mice leads to early death within 15 h after birth due to respiratory failure (Forrest et al., 1994). Therefore, only inducible or subregion-specific GluN1 knockouts can be used for behavioral analysis. However, a limiting factor is the low number of specific promoters or molecular technologies available for such anatomically restricted manipulations. A number of forebrain and hippocampus-specific promoters have been used to drive specific transgenic expression of Cre recombinase in different regions. Using this approach, distinct roles for NMDARs in different regions of the hippocampus have been described. Nevertheless, the transgenic promoter's expression pattern during the lifetime of the animal is often not clearly defined, constituting an important drawback for NMDAR functional analysis. For example, it has been reported that CA1-specific knockout of GluN1 strongly impairs spatial learning in the Morris water maze, but does not affect a non-spatial 'landmark' version of the task (Tsien et al., 1996). However, there is evidence that a strong component of this impairment might be the knockout of NMDARs in additional regions of the forebrain in those mice (Fukaya et al., 2003; Rondi-Reig et al., 2001; Rondi-Reig et al., 2006; Wiltgen et al., 2010). There is a similar situation for the role of NMDARs in the dentate gyrus. In one model of knockout of GluN1 specifically in the granule cells of the

dentate gyrus, no effect on contextual fear conditioning itself was found, but an inability to differentiate between two related contexts (McHugh et al., 2007). On the other hand, in a different model of GluN1 knockout in dentate gyrus (DG) granule cells, no deficit in spatial pattern separation was found (Niewoehner et al., 2007).

In order to study the involvement of NMDARs in different phases of learning, inducible systems are necessary to temporally restrict the onset—and offset—of the knockout. Using a doxycycline (Dox)-inducible forebrain-specific GluN1 knockout mouse, it was first stated that NMDARs could play a role in the consolidation processes occurring weeks after learning of hippocampus-dependent tasks such as Morris water maze or contextual fear conditioning (Shimizu et al., 2000). In this study, an exogenous GFP-tagged GluN1 subunit was expressed in the absence of Dox for 'reversibility'. Knockout of GluN1 during or right after training significantly impaired further recall one month later, whereas when the knockout was performed three weeks after conditioning, no effect was observed in the one-month retrieval test. The same mouse line was analyzed in another long-term experiment (Cui et al., 2004). Using this model, it was shown that nine-month retrieval of cued and contextual fear conditioning was impaired if NMDARs were removed during a four-week period starting six months after training, showing that NMDAR expression was required during resting periods for normal retrieval of memory at later time-points.

Regarding the role of amygdala NMDARs in learning, only one study has been published so far. In that study, knockout of GluN1 in the CeA by recombinant adeno-associated virus (rAAV)-mediated Cre recombination in *GluN1*$^{2lox/2lox}$ mice inhibited the expression of conditioned place aversion induced by opioid withdrawal in morphine-addicted mice (Glass et al., 2008). The rAAV-mediated approach provides alternative methods for the analysis for NMDARs in defined regions of the brain and several examples are presented in the following section.

1.5. Virus-based methods for gene manipulations in the brain

A significant limitation of transgenic methods for the modification of gene expression in mice is the dependence on cell-type-specific promoters that are sufficiently strong, and are active at an appropriate time point in the life of the animal. Stereotaxic virus-mediated gene manipulations are, so far, the only feasible alternative for the reliable selective alteration of gene expression in brain regions such as the amygdaloid complex. Several viral vectors are available for gene delivery in neurons, including lenti-, herpes and rabies viruses, but I will focus on rAAV systems, since these vectors are easy to manipulate and are handled at a low biosecurity level.

AAVs are small (~26 nm) paraviruses consisting of a single-stranded 4.7-kb DNA genome and a simple, non-enveloped icosahedral protein coat (Klein et al., 2002; Peel and Klein, 2000) and require a helper virus for productive infection (Atchison, 1970; Casto et al., 1967; Richardson and Westphal, 1984). An estimate of 85% of human adults are carriers for AAV with no associated pathology (Muzyczka, 1992).

Recombinant AAVs are unable to replicate since 96% of the viral genome is removed, leaving in the virus only two 145 bp inverted terminal repeats (ITRs), which are necessary for packaging (McLaughlin et al., 1988; Samulski et al., 1989), however, a 4.7-kb limit still applies. A great advantage of the usage of rAAV vectors is their lack of toxicity (Tenenbaum et al., 2004) and their long-lasting expression of the delivered genes without triggering immune responses (Peel and Klein, 2000). Moreover, rAAV vectors do not integrate into the mouse genomes or do it with a very low frequency, minimizing possible effects on the host cells due to integration (Nakai et al., 2001).

A variety of tissues have been successfully targeted by rAAVs including lung, muscle, brain, spinal cord, retina and liver (Zolotukhin et al., 1999). Therefore, rAAVs have been proposed as good candidates for gene therapy in the treatment of neurological conditions (Anderson, 1998; Monahan and Samulski, 2000). Moreover, the onset of expression of the delivered genes can be controlled by drugs, such as tetracycline, RU486 or rapamycin (Haberman and McCown, 2002). In a recent notable example, a successful clinical trial was

performed for treatment of Parkinson's Disease using bilateral rAAV-mediated expression of glutamic acid decarboxylase in the subthalamic nucleus, leading to an improvement of the symptoms of the disease (LeWitt et al., 2011).

1.5.1. Tetracycline-controlled rAAV-mediated gene expression

Stereotaxic delivery of rAAV into the brain provides a degree of anatomical specificity that cannot be obtained by classical transgenic methods. Additionally, temporal regulation of gene expression can be achieved by using the tetracycline-controlled transcriptional trans-activator (tTA) system, based on the tetracycline resistance operon from *Escherichia coli* (Gossen and Bujard, 1992). In general terms, the system relies on the exogenous expression of tTA, which binds to a set of seven tetracycline operators ($TetO_7$) directly upstream from a minimal cytomegalovirus promoter containing a TATA-box transcription start site (P_{tet}), thus driving expression of the gene(s) of interest under that promoter. In the presence of tetracycline or its derivative Dox, tTA cannot bind the $TetO_7$ and the promoter is silent. A variation of this system consists in using a reverse tTA (rtTA), which has been modified so that it requires Dox presence in order to bind to $TetO_7$ and drive gene expression (Gossen et al., 1995; Hecht et al., 1993).

For use in rAAV, the tTA or rtTA gene can be packed in one virus, while another virus containing the P_{tet} responder is simultaneously delivered (McGee Sanftner et al., 2001; Zhu et al., 2007). In order to drive expression of two genes simultaneously, several approaches are available. The first one consists of a bidirectional version of the promoter P_{tet} (P_{tetbi}). Moreover, internal ribosomal entry sites have also been used, but the degree of expression of the second gene can be a limiting factor. More recently, self-cleaving viral peptide bridges, such as the 18-aminoacid 2A-peptide from the picornavirus family (Ryan et al., 1991), have been adapted for use in rAAV vectors to efficiently express two or three genes simultaneously in comparable amounts (Tang et al., 2009).

By combining the tTA/rtTA systems with rAAV-mediated expression of Cre recombinase, the removal of loxP sites for knocking out genes in the mouse brain can be delimited both anatomically and temporally, thus enabling

important applications. In this study, I applied these tools to restrict the knockout of GluN1 and GluA1 subunits to the basolateral amygdala after a defined time point to investigate a particular phase of emotional learning.

1.5.2. Neuronal silencing using tetanus toxin light chain

Finally, the rAAV system can also be used for the expression of gene products that directly modify neuronal activity. This approach has only started recently and has proven to have enormous potential for the study of brain function.

The tetanus toxin light chain (TTLC), a fragment of the tetanus neurotoxin from *Chlostridium*, cleaves the synaptic protein VAMP2 (Link et al., 1992; Schiavo et al., 1992) and inhibits release of neurotransmitter vesicles in neurons (Schoch et al., 2001; Südhof, 1995). The expression of TTLC has been used in transgenic mice for the reversible rtTA-regulated silencing of granule cells in the cerebellum (Yamamoto et al., 2003), in olfactory sensory neurons (Yu et al., 2004), and more recently, in CA3 neurons of the hippocampus (Nakashiba et al., 2008). TTLC expression has also been used for the hemilateral silencing of substantia nigra neurons in a rat model of Parkinson's disease using adenoviral vectors (Yang et al., 2007).

So far, TTLC-mediated neuronal silencing in the amygdala has not yet been reported. In this study, I used rAAV gene delivery of TTLC as a proof-of-concept experiment, showing that rAAV-mediated gene expression modifications can be applied for the study of amygdala-related learning. However, the potential of reversible neuronal silencing in this brain region for the study of different phases of learning still remains to be explored.

1.6. Aim of thesis

Ionotropic glutamate receptors play an essential role in the mechanisms of neuronal plasticity in the brain. Particularly in learning and memory, AMPARs and NMDARs are key to the changes in synaptic transmission. A great deal of knowledge has been gained from genetic mouse models with altered AMPAR and NMDAR signaling, which points to a complex scenario for the roles of these two types of receptors. Nevertheless, important limitations are associated

with the transgenic and pharmacological methods that have been used so far for the study of the involvement of glutamate receptors in mental processes. My goal is to gain insight into the role of the two main populations of AMPARs in principal neurons—GluA1- and GluA3-containing receptors—in short- and long-term memory processes through the behavioral analysis of mice deficient for each of these subunits. Additionally, I aim to apply rAAV-mediated gene delivery in the study of amygdala-dependent learning and, particularly, the involvement of NMDARs in long-term memory.

2. Results

2.1. *Emotional memory in GluA3 knockout mice*

2.1.1. Exploratory behavior of *GluA3*$^{-/-}$ mice

An assessment of general exploratory behavior is of great importance for a variety of behavioral tests that rely on measurement of mouse locomotion. The global GluA3-deficient mouse line, *GluA3*$^{-/-}$ (Sanchis-Segura et al., 2006), was tested in order to find out what behavioral phenotype arises when GluA3-containing AMPARs are absent.

GluA3$^{-/-}$ mice (n = 13 males; age 17 ± 0.2 weeks) and wild-type littermates (Control n = 11 males; age 16 ± 0.3 weeks) were used for these experiments. Observation of exploratory activity in the open field arena (Figure 1a) for 6 min revealed that the control group traveled a longer distance (Figure 1b; $t_{22} = 3.8$, $p = 0.001$), indicating a hypoactive behavior of *GluA3*$^{-/-}$ mice. However, the time spent in the center of the arena for all mice was not significantly different (Mann-Whitney $U = 50$, $p = 0.22$), indicating that the global anxiety levels were similar for both groups (Appendix Table 7, Figure 1c).

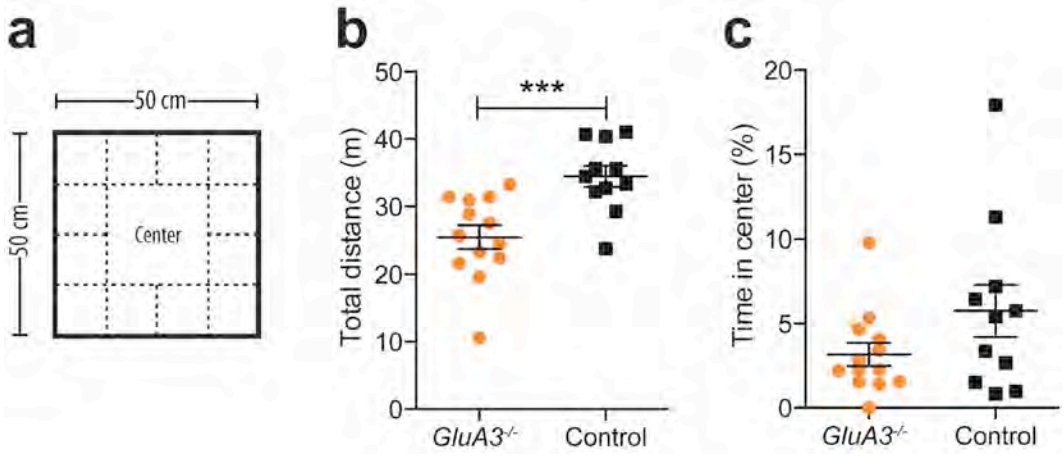

Figure 1. Open field test for *GluA3*$^{-/-}$ mice
a, Diagram of the open field: the 60 cm x 60 cm arena was divided in 16 equal regions, with the four internal squares constituting the center. **b,** Scatter plot of the total distance traveled during the 6 min observation calculated from the video recording: *GluA3*$^{-/-}$ mice were significantly less explorative The horizontal line corresponds to the mean. **c,** Scatter plot of the percentage of time spent in the center area of the open field with the mean shown as a horizontal line. No significant difference was observed between knockouts and controls. Error bars, s.e.m. ***$p = 0.001$

2.1.2. General cognitive ability of *GluA3*$^{-/-}$ mice

The puzzle-box test was used to assess the general cognitive ability of *GluA3*$^{-/-}$ mice in a series of executive tasks with increasing difficulty to escape from a lit compartment (Abdallah et al., 2011). For each task, the latency to escape from the bright compartment and enter the dark compartment of the box was measured and the test was stopped after a time limit of 3 or 4 min. A censored-subject statistical analysis was performed, in which the log-rank Mantel-Cox test was used to compare the 'survival' curves—i.e. the plot of the percentage of mice reaching the goal within a particular latency—between genotypes on different trials and tasks and the Bonferroni correction was applied when comparing more than two curves (Appendix Table 8).

In the first task, animals simply passed through an 'open door' opening from the light to the dark compartment. No differences were found in the escape latency for *GluA3*$^{-/-}$ and controls, indicating that the motivational drive to escape from the brightly lit open arena was similar for both genotypes (Figure 2a).

In the second task, animals had to cross to the dark compartment using an underpass, in the absence of an open door (Figure 2b). When this new task was presented, both groups of mice initially had difficulties in achieving escape into the dark chamber (task 2, trial 1), but controls were able to do this reliably during further trials (trials 2 and 3). *GluA3*$^{-/-}$ mice were significantly impaired in the solving of this task, as shown by the still high latency to enter the dark during trial 2, which was significantly different from the wild types ($C^2_{1,N=24}$ = 11.49, p = 0.0007). Nevertheless, knockouts were also able to learn to solve the task, as evidenced by the improved latency to escape the light chamber and the absence of significant differences compared to control mice in trial 3.

In task 3, mice had to dig their way through the sawdust-blocked underpass to gain access to the dark compartment (Figure 2c). This increase in the difficulty of the task affected primarily *GluA3*$^{-/-}$ mice, which were strongly impaired in their ability to solve the task compared with the wild types ($C^2_{1,N=24}$ = 6.961, p = 0.0083). On the second trial of this task, the difference was less marked ($C^2_{1,N=24}$ = 4.478, p = 0.0343) and more so in the third trial ($C^2_{1,N=24}$ =

3.918, $p = 0.0478$). This shows that *GluA3*$^{-/-}$ mice were also able to learn to solve this task, although it was more challenging for them than for wild-type mice.

In a final variation of the problem-solving test —task 4—, mice needed to remove a cardboard plug to enter the dark compartment (Figure 2d). The behavior in this task was similar to that in the previous one. *GluA3*$^{-/-}$ mice were initially strongly impaired compared with controls (trial 1, $C^2_{1,N=24} = 5.929$, $p = 0.0149$), but there were no significant differences in subsequent trials (trial 2, $C^2_{1,N=24} = 3.116$, $p = 0.0775$; trial 3, $C^2_{1,N=24} = 2.160$, $p = 0.1416$). However, mice from both groups were able to learn how to solve this task.

A digging test was performed in order to exclude the possibility that the results of the puzzle box test could be explained by impairment in motor ability or motivation or ability to dig (Figure 2e). Mice were placed in a Makrolon type II cage with 5-cm deep embedding and the time spent digging as well as the latency to start to dig were assessed. *GluA3*$^{-/-}$ mice spent as much time (*GluA3*$^{-/-}$ 18.36 ± 3.269 s; Control 16.19 ± 5.15 s; $t_{22} = 36.65$, $p = 0.7175$) and had a similar latency to start digging as the wild-type controls (*GluA3*$^{-/-}$ median 90 s; Control median 110 s; $C^2_{1,N=24} = 0.7491$, $p = 0.3868$).

In summary, these results show that *GluA3*$^{-/-}$ mice are able to solve complex executive tasks and do not have major motor or motivational problems, while they possess a subtle cognitive impairment.

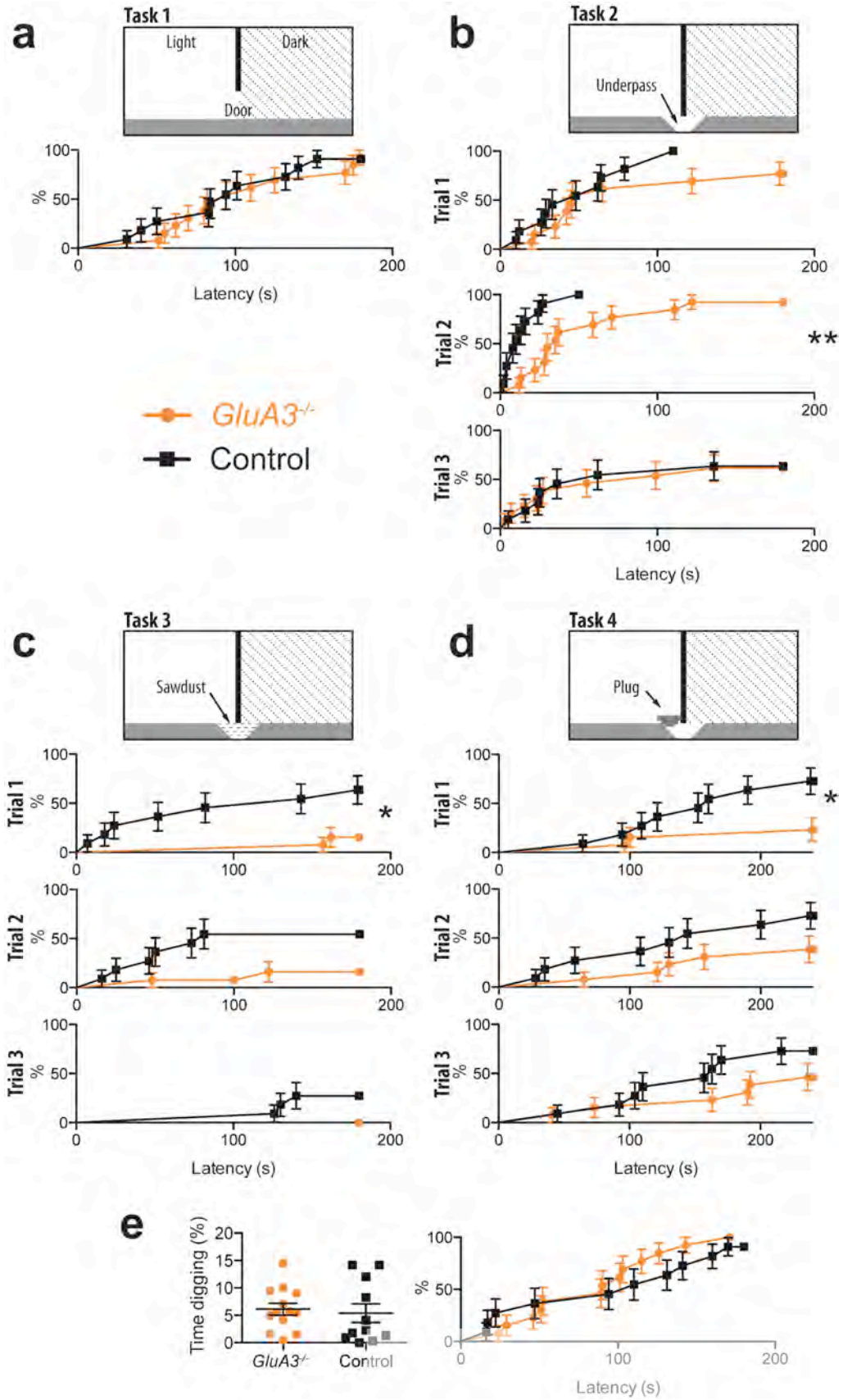

Figure 2. General cognitive ability of *GluA3*$^{-/-}$ mice assessed in the puzzle-box test
a, Lateral view diagram of the puzzle box depicting the light and dark compartments communicated by an open door in task 1. Below the scheme: 'survival' curve for the latency to enter the dark area showing the percentage of animals that finished the task

at a particular time within 180 s. **b,** In task 2, mice can only enter the dark compartment through an underpass (diagram). Below: 'survival' curves for the three trials of this task. A left-shifted curve indicates that the mice quickly and successfully finished the task. A right-shift indicates difficulties in finishing the test. **c,** In task 3, the underpass is filled with sawdust and the mice dig through it to enter the dark. Below: 'survival' curves for the three trials of this task. A down-shifted curve indicates that few of the mice were able to successfully finish the task. **d,** In task 4, the communicating underpass was blocked with a cardboard plug, which had to be removed by the mice. Below: 'survival' curves for the three trials with a time limit of 240 s. **e,** Scatter plot for the performance in the digging test measured by the percentage of time spent digging. The horizontal line indicates the mean. Next to it, 'survival' curve for the latency to start digging in the digging test. Both the percentage of time spent digging in sawdust in a separate test and the latency to start digging were similar for *GluA3*$^{-/-}$ and wild-type mice. Error bars, s.e.m. *$p < 0.05$, ***$p < 0.001$.

2.1.3. *GluA3*$^{-/-}$ mice in fear conditioning and extinction

To study the role of GluA3-containing AMPARs in fear learning, cued Pavlovian fear conditioning was performed on the same cohort of mice with an acquisition phase consisting of three tone-shock pairings (Figure 3a). To test for retrieval of the cued association a memory test was performed by re-exposing the mice to the tone and measuring the fear response 24 h after acquisition and on four additional subsequent days. Therefore, the cued tests constituted extinction trials and are termed E1-E5 in the following analysis.

The same cohort of male *GluA3*$^{-/-}$ mice (n = 13; age 24 ± 0.3 weeks) and littermate wild-type controls (n = 11; age 23 ± 0.5 weeks) were trained in the fear-conditioning protocol shown in Figure 3a, and the percentage of immobility was quantified from infrared sensor readings (movement of less than 1 cm/s). There were no differences between both genotypes during the first 6 min of the acquisition protocol, showing that both groups have a similar baseline activity. During this phase, *GluA3*$^{-/-}$ mice and wild types sequentially increased their immobility in response to each tone-shock pairing (Figure 3b). Two-way repeated measures ANOVA showed a significant effect of genotype ($F_{1,22} = 12.27$, $p = 0.0020$), time ($F_{14,22} = 27.85$, $p < 0.0001$) and interaction ($F_{14,22} = 3.780$, $p < 0.0001$). Post hoc comparisons revealed that the final immobility levels were higher for the *GluA3*$^{-/-}$ mice than for the wild types (Appendix Table 9). Interestingly, each presentation of the tone was accompanied by decreased immobility during the 30 s tone presentation.

When tested for cued retrieval of fear 24 h after acquisition, both groups of animals increased their immobility in response to the tone (Figure 3c), but the strength of the memory was different for both genotypes ($F_{1,22}$ = 23.31, p < 0.0001; time effect $F_{13,22}$ = 16.94, p < 0.0001; interaction $F_{13,22}$ = 3.122, p = 0.0002). Post hoc Bonferroni-corrected t-tests revealed that *GluA3*$^{-/-}$ mice moved significantly less than their wild-type littermates during the first 6 min of the tone presentation (Appendix Table 9).

In order to test if the mice had learned to associate the tone as a prediction of the foot shock, total immobility before and during the CS presentation was compared (Figure 3d). There was a significant effect of genotype ($F_{1,44}$ = 13.15, p = 0.0007) and tone ($F_{1,44}$ = 42.59, p < 0.0001). In response to the tone, *GluA3*$^{-/-}$ mice moved significantly less than before the tone and the same was true for the controls. Therefore, both groups of mice learned the fear association. The total immobility during the CS was higher (~1.5 fold) for *GluA3*$^{-/-}$ mice.

Subsequently, the mice were subjected to an extinction protocol consisting of a repetition of the cued test during four additional days (extinction trials 2-5). The total immobility during the tone presentation (solid lines) and the baseline immobility (dotted lines) are shown in Figure 3(e). Two-way repeated-measures ANOVA showed a significant effect of genotype ($F_{3,44}$ = 9.91, p < 0.0001), trial ($F_{4,44}$ = 11.51, p < 0.0001), and interaction ($F_{12,44}$ = 7.81, p < 0.0001). Post hoc tests revealed that *GluA3*$^{-/-}$ mice exhibited tone-enhanced immobility during E1 and E2, but not in the subsequent tests, whereas control mice only showed significantly more immobility to the tone compared to the baseline at E1 and not in the subsequent days (Appendix Table 11).

Upon completion of the extinction protocol, all animals were able to extinguish the initial CS/US association, as evidenced by the unchanged activity levels in response to the CS presentation in E5. The time line of extinction, however, was different in both groups. This is confirmed additionally by the direct observation of freezing by a blind experimenter, defined as the complete absence of movement except for respiration (Appendix Table 12, Figure 3f).

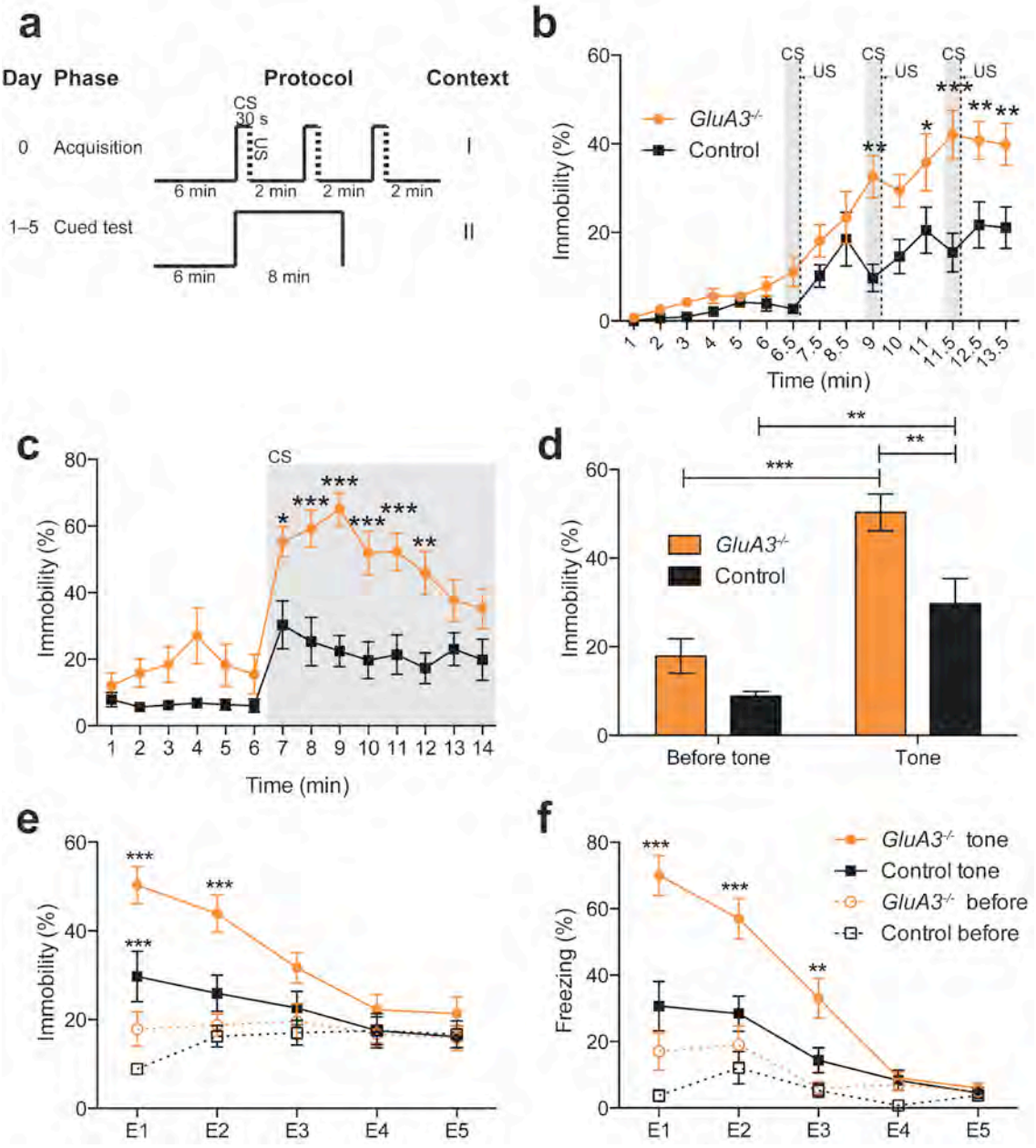

Figure 3. Cued fear conditioning and extinction in *GluA3*$^{-/-}$ mice

a, Schematic representation of the fear conditioning protocol, which consisted of a three-shock acquisition protocol and five extinction tests each every 24 h. The elevated segments indicate tone presentation (CS) and the dotted lines represent the 2 s 0.4 mA foot shock (US). **b**, Immobility during the acquisition phase: *GluA3*$^{-/-}$ mice had a similar baseline activity as wild-types. *GluA3*$^{-/-}$ mice reached significantly higher final immobility levels than wild types after each shock. The gray area represents the CS/US presentation. **c,** Immobility during the cued test 24 h after acquisition: *GluA3*$^{-/-}$ mice showed increased immobility compared to controls during the first 6 min of tone presentation, before habituating in the last 2 min. The gray area represents CS presentation. **d**, Comparison of total immobility in percent during the initial 6 min period and the 8 min tone presentation. Immobility was similar before the tone for both groups, but higher for *GluA3*$^{-/-}$ mice during tone presentation. Both groups of mice showed learning of the fear association, when comparing the fear response before and during the tone. **e,** Immobility levels during the five extinction trials: the dotted lines represent the immobility before the tone presentation, the solid lines show

immobility during the tone presentation. *GluA3*$^{-/-}$ mice showed higher immobility levels during the tone presentation (continuous line) and extinction of the cued memory association took longer to occur. **f,** Comparison of freezing levels during the extinction trials assessed by direct observation by a blind experimenter. Dotted lines represent the period before the tone, solid lines represent freezing during the tone presentation. Error bars, s.e.m. *$p < 0.05$, **$p < 0.01$, ***$p < 0.001$.

2.1.4. *GluA3*$^{-/-}$ mice in passive avoidance

Fifteen weeks after the fear-extinction protocol for the fear memory, another paradigm to test amygdala-dependent fear learning was performed with the same cohort of mice (*GluA3*$^{-/-}$ n = 13, age 39 ± 0.3 weeks; wild-type controls n = 11, age 38 ± 0.5 weeks). In the passive avoidance test, mice are placed on a square open platform (9 cm^2) elevated 1 m above the ground—an aversive situation of exposure to dangers—, and then allowed to explore it. Normally, mice enter immediately into an adjacent more protected dark chamber with a metallic grid floor (habituation phase). After 24 h, the experiment is repeated, this time giving the mice a mild electric shock (0.4 mA, 2 s), upon entering the dark compartment (acquisition phase). When tested 24 h, 37 d or 67 d later, the latency to re-enter the dark compartment is measured (retention tests). The experiment was stopped after 5 or 10 min, if the mouse did not enter. A censored-subject statistical analysis was performed. The log-rank Mantel-Cox test was used to compare the 'survival' curves between genotypes on different trials and tasks and the Bonferroni correction was applied when comparing more than two curves (Appendix Table 13).

During the acquisition phase, the latencies to leave the open platform and enter the dark compartment before the shock administration were statistically identical for *GluA3*$^{-/-}$ and wild-type mice (Figure 4a). Also during the retention tests 24 h and 7 d after initial acquisition, the latency was not significantly different between the two groups. *GluA3*$^{-/-}$ mice are, thus, able to learn to associate entering the dark chamber with a noxious stimulus. Strikingly, the latency to enter was significantly higher in *GluA3*$^{-/-}$ mice, when tested 37 d or 67 d after acquisition. Whereas wild-type mice showed decreased latencies with the passage of time, *GluA3*$^{-/-}$ mice continued to show a strong delay to enter the dark chamber.

Intra-genotype comparisons of the latency to enter the dark compartment at different time points revealed that wild-type mice strongly retained the memory for up to 7 d, but the retrieval efficiency decreased after 37 d, and there was no retention 67 d after acquisition (Figure 4b). On the other hand, *GluA3*$^{-/-}$ mice were able to strongly retain the memory of the shock for up to 67 d (Figure 4c). In summary, these data indicate that *GluA3*$^{-/-}$ mice form a stronger association in the passive avoidance test than wild-type controls and they retain this association for a considerably longer time period.

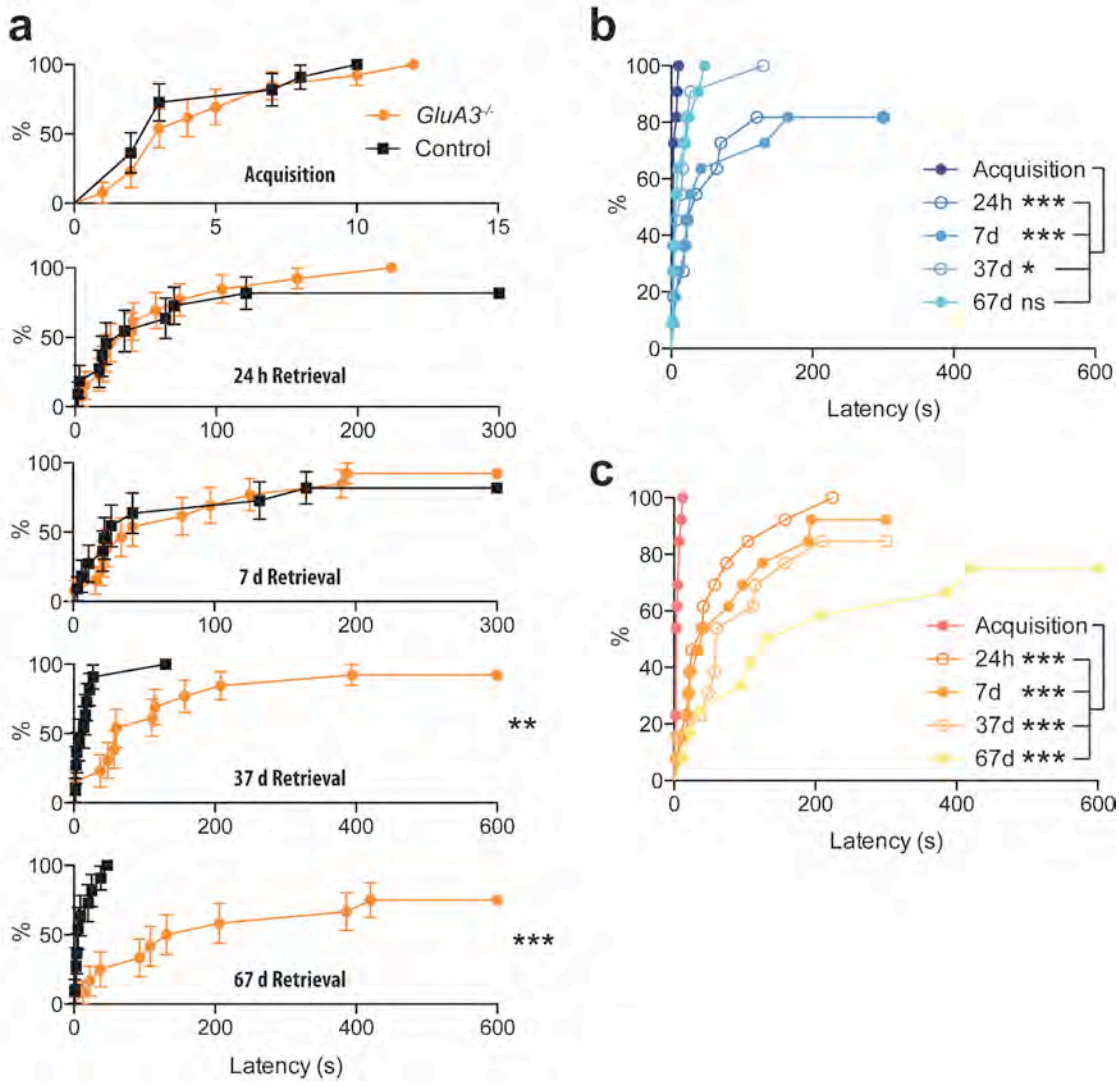

Figure 4. Long-term retrieval of passive avoidance memory in *GluA3*$^{-/-}$ mice
a, 'Survival' curves for the latency to enter the dark compartment during the acquisition phase (before receiving an electric shock) and during subsequent retrieval tests 24 h, 7 d, 37 d, and 67 d later. The Y-axis shows the percentage of mice that entered the dark compartment within the latency indicated in the X-axis. The time limit for the experiment was 600 s. A left-shifted curve indicates immediate entrance of most of the mice into the dark chamber. A right-shifted curve indicates that mice took a

longer time before entering the dark. Before the shock, all mice immediately entered the dark chamber (latency under 15 s). Both *GluA3*$^{-/-}$ and wild types exhibited similar retention of the fear memory 24 h and 7 d later. At further time points of 37 d and 67 d, *GluA3*$^{-/-}$ mice showed significantly stronger retention of the fear association. **b,** Side-by-side comparison of the latency to enter the dark chamber in wild-type mice, during the different phases of testing from the acquisition to the 67 d retrieval test. Wild-types retained the fear association of entering the dark chamber for up to 37 d. **c,** Same comparison as in (b) for *GluA3*$^{-/-}$ mice. These mice strongly retained the fear memory for up to 67 d. In (b) and (c), s.e.m. bars were omitted for clarity. *$p < 0.05$, **$p < 0.01$, ***$p < 0.001$.

2.2.Emotional memory in GluA1 mutant mice

2.2.1. *GluA1*$^{R/R}$ mice in fear conditioning

In order to test whether changes resulting from a point mutation of the GluA1 subunit, such as decreased excitatory drive and Ca^{2+}-permeability of GluA1-containing AMPARs, are enough to have an effect on the performance in fear conditioning, *GluA1*$^{R/R}$ mice (Vekovischeva et al., 2004; Vekovischeva et al., 2001) were analyzed. These mice carry a gene-targeted point mutation in the GluA1-subunit gene in which a single amino acid residue codon has been substituted (Q582R) leading to decreased single-channel conductance and less Ca^{2+}-permeability of their AMPARs (Burnashev et al., 1992). *GluA1*$^{R/R}$ mice have many similarities with complete GluA1 knockout mice, for example, they also exhibit hyperactive behavior in the open field test (Vekovischeva et al., 2004; Vekovischeva et al., 2001).

Male *GluA1*$^{R/R}$ (n = 9; age 14 ± 2 weeks) and C57Bl/6N (n = 9; age 9 weeks) mice were trained in the fear-conditioning paradigm as shown in Figure 5a. The baseline activity of both groups was comparable, as observed during the first 6 min of the acquisition phase. Upon presentation of the first CS-US pairing, the control mice increased their immobility response and continued to increase it after each additional CS-US pair (Figure 5b). *GluA1*$^{R/R}$ mice consistently showed close-to-zero immobility levels even after the three-shock administration. Two-way repeated-measures ANOVA revealed significant differences by genotype ($F_{1,16} = 51.84$, $p < 0.0001$), time ($F_{14,16} = 24.68$, $p < 0.0001$), and interaction ($F_{14,16} = 25.12$, $p < 0.0001$). Bonferroni-corrected post

hoc comparisons restricted the differences between both groups to minutes 8.5–13.5 (Appendix Table 14). These results indicate an inability of *GluA1*$^{R/R}$ mice to express fear in response to an acute painful stimulus.

When tested 24 h later for retrieval of the cued association in a different context, *GluA1*$^{R/R}$ mice consistently showed lower immobility levels than the control group (Figure 5c; genotype effect $F_{1,16} = 37.74$, $p < 0.0001$; time effect $F_{13,16} = 6.03$, $p < 0.0001$; interaction not significant; post hoc t-tests are shown in Appendix Table 14). By comparing the total amount of immobility during the period before the tone was presented and during the tone presentation, it was evident that *GluA1*$^{R/R}$ mice moved significantly more than controls (genotype effect $F_{1,32} = 61.50$, $p < 0.0001$; CS effect $F_{1,32} = 10.44$, $p = 0.003$), both before the tone ($t_{32} = 5.24$, $p < 0.001$) and during the tone ($t_{32} = 5.85$, $p < 0.001$). It was also clear from the results, that both control mice ($t_8 = 4.39$, $p = 0.002$) and *GluA1*$^{R/R}$ mice ($t_8 = 5.74$, $p = 0.0004$) showed increased immobility in response to the tone, indicating that both were able to recall, to a different extent, the tone-shock association (Figure 5d). Therefore, *GluA1*$^{R/R}$ mice were able to recall, although weakly, the association between the tone and the foot shock and showed a mild fear response when the CS was administered, which was however not as strong as that expressed by the wild types.

The contextual component of the fear association was tested 48 h after acquisition. *GluA1*$^{R/R}$ mice also showed lower immobility levels than controls during this test (Figure 5e; genotype effect $F_{1,16} = 12.06$, $p = 0.003$; time effect and interaction not significant; post hoc t-tests are shown in Appendix Table 14). This phenotype was evident, when comparing the total percent of immobility during the context re-exposure for both groups (Figure 5f). The immobility levels of *GluA1*$^{R/R}$ during the context retrieval test were not different from the response during the initial 6 min baseline of the acquisition phase ($t_8 = 1.57$, $p = 0.15$), whereas the controls did increase the fear response during the context retrieval ($t_8 = 5.56$, $p = 0.0005$). This indicates that *GluA1*$^{R/R}$ mice showed a strong impairment in the retrieval of the contextual component of a fear memory.

In summary, when the GluA1 subunit is mutated, mice show an abnormal acute response to noxious stimuli during the acquisition of fear conditioning, but they are able to recall the learned tone-shock association 24 h later. However, the association between the context and the foot shock could not be retrieved 48 h later.

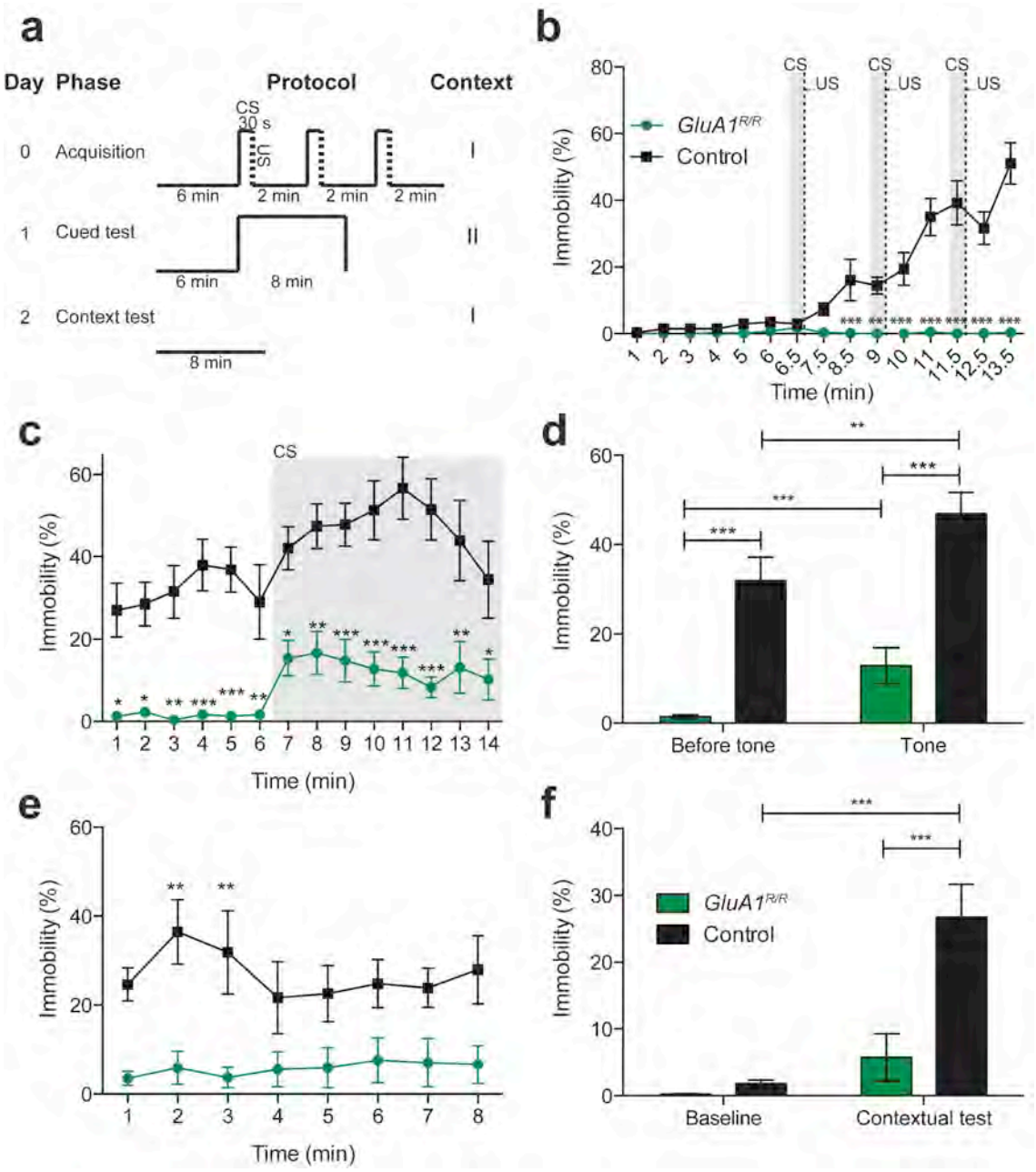

Figure 5. Fear conditioning of *GluA1*$^{R/R}$ mutant mice

a, Schematic representation of the fear conditioning protocol, which consisted of a three-shock acquisition protocol and one cued and one contextual retrieval tests. The elevated segments indicate tone presentation (CS) and the dotted lines represent the 2 s 0.4 mA foot shock (US). The cued retrieval test was performed 1 day later, followed by the context retrieval test 2 days after acquisition. The two different contexts used are

indicated as I and II. **b,** Percentage of immobility during the acquisition phase for *GluA*$^{R/R}$ and controls. The gray area represents the CS/US presentation. **c,** Immobility during the cued test 24 h after acquisition. The gray area represents CS presentation. **d,** Comparison of total immobility in percent during the initial 6 min period and the 8 min tone presentation. Immobility was significantly different between the genotypes before and during the tone, and both *GluA1*$^{R/R}$ and wild-type mice showed learning of the fear association, when comparing the fear response before and during the tone. **e,** Contextual retrieval test by re-exposure to the acquisition context with a 1-min time bin. **f,** Total immobility response during the context test revealing a retrieval impairment in *GluA1*$^{R/R}$ mice and normal learning in controls. *$p < 0.05$, **$p < 0.01$, ***$p < 0.001$.

2.2.2. *GluA1*$^{-/-}$ mice in fear conditioning

To further investigate the role of GluA1-containing AMPARs in the dynamics of emotional fear, global GluA1 knockout mice (Zamanillo et al., 1999) were tested in the Pavlovian fear-conditioning paradigm. These mice also exhibit an abnormal hyperactive behavior in the open-field test (Zamanillo et al., 1999), in a way similar to *GluA1*$^{R/R}$ mice.

GluA1$^{-/-}$ (n = 8, age 43 ± 3.2 weeks) and wild-type littermates (n = 9, age 46 ± 3.6 weeks) were trained in the same fear conditioning protocol used for *GluA3*$^{-/-}$ mice in section 2.1.3 (Figure 6a). The fear response was quantified as immobility level from infrared-sensor readings (movement of less than 1 cm/s). Both groups had a similar baseline activity during the first 6 min of the acquisition protocol. During this phase, *GluA1*$^{-/-}$ mice consistently exhibited close-to-zero immobility levels and there was no increase in the fear response after each tone-shock pairing (Figure 6b). Two-way repeated measures ANOVA showed a significant effect of genotype ($F_{1,15} = 120.3$, $p < 0.0001$), time ($F_{14,15} = 23.55$, $p < 0.0001$) and interaction ($F_{14,15} = 23.05$, $p < 0.0001$). Post hoc comparisons revealed that the wild types moved less than *GluA1*$^{-/-}$ mice after the first tone-shock pairing until the end of the protocol (Appendix Table 15). These results are in strong parallel with the behavior of *GluA1*$^{R/R}$ mice in the acquisition of fear conditioning, showing a clear impairment in the ability to evidence fear after an acute noxious stimulus.

GluA1$^{-/-}$ mice further showed a strong impairment in the retrieval of the cued fear memory 24 h after the acquisition (Figure 6c). During this cued test, the immobility response of these mice was significantly different compared

with that of wild types (two-way repeated-measures ANOVA: genotype $F_{1,15}$ = 6.802, $p < 0.0001$; time $F_{13,15}$ = 10.08, $p < 0.0001$; interaction $F_{13,15}$ = 5.151, $p < 0.0001$). Post hoc tests revealed that the differences were almost exclusively limited to the period of tone re-exposure (Appendix Table 15).

In order to test whether *GluA1*$^{-/-}$ mice were able to learn to associate the tone with a noxious stimulus, even to a lower degree, the total immobility in the cued test before the tone and during the tone presentation was compared (Figure 6d). A significant effect of the genotype ($F_{1,30}$ = 63.12, $p < 0.0001$), time ($F_{1,30}$ = 23.30, $p < 0.0001$) and interaction ($F_{1,30}$ = 11.43, $p = 0.002$) was found. Post hoc comparisons revealed that wild types moved significantly less than *GluA1*$^{-/-}$ both before and during the tone presentation (Appendix Table 16). However, both groups of mice showed learning of the tone-shock association, as indicated by the significant tone-dependent increased immobility in both cases.

In summary, *GluA1*$^{-/-}$ mice were able to learn a cued fear memory, but the weakness of the association indicates a strong impairment in the retrieval of cued memory. This phenotype is very similar to the one observed in *GluA1*$^{R/R}$ mice.

In the extinction protocol for the cued association, *GluA1*$^{-/-}$ mice reduced their immobility response to the tone along the four extinction trials (Figure 6e; Appendix Table 17). Already on E2, *GluA1*$^{-/-}$ mice had similar immobility levels before and during the tone, and on the subsequent extinction trials, immobility was even slightly higher before the tone. This indicates that the weak cued memory formed by *GluA1*$^{-/-}$ was readily extinguished after one trial, in contrast to wild types, which needed four extinction trials to bring their immobility levels to the tone back to the baseline.

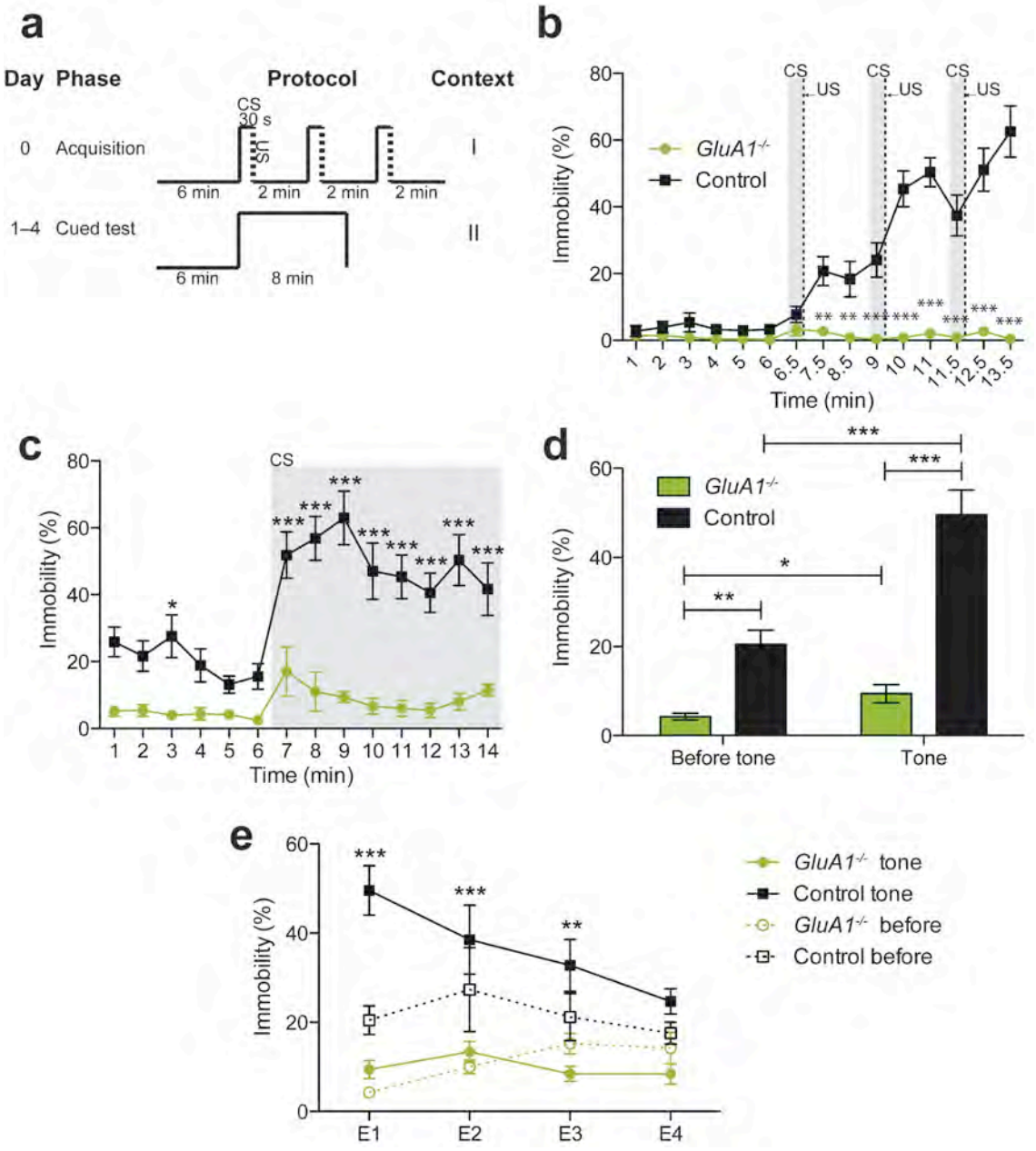

Figure 6. Cued fear conditioning and extinction in *GluA1*$^{-/-}$ mice

a, Schematic representation of the fear conditioning protocol consisting of a three-shock acquisition and four extinction tests each every 24 h. The elevated segments indicate tone presentation and the dotted lines represent the 2 s 0.4 mA foot shock. Two different contexts were used, indicated as I and II. **b**, Acquisition phase: *GluA1*$^{-/-}$ mice started at a similar baseline activity as wild types. *GluA1*$^{-/-}$ mice failed to increase immobility after each tone-shock pairing. The gray area represents each CS/US presentation. **c,** Cued test 24 h after acquisition. *GluA1*$^{-/-}$ mice had a weak increase in immobility to the tone re-exposure compared with controls. The gray area represents tone presentation. **d**, Comparison of total immobility during the initial 6 min period and the 8 min tone presentation. Immobility was lower for *GluA1*$^{-/-}$ mice both before the tone, and during tone presentation, compared with wild types. Both groups of mice showed learning of the fear association, as indicated by the significantly increased immobility response after the tone was presented. **e,** Immobility levels during the extinction trials. Immobility before the tone (dotted line) remained constant during the

extinction protocol for both genotypes. *GluA1*$^{-/-}$ mice showed a rapid extinction of their weak cued fear memory. Error bars, s.e.m. *$p < 0.05$, **$p < 0.01$, ***$p < 0.001$.

2.2.3. *GluA1*$^{-/-}$ mice in passive avoidance

Two weeks after the extinction protocol for the fear memory, the same cohort of mice (*GluA1*$^{-/-}$ n = 8, age 46 ± 3.2 weeks; wild-type littermates n = 9, age 49 ± 3.6 weeks) was tested in the passive avoidance paradigm. The same protocol was used as in section 2.1.4, with the difference that the habituation and acquisition phases took place on the same day. Retrieval tests were performed 24 h, 7 d and 23 d after acquisition. The data and statistical analysis are shown in Appendix Table 18.

No differences were found between the latency to leave the open platform and enter the dark compartment during the acquisition before the shock administration for *GluA1*$^{-/-}$ and wild-type mice (Figure 7a). This latency to enter was also not significantly different during the retention tests 24 h and 7 d after initial acquisition. However, the latency to enter was significantly higher in *GluA1*$^{-/-}$ mice, when tested 23 d after acquisition. Whereas wild-type mice showed decreased latencies with the passage of time, GluA1 knockouts continued to show a strong delay to enter the dark chamber.

Intra-genotype comparisons of the latency to enter the dark compartment at different time points revealed that wild-type mice strongly retained the memory for up to 23 d after acquisition (Figure 7b), as well as *GluA1*$^{-/-}$ mice (Figure 7c). But in the case of the knockouts, the strength of the retention gradually increased with the passage of time, being highest at the later time point of 23 d. In summary, *GluA1*$^{-/-}$ mice formed a stronger association in the passive avoidance test than did wild-type controls and were able to maintain this memory strength for a longer period of time.

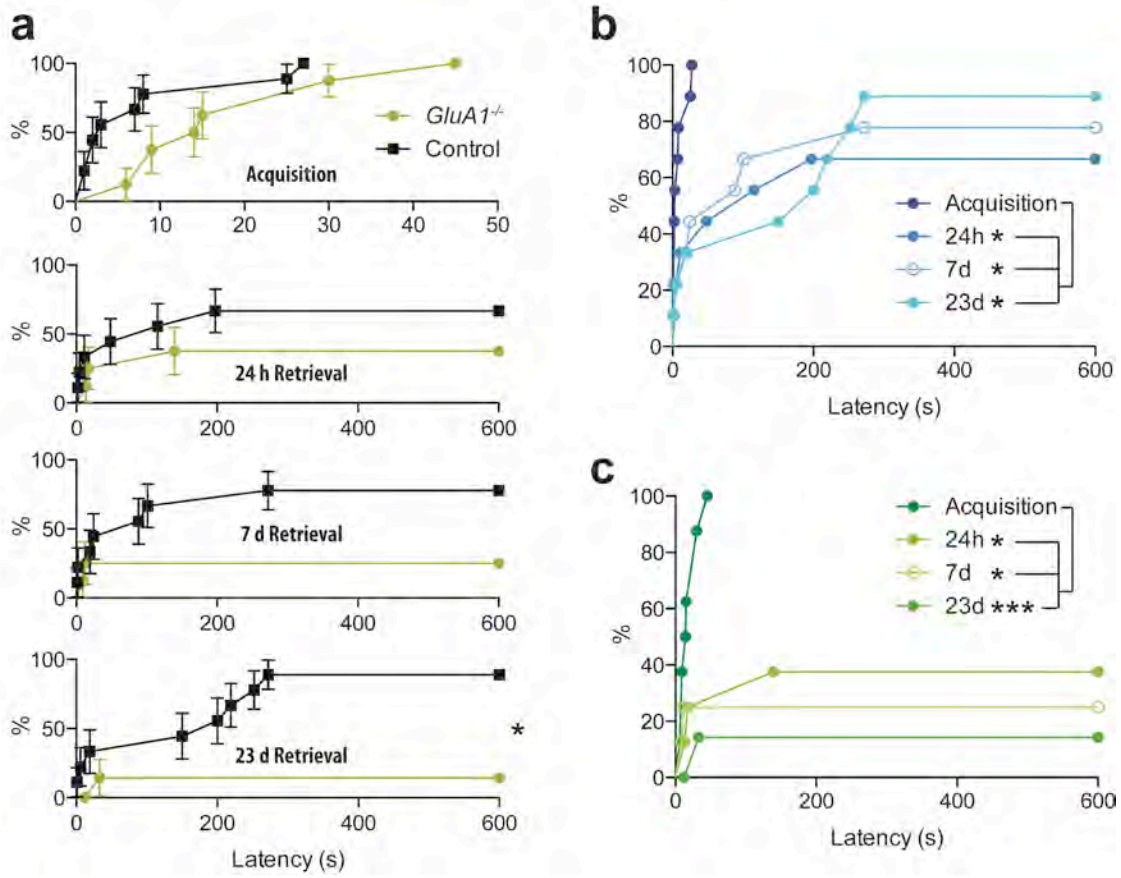

Figure 7. Long-term retrieval of passive-avoidance memory in *GluA1*$^{-/-}$ mice
a, Latency to enter the dark compartment during the acquisition phase (before receiving an electric shock) and during subsequent retrieval tests 24 h, 7 d and 23 d later. The Y-axis shows the percentage of mice that entered the dark compartment within the latency indicated in the X-axis. The time limit for the experiment was 600 s. A left-shifted curve indicates immediate entrance of most of the mice into the dark chamber. A right-shifted curve indicates that mice took a longer time before entering the dark. Before the shock, all mice immediately entered the dark chamber (latency under 15 s). Both *GluA1*$^{-/-}$ and wild types exhibited similar retention of the fear memory 24 h and 7 d later. At 23 d, *GluA1*$^{-/-}$ showed significantly stronger retention of the fear association. **b,** Side-by-side comparison of the latency to enter the dark chamber in wild-type mice, during the different phases of testing from the acquisition to the 67 d retrieval test. Wild types retained the fear association of entering the dark chamber for up to 23 d. **c,** Same comparison as in (b) for *GluA1*$^{-/-}$ mice. These mice strongly retained the fear memory for up to 23 d. In (b) and (c), s.e.m. bars were omitted for clarity. *$p < 0.05$, **$p < 0.01$, ***$p < 0.001$.

2.3. *Long-term passive avoidance in* GluA1$^{-/-}$ *and* GluA3$^{-/-}$ *mice*

In order to analyze the performance of *GluA1*$^{-/-}$ and *GluA3*$^{-/-}$ mice in the passive-avoidance test on a long-term basis, a second cohort of mice was trained, which included animals deficient for each of these subunits, as well as their respective wild-type littermates (Figure 8a).

Four groups of age-matched mice were analyzed: *GluA1*$^{-/-}$ (knockouts, n = 8, age 17 ± 2.02 weeks), *GluA1*$^{+/+}$ (wild types, n = 8, age 15 ± 0.18 w), *GluA3*$^{-/-}$ (knockouts, n = 8, age 16 ± 0.35 w) and *GluA3*$^{+/+}$ (wild types, n = 8, age 16 ± 0.35 w). All subjects were male, except for one *GluA1*$^{-/-}$ female. *GluA1*$^{-/-}$ and *GluA1*$^{+/+}$ mice belonged to the same colony and were littermates. *GluA3*$^{-/-}$ and *GluA3*$^{+/+}$ mice were also littermates and belonged to a different colony.

The same protocol was used as in section 2.1.4, but a slightly higher shock intensity (0.5 mA, 2 s) was applied. The median of the latencies to enter the dark compartment during the different experimental phases is presented in Appendix Table 19. No significant statistical differences were found between the two groups of wild-type mice *GluA1*$^{+/+}$ and *GluA3*$^{+/+}$ in any of the tests (Appendix Table 20). Thus, for the sake of clarity, these groups were merged for further analysis as wild-type controls. A statistical comparison between the knockout groups and the controls is shown in Appendix Table 21.

During the acquisition phase, all mice entered the dark compartment within 1 min, indicating that there was enough motivational drive to escape from the open platform and that the dark chamber itself did not have a particularly aversive component. *GluA3*$^{-/-}$ mice did not differ from the controls during the acquisition, and immediately entered the dark chamber. *GluA1*$^{-/-}$ mice took significantly longer than the controls to enter the dark compartment, although the electric shock had not been administered yet. However, the real significance of this difference on the further outcome of the experiment is questionable.

Twenty-four hours after the electric shock administration, mice were placed again on the open platform for a retrieval test. At this time point, all experimental groups performed similarly and no significant differences were found. In all cases, the latency to enter the dark compartment was significantly

higher than during the acquisition phase, indicating that the mice were able to learn that the entry into the dark chamber is associated with a noxious stimulus.

When tested 7 d later, wild-type mice still exhibited a higher latency to enter the dark compartment than during the acquisition, showing that they were still able to recall the fear association. However, the strength of the fear response was significantly lower for wild types than for GluA1$^{-/-}$ and GluA3$^{-/-}$ mice, as indicated by the higher latency exhibited by the knockouts at this time point. A similar recall pattern was observed at later time points of 37 d and 67 d.

At 161 d after acquisition, the latency to enter was no longer significantly different between *GluA3*$^{-/-}$ and wild-type mice. *GluA1*$^{-/-}$ mice continued to show a higher latency compared to the controls. The latency to enter for the wild types decreased compared to the 67 d test, but it continued to be significantly higher than during the acquisition, showing that these mice were still able to recall the fear association.

For all three groups of mice, there was a continuous increase in the fear response, measured by the latency, during the 24 h, 7 d and 37 d tests. At 67 d, the latency was similar to that of the 37 d time point. Finally, at the latest time point of 161 d, the fear response of the mice decreased back to levels similar to those at 24 h (Figure 8b,c,d).

In summary, it was confirmed that *GluA1*$^{-/-}$ and *GluA3*$^{-/-}$ mice are able to strongly recall a passive avoidance in a more intense fashion for a longer period of time than wild-type littermates.

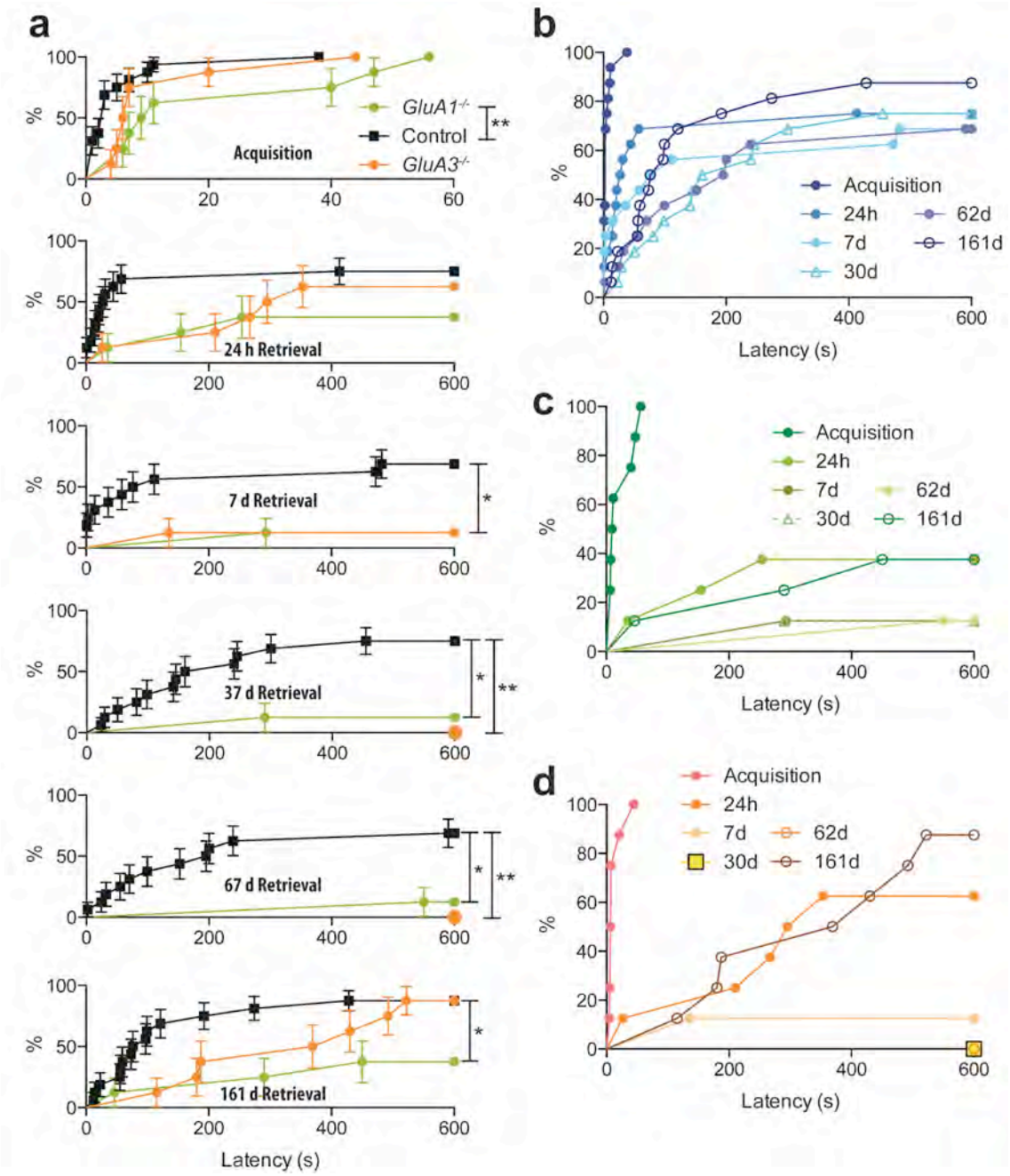

Figure 8. Passive avoidance in *GluA1*$^{-/-}$ and *GluA3*$^{-/-}$ mice

a, Latency to enter the dark compartment during the acquisition phase (before receiving an electric shock) and during subsequent retrieval tests 24 h, 7 d, 37 d, 67 d, and 161 d later. The Y-axis shows the percentage of mice that entered the dark compartment within the latency indicated in the X-axis. The time limit for the experiment was 600 s. A left-shifted curve indicates immediate entrance of most of the mice into the dark chamber. A right-shifted curve indicates that mice took a longer time before entering the dark. Before the shock, all mice immediately entered the dark chamber (latency under 60 s). *GluA1*$^{-/-}$, *GluA3*$^{-/-}$ and wild types exhibited similar retention of the fear memory 24 h later. At further time points of 7 d, 37 d and 67 d, *GluA1*$^{-/-}$ and *GluA3*$^{-/-}$ showed significantly stronger retention of the fear association. At 161 d, *GluA3*$^{-/-}$ mice were no longer different from the controls, and only *GluA1*$^{-/-}$ still exhibited a strong recall of the fear association. **b,** Side-by-side comparison of the latency to enter the dark chamber in wild-type mice, during the different phases of

testing from the acquisition to the 161 d retrieval test. **c,** Same comparison as in (b) for *GluA3*$^{-/-}$ mice. These mice strongly retained the fear memory for up to 161 d. **d,** Same comparison as in (b) for *GluA3*$^{-/-}$ mice. These mice strongly retained the avoidance memory for up to 67 d. In (b), (c) and (d), s.e.m. bars were omitted for clarity. *$p < 0.05$, **$p < 0.01$, ***$p < 0.001$.

2.4. *Long-term fear conditioning in* GluA3$^{-/-}$ *and* GluA1$^{+/-}$ *mice*

In order to find out whether the enhanced long-term retrieval of passive avoidance memories observed in *GluA3*$^{-/-}$ mice could also be observed in a different emotional memory paradigm, I tested these mice in Pavlovian fear conditioning.

A cohort of 37 littermate males corresponding to four different genotypes was used (Table 1). All mice underwent the standard three-shock fear conditioning acquisition protocol (Figure 9a) and were tested for retrieval of cued fear at 24 h or 31 d, depending on the group.

Table 1. Cohort properties for long-term retrieval analysis of fear conditioning. Genotype, sample size, age at the start of the experiment and cued retrieval time points.

Group name	Genotype	*n*	Age (w)	Cued test
***GluA3*$^{-/-}$**	*GluA3*$^{-/-}$ *A1*$^{+/+}$	13	19 ± 0.26	31 d
Control	*GluA3*$^{+/+}$ *A1*$^{+/+}$	4	18.5 ± 0.29	31 d
***GluA3*$^{-/-}$ *A1*$^{+/-}$**	*GluA3*$^{-/-}$ *A1*$^{+/-}$	13	19 ± 0.08	24 h and 31 d
***GluA1*$^{+/-}$**	*GluA3*$^{+/+}$ *A1*$^{+/-}$	7	18 ± 0.28	24 h and 31 d

During the acquisition phase, the baseline activity for all groups was similar (**Figure 9**b). All mice showed increased immobility after each tone-shock pairing. Repeated measures two-way ANOVA revealed a significant global effect of genotype ($F_{3,33} = 10.97$, $p < 0.0001$), time ($F_{14,33} = 51.29$, $p < 0.0001$) and interaction ($F_{42,33} = 2.947$, $p < 0.0001$). Post hoc comparisons showed that *GluA3*$^{-/-}$*A1*$^{+/-}$ and *GluA1*$^{+/-}$ mice did not differ from each other, but moved less than the *GluA3*$^{-/-}$ and controls (

Appendix Table 22). GluA3$^{-/-}$ and control mice did not show immobility levels significantly differently from each other.

To show that the mice were able to learn the tone-shock association, a cued retrieval test was performed 24 h after acquisition for *GluA3*$^{-/-}$*A1*$^{+/-}$ and

GluA1$^{+/-}$ mice (Figure 9c). Both groups of mice showed increased immobility levels in response to the tone. Furthermore, repeated-measures two-way ANOVA revealed a significant global effect of genotype ($F_{1,18}$ = 9.624, $p < 0.0061$), time ($F_{13,18}$ = 14.76, $p < 0.0001$), but not their interaction ($F_{13,18}$ = 0.5415, p = 0.8970). However, post hoc comparisons did not allow determining at what time point these differences occurred (Appendix Table 23). The same mice were tested again at a later time point of 31 d (Figure 9d). Again, the genotype had a significant effect on the immobility levels ($F_{1,18}$ = 5.082, $p < 0.0001$), as did time ($F_{13,18}$ = 5.277, $p < 0.0001$) and their interaction ($F_{13,18}$ = 2.313, p = 0.0067). In summary, both at 24 h and 31 d, *GluA3*$^{-/-}$*A1*$^{+/-}$ moved less than *GluA1*$^{+/-}$ mice.

To avoid the possibility of interference of the first cued test (24 h) on the retrieval in the second cued test (31 d), *GluA3*$^{-/-}$ and control mice were only tested at the 31 d time point (Figure 9e). Repeated-measures two-way ANOVA showed no global significant effect of genotype ($F_{1,15}$ = 2.341, p = 0.1468), but only of time ($F_{13,15}$ = 3.851, $p < 0.0001$) and their interaction ($F_{13,15}$ = 2.398, p = 0.0052).

Due to the variability observed between heterozygous mice for GluA1 and wild-type mice, a comparison of the total immobility levels before and during the tone presentation was made (Figure 9f), revealing a significant effect of genotype ($F_{5,51}$ = 3.027, $p < 0.0001$), tone ($F_{1,51}$ = 45.12, p = 0.0181) and their interaction ($F_{5,51}$ = 2.470, p = 0.0444) by two-way repeated-measures ANOVA. Post hoc tests comparing the total immobility levels before and during the tone revealed in which tests there was significant recall of the tone-shock association (Appendix Table 24). During the 24 h test, both tested groups showed significant recall of the cued association. However, on the long-term at 31 d, only *GluA3*$^{-/-}$*A1*$^{+/-}$ mice robustly recalled this fear memory, whereas *GluA1*$^{+/-}$ did not (Figure 9f). Similarly, the control group of mice did not significantly increase its immobility in response to the tone at 31 d, showing an impaired recall of the fear association. On the other hand, *GluA3*$^{-/-}$ mice were still able to robustly recall the tone-shock memory even after 31 d.

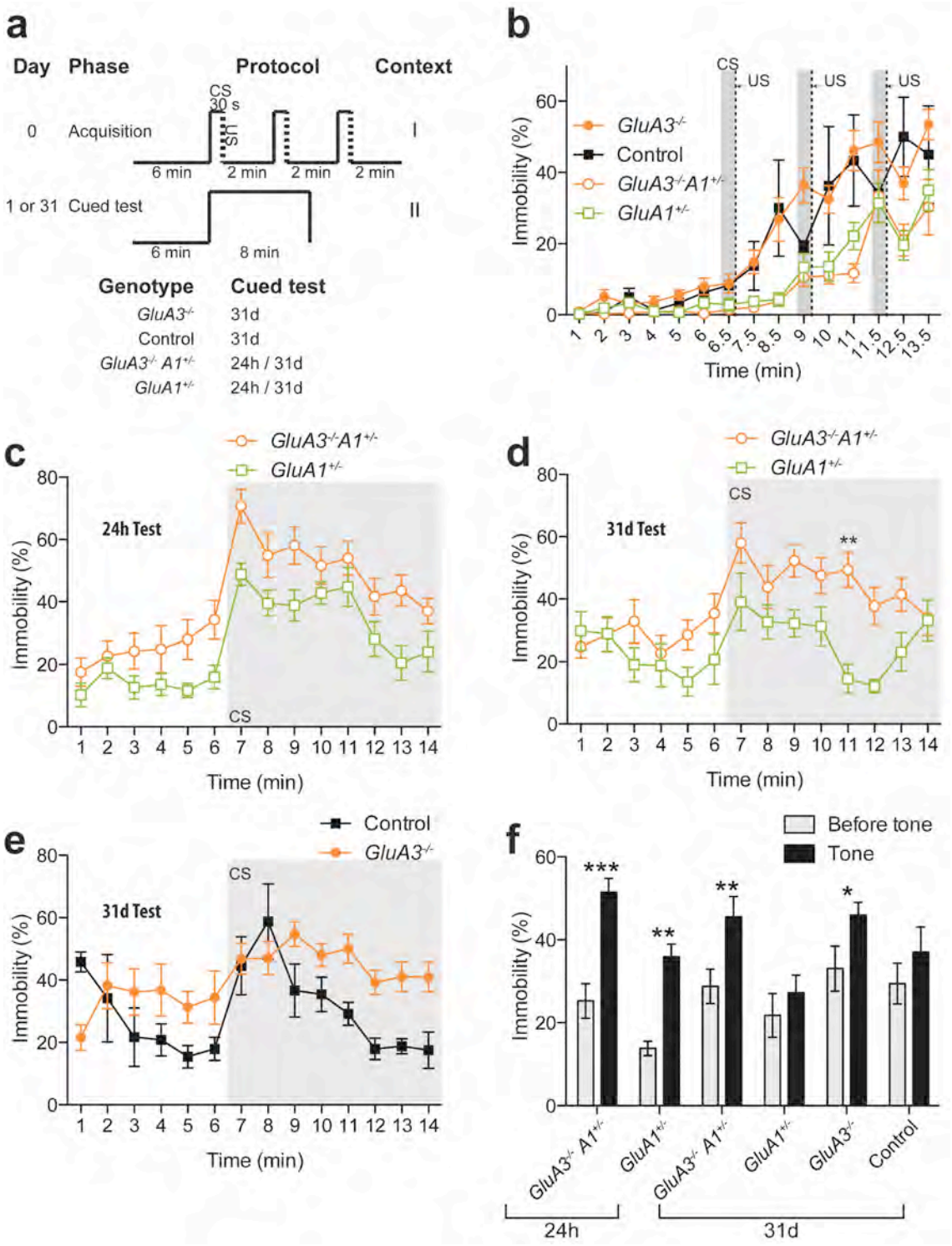

Figure 9. Long-term retrieval of fear conditioning in *GluA3*$^{-/-}$ and *GluA1*$^{+/-}$ mice
a, Schematic representation of the fear conditioning protocol consisting of a three-shock acquisition and either one or two cued tests. The elevated segments indicate tone presentation and the dotted lines represent the 2 s 0.4 mA foot shock. *GluA3*$^{-/-}$ and control mice were tested for retrieval of the cued memory 31 d after acquisition. *GluA3*$^{-/-}$*A1*$^{+/-}$ and *GluA1*$^{+/-}$ mice were tested at two time points: 24 h and 31 d after acquisition. Two different contexts were used as indicated by I and II. **b**, Acquisition phase: All mice started with a similar baseline activity. *GluA3*$^{-/-}$*A1*$^{+/-}$ and *GluA1*$^{+/-}$ had a globally lower immobility response after each tone-shock pairing. *GluA3*$^{-/-}$ mice showed slightly higher immobility levels than the controls. The gray area represents

each CS/US presentation. **c,** Cued test 24 h after acquisition. *GluA3$^{-/-}$A1$^{+/-}$* moved slightly less than *GluA1$^{+/-}$* mice before and during the CS. A similar comparison was found on the 31 d cued test (**d).** The gray area represents tone presentation. **e**, Cued test 31 d after acquisition: *GluA3$^{-/-}$* mice had slightly higher immobility levels than the controls at this time point. **f,** Comparison of total immobility during the initial 6 min period and the 8 min tone presentation in the 24 h and 31 d retrieval tests. At 24 h, both *GluA3$^{-/-}$A1$^{+/-}$* and *GluA1$^{+/-}$* were able to recall the tone-shock association, whereas only *GluA3$^{-/-}$A1$^{+/-}$* showed significant recall in the 31 d test. Similarly, *GluA3$^{-/-}$*, but not control mice, moved significantly more in response to the tone during the 31 d retrieval test. $*p < 0.05$, $**p < 0.01$, $***p < 0.001$.

2.5. *Amygdala neuron silencing by rAAV-mediated TTLC expression*

The amygdaloid complex is an essential structure for the learning of emotionally relevant information. Genetic manipulation of the amygdala is not practicable through classical transgenic methods in a specific manner because of the lack of specific promoters that target gene expression in this brain region. Therefore, a rAAV-mediated approach was taken to deliver genes into the amygdala by stereotaxic injection. First, behavioral alterations were tested after expression of TTLC in amygdala neurons, as a proof-of-principle experiment for the applicability of the rAAV systems to modify behavior.

2.5.1. Injection of rAAVs for TTLC expression in the amygdala

One cohort of littermate male C57Bl/6N mice was used in these experiments. One group was injected bilaterally into the amygdala with a 1:2 mixture of rAAV-syn-tTA and rAAV-P_{tetbi}-TTLC-tdTomato (TTLC, n = 6, age 10 weeks; Figure 10a; Virus sources Section 7.5.4). A second group of uninjected males was used as a control (n = 4; age 10 weeks). The neuron-specific human synapsin promoter (syn) drives expression of tTA, which binds to the bidirectional tetracycline-activated promoter (P_{tetbi}) and in turn drives simultaneous expression of TTLC and the red-fluorescent protein tandem-dimer tomato (tdTomato).

Post-mortem histological analysis of the cohort revealed that tdTomato expression in neurons of the amygdala nuclei (Figure 10b) could be used to determine the area of infection by the virus. Infected neurons were found in the

lateral amygdala, the basal amygdala, the central amygdala and part of the piriform cortex (Figure 10c).

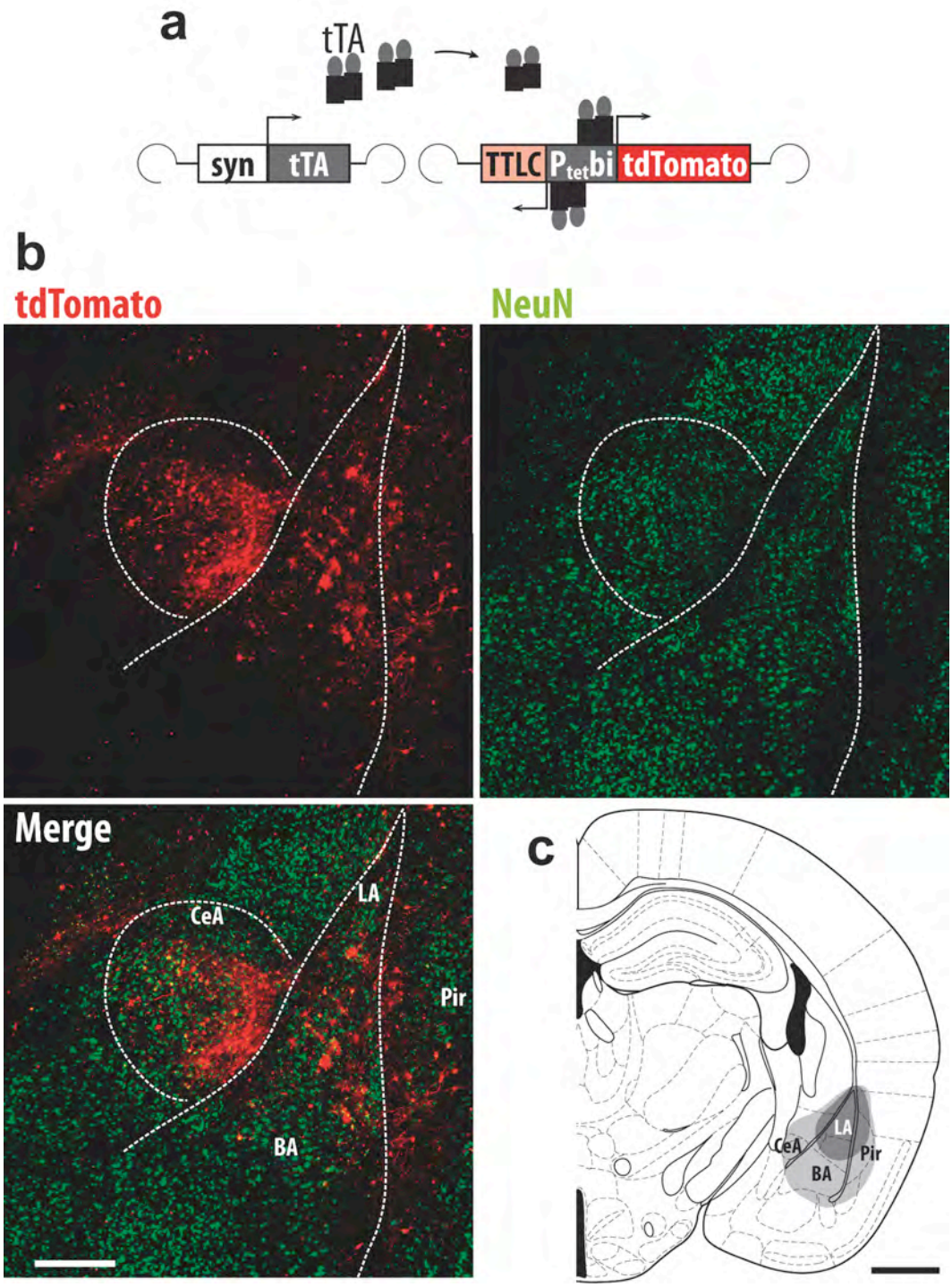

Figure 10. Expression of tdTomato in mice injected with rAAV for expression of TTLC for amygdala neuron silencing

a, Schematic representation of the viral system for TTLC expression in neurons. The neuron-specific human synapsin promoter (syn) drives expression of the tetracycline trans-activator (tTA), which binds to the bidirectional tetracycline-activated promoter (P_{tetbi}) and in turn drives simultaneous expression of TTLC and the red-fluorescent protein tdTomato. **b,** Immunostaining against NeuN shows infected neurons in the lateral amygdala (LA), basal amygdala (BA), central amygdala (CeA) and part of the

piriform cortex (Pir). Scale bar, 200 μm. **c,** Extent of infection in the cohort of mice analyzed. The smallest area of infection is shown in dark gray, the largest in light gray. Scale bar, 1 mm.

2.5.2. Exploratory behavior after amygdala neuron silencing

Twenty days after bilateral rAAV injection into the amygdala, mice were allowed to explore the open-field arena during 10 min. There were no significant differences in the exploratory behavior of amygdala-silenced mice, measured as the total distance traveled in the open-field arena (Appendix Table 25; Figure 11a). The total distance decreased significantly with time indicating normal habituation to the novel environment (repeated-measures ANOVA, $F_{9,8} = 5.441$, $p < 0.0001$). The virus injection had no significant effect ($F_{1,8} = 0.0006$, $p = 0.9809$) nor did the interaction of these two factors ($F_{9,8} = 1.861$, $p = 0.0719$).

Mice were also tested in the light-dark preference test, 35 d after rAAV injection, by measuring the time spent in each of two symmetrical compartments communicated by a small door (~4 cm wide), one brightly-lit, the other dark and covered. Both the TTLC and control groups exhibited a similar preference for the dark compartment (Appendix Table 25), indicating that the rAAV injection and silencing of neurons did not cause higher levels of anxiety. This was indicated both by the percentage of time spent in the dark (Figure 11b) or the number of entries into the dark compartment (Figure 11c).

Consistent with these observations, the elevated plus maze produced similar results 36 d after rAAV injection (Appendix Table 25). In this test, mice were placed on an elevated plus-shaped maze, with two opposed arms with flanking walls that protect mice from falling, and two open arms without walls and the time spent in both of these types of arms was measured. No significant differences were observed between the amygdala-silenced and the control groups (Figure 11d).

Together, these results show that rAAV-injected mice show similar general exploration behavior and anxiety levels and, therefore, can be used in order to assess memory impairments by amygdala silencing in the following experiments.

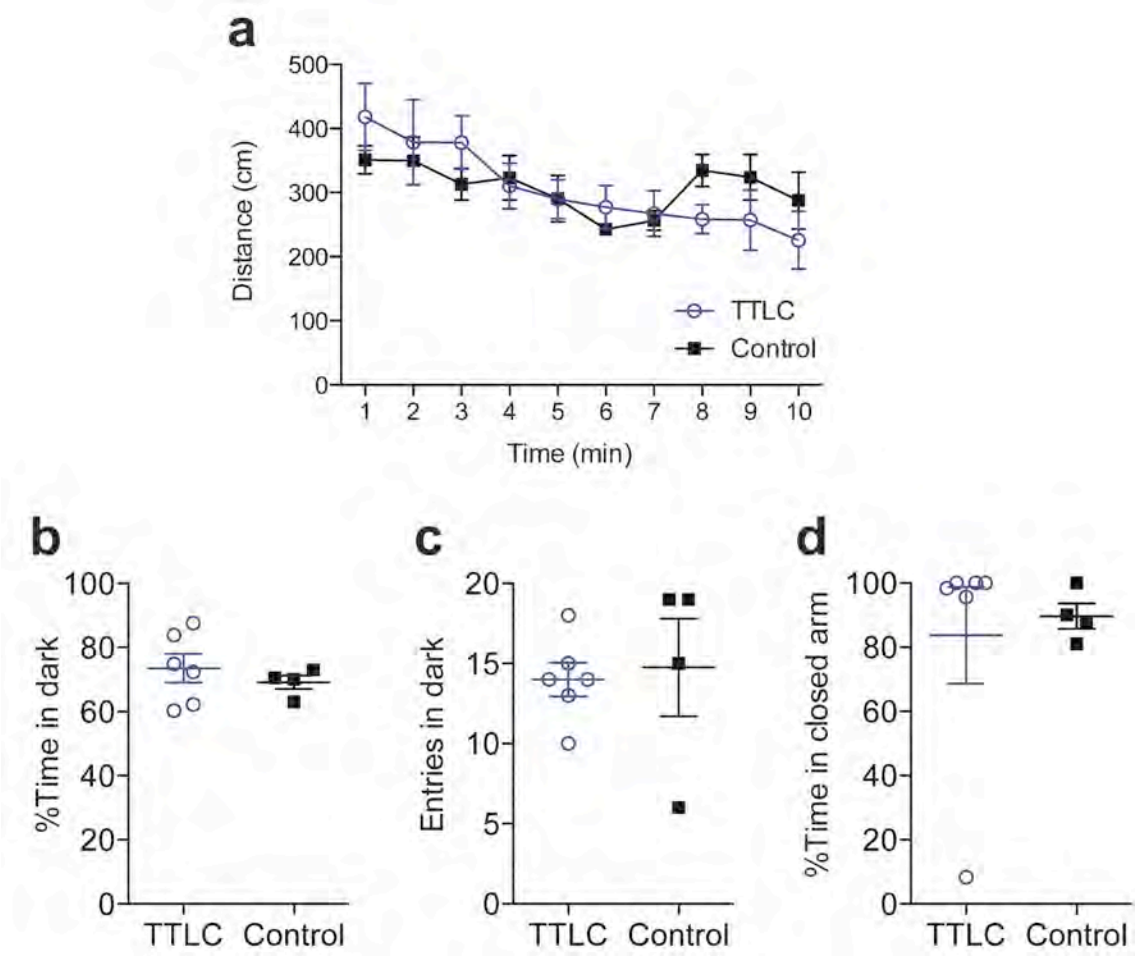

Figure 11. General exploratory behavior and anxiety in amygdala-silenced mice
a, Total distance traveled in the open field arena was not different for TTLC and control mice during a 10 min period. **b,c,** Light dark test: no significant difference was found between TTLC and control mice neither for the amount of time spent in the dark chamber (**b**), nor for the number of entries into the dark compartment (**c**). **d,** Elevated plus-maze: TTLC and control mice did not differ significantly in the amount of time spent in the closed arm.

2.5.3. Fear conditioning after amygdala neuron silencing

Mice underwent acquisition of the fear-conditioning paradigm 42 d after rAAV injection (n = 10, age 16 weeks). A modified paradigm with only one tone-shock pairing was performed with this cohort of mice (Figure 12a). The acquisition phase consisted of an initial habituation phase of 2 min, followed by a tone presentation for 30 s ended by a 2 s 0.8 mA foot shock and an additional 30 s exploration. Both groups had identical baseline activity during the first 2 min (Figure 12b). After the shock administration, both amygdala-silenced and

control mice slightly increased their immobility. Two-way repeated measures ANOVA showed a significant effect of time ($F_{3,8}$ = 6.974, p = 0.0016), but not of the virus injected ($F_{1,8}$ = 0.4273, p = 0.5317) or the interaction ($F_{3,8}$ = 0.1262, p = 0.9437). This indicates that amygdala-silenced mice were able to show acute fear expression during acquisition.

After 24 h, mice were tested for retrieval of contextual fear by re-exposure to the acquisition context for 5 min (Figure 12c). Two-way repeated-measures ANOVA revealed a significant effect of time ($F_{4,8}$ = 4.205, p = 0.0076), and a trend for differences by the virus injected ($F_{1,8}$ = 4.325, p = 0.0712) and the interaction ($F_{4,8}$ = 2.014, p = 0.1161). Post hoc Bonferroni-corrected t tests showed that TTLC-expressing mice were significantly more immobile during the first minute of observation, after which both control and TTLC mice habituated to the context (Appendix Table 26). The same test was performed 41 d after acquisition, with no significant effect of the virus injected (Figure 12c; $F_{1,8}$ = 1.704, p = 0.2281), a significant effect of time ($F_{4,8}$ = 4.614, p = 0.0047), and no significant interaction ($F_{4,8}$ = 0.6447, p = 0.6347). Post hoc tests showed no significant differences during the duration of the test.

Cued fear retrieval was tested 48 h after acquisition in a different context, where mice were allowed to explore the chamber for 3 min followed by 3 min of tone presentation (Figure 12d). Two-way repeated-measures ANOVA showed that the virus injection had a significant effect on the immobility ($F_{1,8}$ = 14.57, p = 0.0051), as did time ($F_{5,8}$ = 3.012, p = 0.0212), but not their interaction ($F_{5,8}$ = 1.213, p = 0.3208). Post hoc multiple comparisons revealed that TTLC mice moved significantly less at the beginning of the test and at the beginning of the tone presentation. The same cued test was performed 42 d after acquisition and a significant effect of the virus was observed (Figure 12d; $F_{1,8}$ = 17.96, p = 0.0028), but not of time ($F_{4,8}$ = 2.054, p = 0.0916), or their interaction ($F_{3,8}$ = 1.482, p = 0.2173). Again, at 42 d, post hoc comparisons revealed that TTLC mice moved significantly less during the first minute of tone presentation. These results indicate a strong impairment in the retrieval of the cued component of the fear memory both on the short term (48 h) and on the long term (42 d).

Quantification of fear by direct observation of total freezing by a blind experimenter yielded similar results (Appendix Table 27). By this method, a more marked impairment after amygdala silencing in contextual fear (Figure 12e,f) was observed ($F_{1,8}$ = 13.12, p = 0.0068), but not of time ($F_{1,8}$ = 2.159, p = 0.1799), or their interaction ($F_{1,8}$ = 0.5854, p = 0.4662). Similarly, a marked effect of TTLC expression in the cued retrieval test (Figure 12e,g) was evidenced ($F_{1,8}$ = 15.51, p < 0.0001), as well as for the interaction of virus and time ($F_{3,8}$ = 16.62, p < 0.0001), but not of time alone ($F_{1,8}$ = 0.01060, p = 0.9193).

In summary, amygdala silencing by rAAV-mediated expression of TTLC in neurons strongly impaired short-term and long-term cued fear retrieval, and, less markedly, contextual fear retrieval.

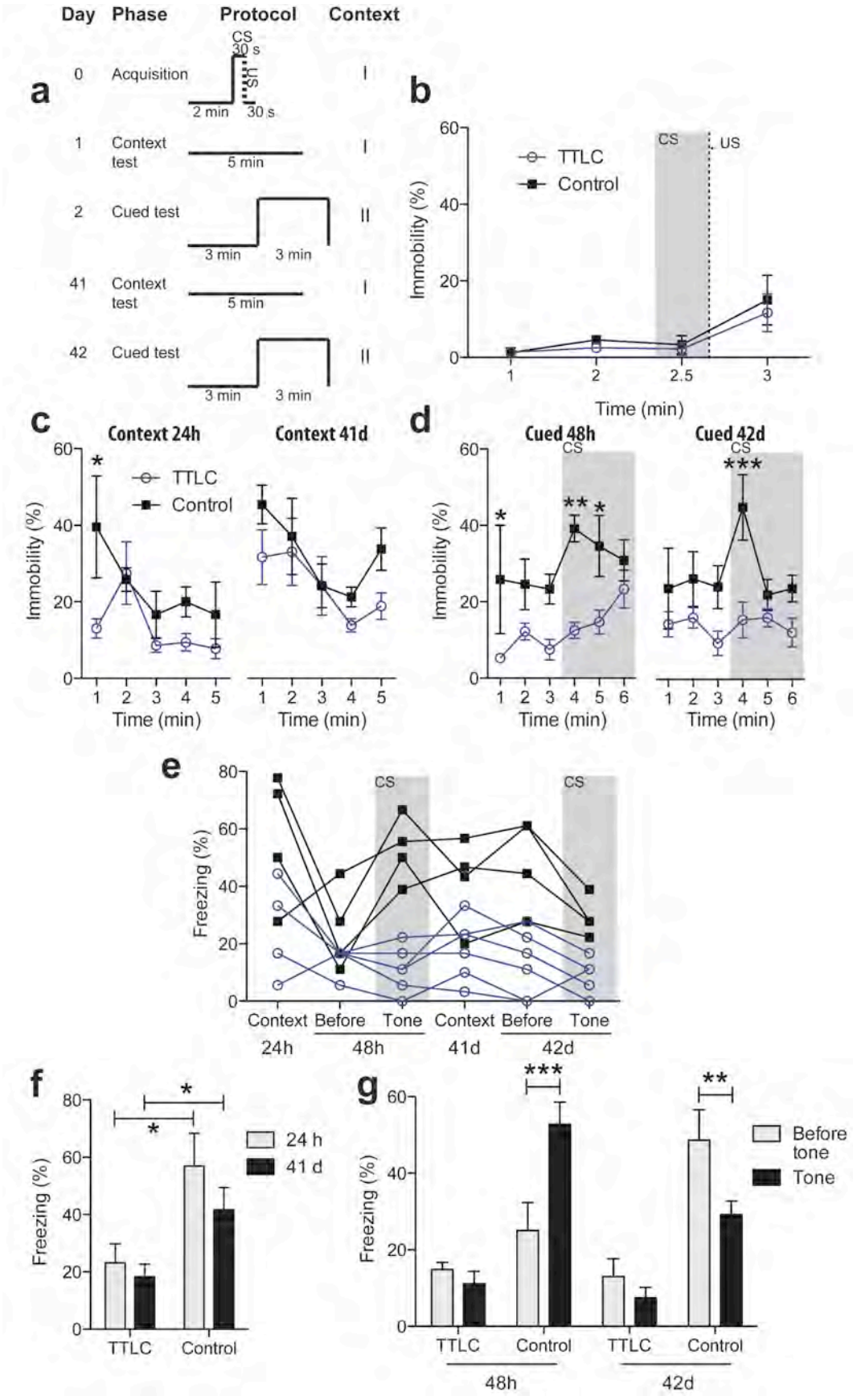

Figure 12. Fear conditioning after amygdala neuron silencing by TTLC expression
a, Schematic representation of the fear conditioning protocol consisting of a one-shock acquisition phase and contextual retrieval tests after 24 h and 41 d, as well as cued

retrieval tests after 48 h and 42 d. The elevated segments indicate tone presentation and the dotted line represents the 2 s 0.8 mA foot shock. Two different contexts were used as indicated by I and II. **b**, Acquisition phase: amygdala-silenced mice started at a similar baseline activity as controls. Both groups increased immobility after the shock. The gray area represents the period of CS presentation coupled with US. **c,** Contextual retrieval after 24 h showed an initial impairment in TTLC mice before all mice habituated. After 41 d, the contextual retrieval impairment of TTLC mice was less marked. **d,** Cued retrieval after 48 h: TTLC mice were strongly impaired when the tone was presented. The gray area represents tone presentation. After 42 d, cued fear retrieval continued to be impaired in TTLC mice. **e,** Scatter-plot for individual freezing scores during the contextual and cued retrieval tests (before and during the CS) for controls and TTLC mice. **f,** Comparison of total freezing during the 5 min of contextual test 24 h and 48 h after acquisition. Amygdala-silenced mice were impaired at both time points. **g,** Total freezing before and during the tone presentation of the cued retrieval tests at 48 h and 41 d. TTLC mice were strongly impaired at both time points. *$p < 0.05$, **$p < 0.01$, ***$p < 0.001$.

2.5.4. Passive avoidance after amygdala neuron silencing

In order to test whether the blockade of amygdala neuronal transmission also impairs types of emotional memory other than fear conditioning, the passive-avoidance paradigm was used 90 d after the last cued fear test (154 d after rAAV injection). This paradigm has also long been known to depend on intact amygdala function. Silencing of the amygdala by TTLC expression significantly impaired the ability of the mice to associate the entrance into a dark compartment with the administration of an electric foot shock (Appendix Table 28).

During the acquisition phase, both groups of mice entered the dark chamber within 30 s and there were no significant differences between them (Figure 13a,b). Once inside, mice received a 0.7 mA 2 s foot shock and remained additional 60 s in it. After 24 h, wild-type control mice had a significantly higher latency to enter the dark chamber compared to the acquisition phase, showing that these mice learned to associate the entry with a noxious stimulus (Figure 13c). In contrast, all TTLC mice but one entered the dark compartment with latency not significantly different from that during the acquisition (Figure 13c). There was one outlier TTLC mouse that did not enter the dark chamber at all. At the 24 h retention time point, the amygdala-silenced group exhibited a significantly lower latency compared to the wild-type controls, if the one TTLC

outlier was excluded. If it was included, there still was a trend, but this was not statistically significant (Figure 13c).

In summary, these data indicate that silencing of amygdala synaptic transmission by TTLC expression strongly impairs the ability to associate the entry into a particular context with a noxious stimulus in the passive avoidance. In turn, these observations support the application of rAAV-mediated modifications of gene expression in neurons of the amygdala for the study of behavioral phenotypes, which is the subject of the next section.

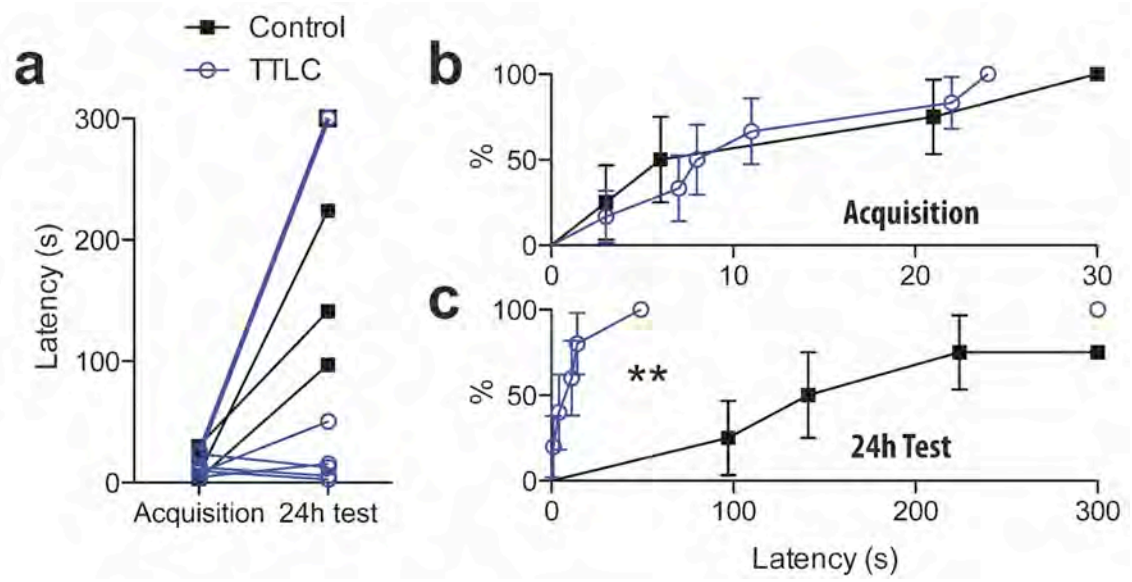

Figure 13. Passive avoidance after amygdala silencing by TTLC expression
a, Before/after display of the latency to enter the dark compartment during the acquisition and the 24 h retention test for control and TTLC mice. **b,** 'Survival' curve for the latency to enter the dark chamber during the acquisition phase, all mice entered under 30 s to avoid staying exposed on the open platform. **c,** In the retention test, 24h after the foot shock presentation, control animals exhibit a longer latency to enter. Amygdala-silenced TTLC mice do not show fear learning and remain with a significantly shorter latency to enter in the retrieval test compared to the controls. **p<0.01

2.6.Fear-conditioning retrieval after GluN1 and GluA1 deletion in the basolateral amygdala

Since the BLA is intricately linked to the acquisition and retrieval of fear conditioning, genetic modifications specific to this region are required to understand the role played by AMPARs and NMDARs in long-term retrieval processes. There are no transgenic methods available that allow restriction of gene targeting to the BLA. Therefore, stereotaxic rAAV-mediated Cre recombinase expression was used in this study to knock out the GluN1—and therefore NMDARs—and GluA1 genes in the BLA. Furthermore, temporal specificity was added to the BLA knockout by taking advantage of the doxycycline (Dox)-induced reverse tetracycline trans-activator (rtTA) system for the control of Cre recombinase expression.

2.6.1. Doxycycline-inducible recombination in the BLA of *Rosa26-lacZ^{2lox}* mice

In order to test the inducible Dox-activated rtTA system for expression of Cre recombinase in neurons, rAAVs were injected into the BLA of three heterozygous 24-week-old female mice with a Rosa-locus knock-in of beta-galactosidase with a loxP-flanked transcriptional-silencing cassette *Rosa26-lacZ$^{2lox/wt}$* (Soriano, 1999). Each mouse was injected with 500 nl of a mixture of rAAV-syn-rtTA and rAAV-P_{tetbi}-iCre-tdTomato in a 1:2 ratio (Figure 14a; Virus sources Section 7.5.4). The synapsin promoter drives neuron-specific expression of the synthetic transcription factor rtTA, which binds to the tetracycline operator elements of the P_{tetbi} bidirectional promoter in the presence of Dox. Therefore, upon Dox administration, simultaneous expression of Cre recombinase and tdTomato is induced.

Seven days after AAV injection, Dox was injected intra-peritoneally in two of the *Rosa-lacZ$^{2lox/wt}$* mice and all three mice were perfused 48 h later. The brains were sliced at 100 µm thickness and X-Gal staining was performed. Mice treated with Dox exhibited expression of beta-galactosidase in the BLA, indicating recombination of the floxed transcriptional silencing cassette by Cre recombinase (Figure 14b). Dox treatment also induced expression of tdTomato

in the BLA (Figure 14d). In the absence of Dox treatment, no recombination occurred (Figure 14c), and no tdTomato fluorescence was observed (Figure 14e). Recombination was limited to the basal part of the BLA, extending to the apical part of the lateral amygdala, but was also found in portions of the piriform cortex and the striatum. The central amygdala was not infected.

In summary, the rAAV-mediated Dox-inducible Cre/LoxP system can be used to effectively modify gene expression in neurons of the BLA in an anatomically and temporally restricted fashion.

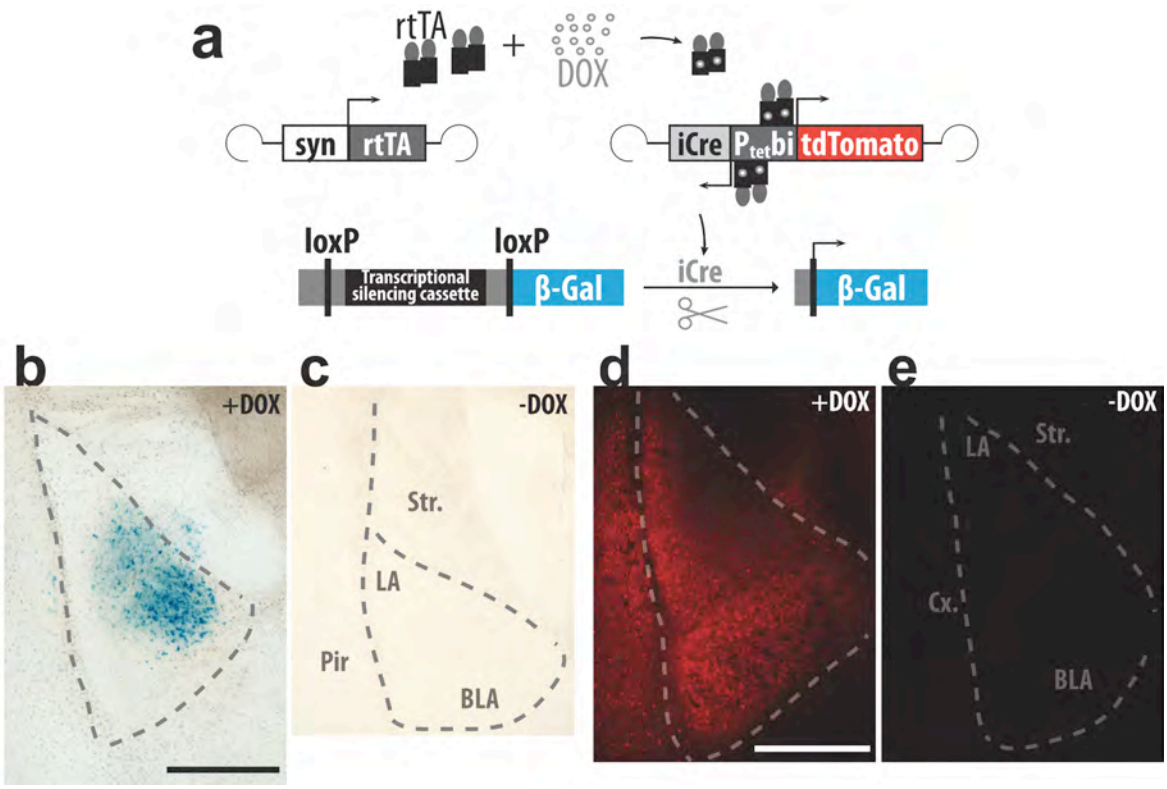

Figure 14. Recombination of loxP-flanked transcriptional silencing cassette of beta galactosidase in *Rosa26-lacZ*^{2lox} mice by Cre expression
a, Schematic representation of the rAAV mixture injected. In presence of Dox, rtTA expressed in infected neurons binds to the bidirectional P_{tetbi} promoter and induces expression of Cre recombinase and tdTomato. Cre recombines the loxP sites flanking the transcriptional silencing cassette in *Rosa26-lacZ*^{2lox} mice leading to beta-galactosidase expression. **b,** Dox-treated (+DOX) AAV-injected mice show recombination evidenced by lacZ staining in the BLA (blue). **c**, In the absence of Dox (-DOX), no lacZ staining is observed. **d,** tdTomato expression after Dox treatment. **e,** In the absence of Dox, no tdTomato fluorescence was observed. Syn: synapsin promoter. rtTA: reverse tetracycline trans activator. Dox: doxycycline. LA: lateral amygdala. Str.: striatum. BLA: basolateral amygdala. Pir: piriform cortex. Scale bars, 500 µm.

2.6.2. Retrieval of a consolidated fear-conditioning memory after GluN1 knockout in the BLA

My goal was to test the involvement of NMDARs and AMPARs in the BLA in memory processes following fear memory acquisition. For gene knockout, rAAV-mediated Cre expression in mice with loxP-flanked alleles was used. Mice carrying loxP-flanked GluN1 alleles were used as a model for NMDAR knockout, since NMDA receptors cannot be formed without the GluN1 subunit (Schüler et al., 2008). Also, GluA1 is an important subunit of AMPARs in the amygdala, but only the GluA1-containing AMPAR population is knocked-out in GluA1 floxed mice after Cre recombination (Zamanillo et al., 1999).

A detailed clarification of the terminology used for each experimental group is shown in Table 2, where 'rAAV mix' refers to the rAAV-syn-rtTA and rAAV-P_{tetbi}-iCre-tdTomato mixture in ratio 1:2 that was bilaterally injected into the amygdala in all mice. Two *GluN1*$^{\Delta BLA}$ and two *GluA1*$^{\Delta BLA}$ mice were excluded from the behavioral data analysis because only unilateral BLA infection was found in these animals after post-mortem analysis.

Table 2. Terminology for experimental groups in this study, sample size and age at the time of injection.

Genotype	Before DOX	After DOX	N	Age (w) at injection
GluN1$^{2lox/2lox}$ injected with rAAV mix	***GluN1***^{2lox}	***GluN1***$^{\Delta BLA}$	8 (originally 10)	9.4 ± 0.2
GluA1$^{2lox/2lox}$ injected with rAAV mix	***GluA1***^{2lox}	***GluA1***$^{\Delta BLA}$	5 (originally 7)	22
C57Bl/6N injected with rAAV mix	**Control**	**Control**	9	9

A series of behavioral tests was performed with the purpose of analyzing the effect of GluN1 and GluA1 knockout in the BLA *after* acquisition of a fear conditioning memory (Figure 15). The protocol was based on the idea of allowing sufficient time for rAAV infection and expression of rtTA in the infected neurons. After 26 d, acquisition of cued fear conditioning was performed and no further manipulations of the mice were carried out for 48 h, to avoid any interference with the molecular consolidation processes that occur during this time window. Two days later, short contextual and cued fear

retrieval tests were performed to assess whether all mice learned the tone-shock association. Up to this point, mice did not express Cre and therefore still had functional GluN1 or GluA1 alleles. Seven days after acquisition, treatment with Dox was started with one intra-peritoneal injection and continued with Dox in the drinking water for additional 23 d. This period of time was chosen so that enough Cre recombinase expression is achieved, recombination of the floxed genes has occurred, and loss of NMDARs and GluA1-containing AMPARs at the synapses has taken place. At this time point, GluN1 and GluA1 have been knocked out in the infected neurons of the BLA. The Dox treatment was then stopped to avoid state-dependent interference on the following behavioral tests. The effect of the gene knockout on the retrieval of the cued and contextual fear memories was assessed with a longer testing protocol.

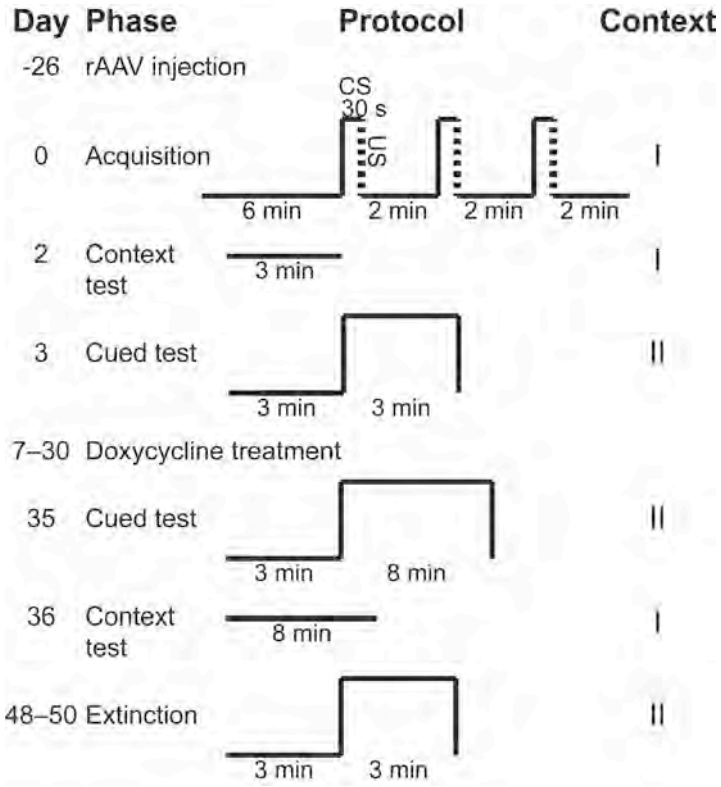

Figure 15. Fear conditioning protocol for *GluN1*$^{\Delta BLA}$ and *GluA1*$^{\Delta BLA}$ mice
A three-shock acquisition protocol was performed 26 d after rAAV injection, in which a 7.5 kHz tone (elevated line, CS) and 0.4 mA 2 s foot shock (dotted line, US) were applied. One contextual and one cued fear test were performed before the Dox treatment and after the knockout induction. Then, extinction of cued fear was conducted. A reacquisition protocol was performed to test for acute fear expression, followed by one final additional cued test. Context I refers to a transparent plexiglass chamber with metallic grid floor and ethanol smell. Context II consisted of a black plastic box with opaque plastic floor and acetic acid smell.

All three groups, *GluA1*^{2lox} (n = 5), *GluN1*^{2lox} (n = 8) and control mice (n = 9), were trained in the same fear-conditioning acquisition protocol (**Figure 16**a). The baseline mobility levels of all mice were similar during the first 6 min. All mice jumped and emitted vocalizations upon experiencing foot shocks, and gradually increased their immobility as evidenced by a significant effect of time (two-way repeated-measures ANOVA, $F_{14,19}$ = 33.59, p < 0.0001), without significant differences between the genotypes ($F_{2,19}$ = 0.9422, p = 0.4072) and no interaction ($F_{28,19}$ = 1.057, p = 0.3922). Therefore, all groups showed a similar behavior in the acquisition of a fear-conditioning memory (Appendix Table 29).

In order to test that all mice acquired the tone/shock association, a contextual and a cued retrieval test were performed three and four days later, respectively (**Figure 16**b,c; Appendix Table 30, 31). Both immobility detected by infrared sensors and freezing assessed by direct observation were analyzed. Re-exposure to the acquisition context triggered low (~20%) levels of immobility and freezing and no significant effect of genotype (**Figure 16**b; immobility, $F_{2,19}$ = 0.2960, p = 0.7472; freezing $F_{2,19}$ = 1.677, p = 0.2134). Time had a significant effect on immobility ($F_{2,19}$ = 4.374, p = 0.0195), as did the genotype-time interaction ($F_{4,19}$ = 4.113, p = 0.0072). *GluA1*^{2lox} mice had a tendency to increase immobility and freezing with time, but post hoc Bonferroni-corrected t tests did not reveal the exact origin of the differences. In general, the low freezing levels during this test indicate that the contextual component of the fear memory was not particularly strong in this cohort of mice.

In the cued retrieval test, all mice showed little freezing and immobility during the initial three minutes and their fear levels significantly increased upon tone presentation (**Figure 16**c; immobility, $F_{5,19}$ = 37.60, p < 0.0001; freezing $F_{5,19}$ = 70.62, p < 0.0001). There was no significant effect of genotype (immobility, $F_{2,19}$ = 2.014, p = 0.1610; freezing $F_{2,19}$ = 2.922, p = 0.0783) or the interaction (immobility $F_{10,19}$ = 1.259, p = 0.2647; freezing $F_{2,19}$ = 1.677, p = 0.2134). Post hoc t tests showed that immobility and freezing levels of the *GluN1*^{2lox} and control mice were not significantly different, whereas the *GluA1*^{2lox} mice tended to freeze more in response to the tone, and this trend was significant in minute 6. In summary, all three groups of mice exhibited fear in

response to re-exposure to the tone, indicating that the cued component of the fear memory was strong.

Upon the start of the 23-day Dox treatment, Cre-dependent recombination is triggered and GluN1 and GluA1 are knocked out in the rAAV infected neurons. Five days after the Dox treatment was stopped, retrieval of the cued fear memory was tested in order to assess the effect of GluN1 and GluA1 knockout in the BLA (**Figure 16**e). All groups had similar baseline freezing levels during the initial three minutes of the test and these increased in response to the tone presentation (time effect, $F_{10,19} = 22.29$, $p < 0.0001$). Two-way repeated-measures ANOVA revealed only a trend in the effect of genotype, which was not significant ($F_{2,19} = 3.223$, $p = 0.0624$). Nevertheless, there was a significant interaction between time and genotype ($F_{20,19} = 2.642$, $p = 0.0003$), indicating that the genotype of the mice did not have a general effect over the whole duration of the test, but that this effect was time-specific. Post hoc multiple comparisons with *t* tests showed that *GluN1*$^{\Delta BLA}$ failed to reach the same freezing levels as the controls during the first two minutes of the tone, after which all mice decreased their freezing response due to habituation. On the other hand, *GluA1*$^{\Delta BLA}$ were not impaired in the tone-dependent increase of freezing, and they showed decreased habituation, as evidenced by the higher freezing levels during minute 7 compared to control and *GluN1*$^{\Delta BLA}$ mice. The immobility data for this test showed similar results (**Figure 16**f), with an increase from minute 3 to 4 for all mice. This tone-dependent increase in immobility was higher for control mice than for *GluN1*$^{\Delta BLA}$. However, due to the high variation of the infrared sensor data, factorial ANOVA was not able to detect such a specific impairment (genotype $F_{2,19} = 0.7554$, $p = 0.4834$; time $F_{10,19} = 3.408$, $p = 0.0004$; interaction $F_{20,19} = 0.9146$, $p = 0.5691$).

In contrast to the cued fear component, the contextual retrieval test after Dox treatment revealed no gross differences between *GluN1*$^{\Delta BLA}$, *GluA1*$^{\Delta BLA}$ and control mice (**Figure 16**d). All mice showed comparably low levels of immobility during the duration of the test (genotype $F_{2,19} = 0.6770$, $p = 0.5200$; time $F_{7,19} = 1.836$, $p = 0.0854$; interaction $F_{14,19} = 1.499$, $p = 0.1196$), indicating that the context did not have a major component in the fear-conditioning memory in

this cohort.

The inducible nature of the genetic manipulation performed in this study allows for the intra-subject comparison of memory retrieval before and after the gene knockout. For this purpose, the freezing levels during the first three minutes of tone presentation were compared before and after the Dox treatment (**Figure 16**g). The genotype of the mice alone did not reach a significant effect on the fear levels ($F_{2,19}$ = 3.041, p = 0.0715). Time, however, did have a significant effect ($F_{1,19}$ = 19.96, p = 0.0003). Moreover, the interaction of genotype and time significantly affected freezing ($F_{2,19}$ = 4.718, p = 0.0217). Post hoc Bonferroni comparisons showed that the freezing levels of control mice did not differ significantly before and after Dox administration (Appendix Table 32), indicating that the drug treatment alone did not influence amygdala function and that there was no significant time-dependent decrease in memory strength. *GluN1*$^{\Delta BLA}$ mice, however, showed significantly less freezing after gene knockout, evidencing impairment in retrieval of cued fear. In the case of *GluA1*$^{\Delta BLA}$ mice, these froze more than controls during the first cued test and showed a significant decrease in freezing levels after GluA1 BLA knockout, reaching control levels.

Due to the inter-group variability in freezing during the first cued test, a relative change in freezing was calculated to include within-subject variation, normalizing with the initial cued freezing of each mouse before Dox (**Figure 16**h). The relative change was computed with the formula:

$$\Delta Freezing_{relative} = \frac{Freezing_{after} - Freezing_{before}}{Freezing_{before}}$$

One-way ANOVA showed that the genotype of the mice had a significant effect on this parameter ($F_{2,19}$ = 5.350, p = 0.0144). Bonferroni's multiple comparisons showed that *GluN1*$^{\Delta BLA}$ mice had a significantly more negative mean relative change, indicating a decrease in freezing after knockout in BLA, compared to controls (Appendix Table 33). The mean relative change of the controls was close to zero, indicating little or no change after Dox treatment. *GluA1*$^{\Delta BLA}$ mice, on the other hand, showed a negative trend in their freezing relative change, but it was not significantly different from the controls.

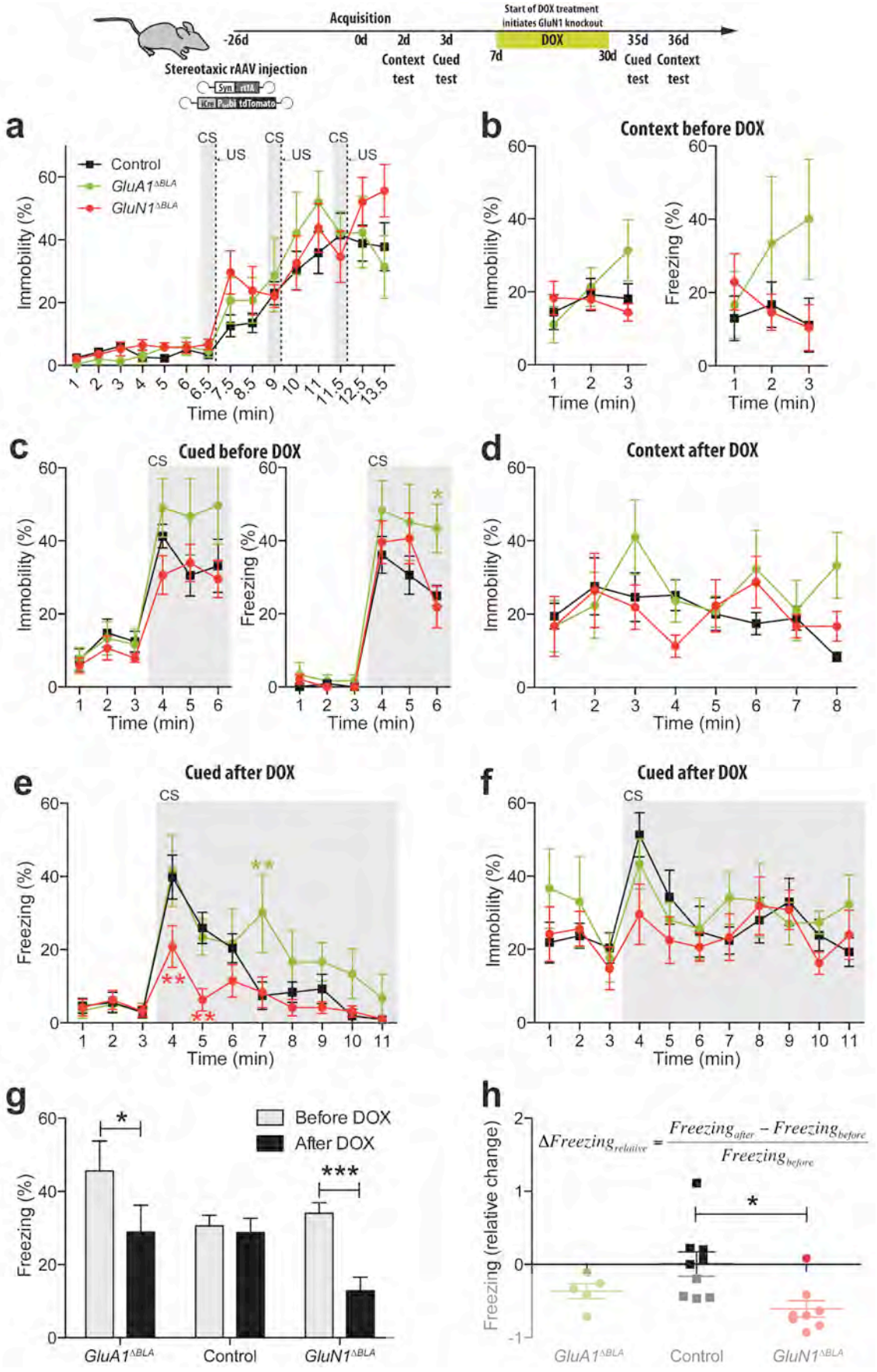

Figure 16. Retrieval of cued fear conditioning before and after knockout of GluN1 and GluA1 in the BLA by Dox-induced Cre recombinase expression

Top, Schematic time-line of the experimental design. Mice were injected with rAAV-syn-rtTA and rAAV-P_{tetbi}-iCre-tdTomato 26 d before acquisition of fear conditioning. Dox treatment was started 7 d later during 23 d. Contextual and cued retrieval tests were performed before and after the Dox treatment. **a,** Three-shock acquisition of cued fear conditioning. All mice gradually increased their freezing after each tone-shock pairing. The gray areas represent CS/US pairings. **b,** Contextual component of the fear memory 2 d after acquisition, before Dox treatment, measured by immobility and freezing. **c,** All three groups showed increased freezing when the tone was presented in a cued test 3 d after acquisition. The gray area indicates the CS presentation. **d,** Retrieval of contextual fear after Dox treatment, no significant differences in immobility between the three groups were observed. **e,** Cued fear retrieval after Dox treatment, 35 d after acquisition. *GluN1*$^{\Delta BLA}$ mice froze significantly less than controls during the first two minutes of tone presentation. *GluA1*$^{\Delta BLA}$ mice froze more than control mice during minute 7. **f,** Immobility levels during the cued retrieval test after Dox treatment reflect a similar trend as freezing. **g,** Total freezing levels during the three initial minutes of tone presentation of the cued tests before and after Dox treatment. Mice froze significantly less after GluN1 knockout and after GluA1 knockout, whereas freezing levels remained similar after Dox treatment in control mice. **h,** The relative change in freezing during the three initial minutes of tone presentation after DOX treatment, calculated by the formula shown, was more negative for *GluN1*$^{\Delta BLA}$ mice than for controls. *$p < 0.05$, **$p < 0.01$, ***$p < 0.001$.

As a next step, the extinction of cued fear in *GluN1*$^{\Delta BLA}$ or *GluA1*$^{\Delta BLA}$ was analyzed, in order to assess whether the fear memory in these groups was as persistent as in control mice. An extinction trial consists of the non-reinforced re-exposure to the CS in the absence of US. The cued retrieval test after Dox treatment was considered as the first extinction trial, and three additional trials were carried out starting 12 d later on three consecutive days. In the extinction trial 2 (E2; Figure 17a), control and *GluA1*$^{\Delta BLA}$ mice still showed increased immobility upon onset of the tone, whereas *GluN1*$^{\Delta BLA}$ continued to exhibit retrieval impairment. In E3 (Figure 17b), all three groups stopped to show tone-induced increase in immobility, an observation further confirmed during E4 (Figure 17c). When comparing the first 3 min of tone presentation across all extinction trials (Figure 17d), it becomes evident that extinction took place (time effect, $F_{3,19} = 4.712$, $p = 0.0052$), but that there were no significant differences by genotype ($F_{2,19} = 1.640$, $p = 0.2203$; interaction $F_{6,19} = 0.4511$, $p = 0.8412$).

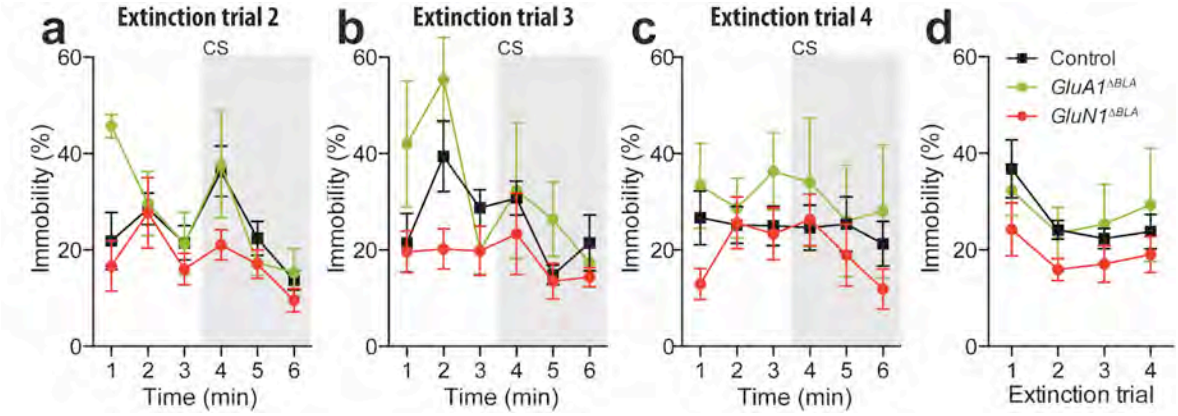

Figure 17. Extinction of cued fear in *GluN1*$^{\Delta BLA}$ and *GluA1*$^{\Delta BLA}$ mice
a, During extinction trial 2, *GluA1*$^{\Delta BLA}$ and control mice still show a tone-dependent increase in immobility, in contrast to *GluN1*$^{\Delta BLA}$. This cued fear memory is absent during extinction trials 3 (b) and 4 (c). The gray area indicates the period of CS presentation. **d,** The immobility during the first 3 min of tone presentation across extinction trials decreased significantly, but there were no significant differences between genotypes. The first extinction trial corresponded to the cued retrieval test after Dox treatment.

2.6.3. Exploratory behavior after GluN1 and GluA1 knockout in the BLA

As a test for general exploratory behavior, *GluN1*$^{\Delta BLA}$ and *GluA1*$^{\Delta BLA}$ mice were tested in the open field for 5 min, 69 d after the initial fear-conditioning acquisition (Figure 18a). The total distance traveled did not differ significantly between genotypes (two-way repeated-measures ANOVA, $F_{2,19}$ = 1.690, p = 0.2112). There was a significant effect of time ($F_{4,19}$ = 4.164, p = 0.0042) but not of the interaction between these two factors ($F_{8,19}$ = 1.159, p = 0.3349). This indicates that the gross exploratory activity of all three groups was similar. Moreover, the percentage of time spent in the center area of the square arena (inner 30 x 30 cm²; Figure 18b) was not significantly different between the genotypes (one-way ANOVA, $F_{2,19}$ = 2.204, p = 0.1378), although the variability was high. These results indicate that none of the groups had particularly high anxiety levels, and their behavior was comparable.

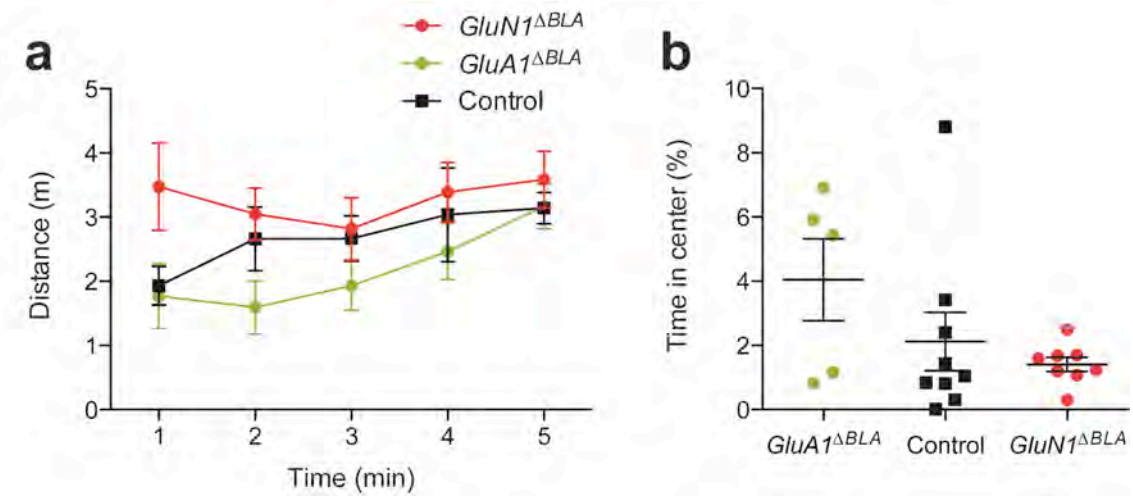

Figure 18. Open-field behavior of *GluN1*$^{\Delta BLA}$ and *GluA1*$^{\Delta BLA}$ mice
a, Total distance traveled during the test in 1 min time bins. **b,** Scatter plot of the percentage of time spent in the center region of the open-field arena.

2.6.4. Visual-association swimming task after GluN1 and GluA1 knockout in the BLA

As a final control test, mice from all three groups were trained in a visual-association swimming task in order to rule out that any group was unable to associate two different stimuli. The test was performed 124 d after the initial acquisition of fear conditioning and consisted of a modification of the protocol developed by Prusky and colleagues (2000). The training starts with one day of habituation to a small swimming pool. Mice swim from an initial start position to a hidden escape platform located behind a door marked by a salient star-shaped visual cue. Ten trials were performed from three different starting positions each located further apart from the goal platform (Figure 19a). On the following day, mice were trained in a larger swimming pool with two different goal options, one marked by the visual cue and containing the hidden platform (correct choice), and the other without cues or platform (wrong choice). Both options are randomly presented on the left or the right for each trial. Mice learn to swim towards the visual cue along five blocks of ten trials distributed on three consecutive days. Six mice from each group were tested (Figure 19b). Two-way repeated measures ANOVA showed that mice were able to learn this task and improve their performance over time ($F_{4,15}$ = 12.74, p < 0.0001). There

were no differences between the genotypes ($F_{2,15}$ = 0.2285, p = 0.7984) and there was no significant interaction with time ($F_{8,15}$ = 0.3631, p = 0.9359). It becomes clear from this result, that the impairments in cued fear retrieval for *GluN1*$^{\Delta BLA}$ and *GluA1*$^{\Delta BLA}$ mice are not simply due to a general cognitive impairment or inability to form general associations.

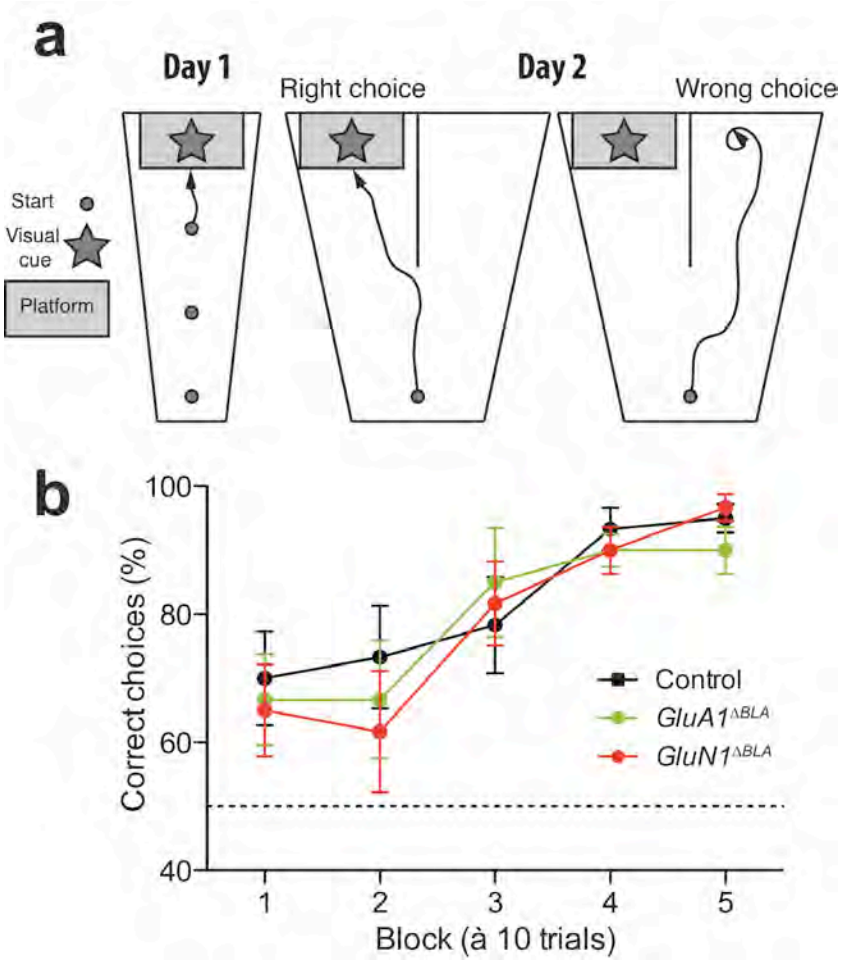

Figure 19. Visual association swim task for *GluN1*$^{\Delta BLA}$ and *GluA1*$^{\Delta BLA}$ mice
a, Schematic representation of the testing apparatus and design. On day 1, mice habituate to the swimming task in a one-option pool, where they swim to a goal hidden platform marked by a salient visual cue, starting from three different gradually more distant positions. On days 2–4, mice swim in a larger pool with two goal options and learn that the visual cue—and not the left/right position—predicts the location of the hidden platform. **b,** The percentage of correct choices improves across the test blocks for all groups of mice without a significant effect of the genotype. The dotted line indicates the chance level.

2.6.5. Doxycycline-induced GluN1 and GluA1 knockout in the BLA

The histological post-mortem analysis of tdTomato expression was used to assess the extent of infection of the BLA in *GluN1*$^{\Delta BLA}$ and *GluA1*$^{\Delta BLA}$ mice after the behavioral experiments were finished (Figure 20). Immunostaining against Cre recombinase showed that recombination was restricted to the BLA and a small portion of the piriform cortex. The neuronal nuclei marker NeuN was used in immunostaining to show that tdTomato expression was neuron-specific.

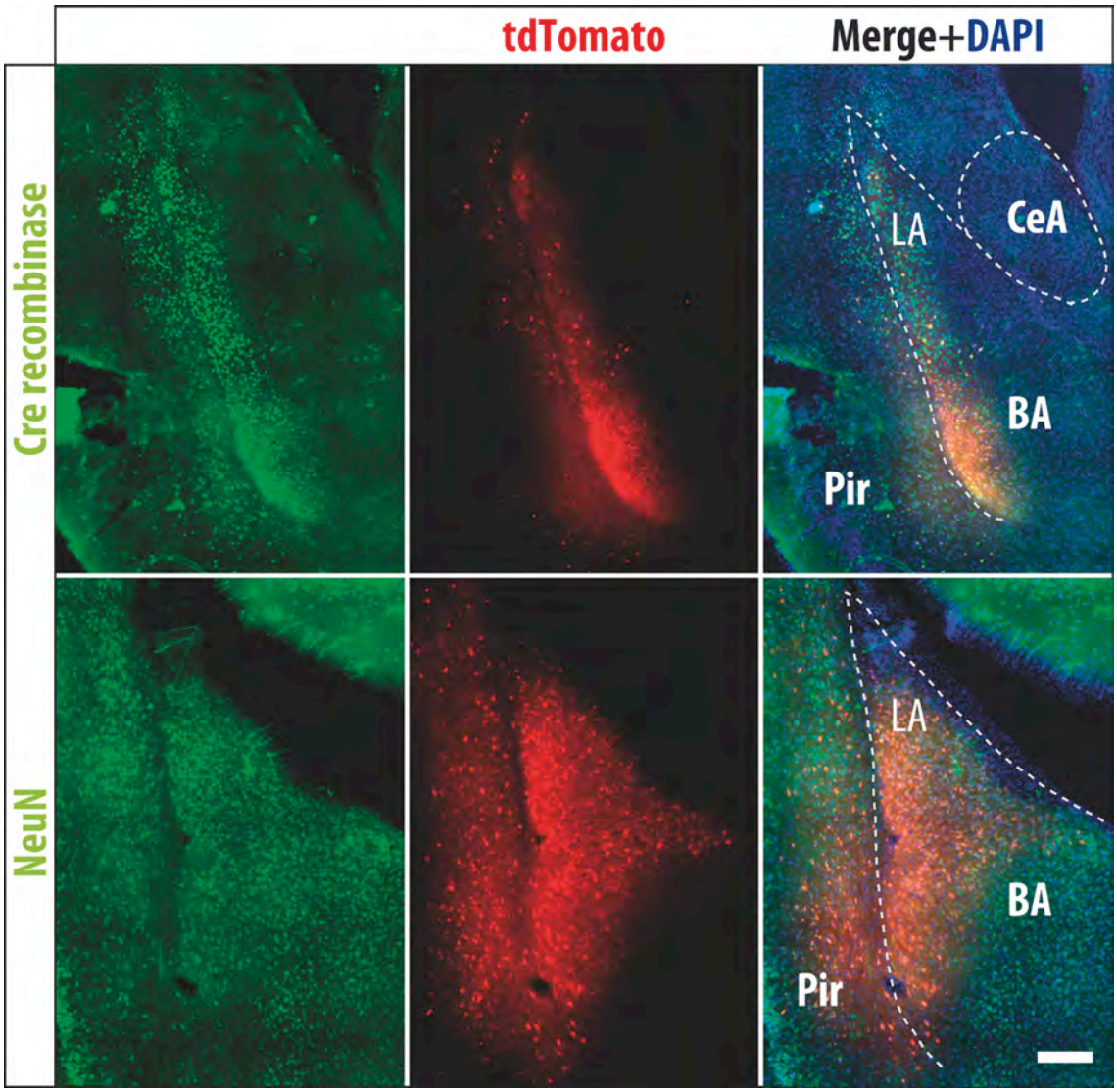

Figure 20. Histological analysis of rAAV-mediated Cre expression in the BLA
Fluorescence immunostaining against Cre recombinase showing restricted expression mostly in the BLA. Cre expression overlapped with the red fluorescence of tdTomato. NeuN immunostaining shows that the cells expressing tdTomato are mature neurons. Scale bar, 200 µm.

A set of examples of Cre immunostaining in *GluN1*$^{\Delta BLA}$ and *GluA1*$^{\Delta BLA}$ mice is shown in Appendix Figure 33. An estimate of 30–60% of the BLA showed rAAV infection, and within an infected region ~90% of the NeuN-positive cells were also Cre-positive.

Furthermore, in order to obtain evidence that the knockout of GluA1 had taken place, 3,3'-Diaminobenzidine (DAB) immunohistochemistry was performed against the GluA1 subunit using a peroxidase-labeled antibody (Figure 21a). GluA1 staining was absent in the infected area of the BLA in *GluA1*$^{\Delta BLA}$ mice, while it was strongly present in the case of rAAV-injected control mice. This was not an artifact of the staining procedure, since other regions known to express high levels of GluA1, such as the hippocampus, exhibited normal staining in *GluA1*$^{\Delta BLA}$ mice.

In the case of NMDARs, no reliable immunostaining protocol against GluN1 is available. Therefore, slice electrophysiological recordings of rAAV-infected BLA neurons were obtained in *GluN1*$^{\Delta BLA}$ and control mice. In *GluN1*$^{\Delta BLA}$ mice, the NMDAR component was completely absent from this neuron population (Paolo Botta and Andreas Lüthi, personal communication).

After the post-mortem injection-site analysis, the variability of the infected area in the cohort of mice was assessed, showing that rAAV infection was mostly restricted to the BLA, but often extended to the deeper layers of the piriform cortex (Figure 21b,c; Appendix Figure 33). Importantly, the output region of the amygdaloid complex, the CeA, was spared from rAAV infection and gene knockout. These results constitute an important reminder of the limitations of the virally-mediated gene manipulation approaches, in which great anatomical specificity can be achieved but with often large variability.

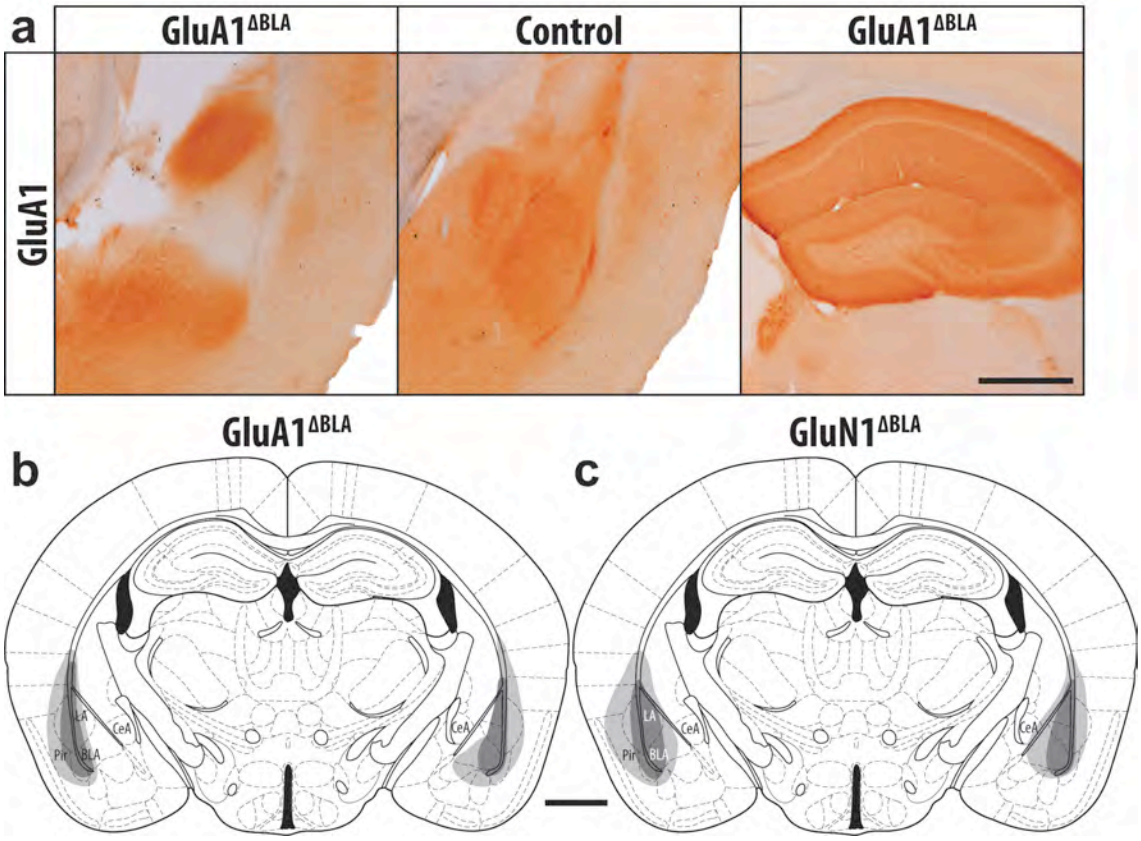

Figure 21. Histological analysis of *GluA1*$^{\Delta BLA}$ and *GluN1*$^{\Delta BLA}$ mice 6 months after rAAV injection

a, DAB-peroxidase immunostaining against the GluA1 shows absence of the subunit in the BLA of *GluA1*$^{\Delta BLA}$ mice, whereas it is expressed normally in control mice. GluA1 expression in the hippocampus of *GluA1*$^{\Delta BLA}$ mice was normal. Scale bar, 500 µm. **b,** Extent of infection in the brains of *GluA1*$^{\Delta BLA}$ mice. **c,** Infection area in the brains of *GluN1*$^{\Delta BLA}$ mice. The smallest area of infection is shown in dark gray, the largest in light gray. Scale bar, 1 mm.

3. Discussion

3.1. The subtle effects of AMPAR subunit knockout

AMPARs have an essential function in mediating glutamatergic synaptic transmission and are represented by two populations in forebrain principal neurons: GluA1-containing and GluA3-containing AMPARs. Paradoxically, complete constitutive absence of one of either of these receptor populations yields only subtle behavioral effects. In the following sections, I will elaborate on the behavioral analysis of the general cognitive ability and emotional memory of *GluA3*$^{-/-}$ and *GluA1*$^{-/-}$ mice.

3.1.1. General cognitive ability of *GluA3*$^{-/-}$ mice

I analyzed the general cognitive ability of *GluA3*$^{-/-}$ mice using the puzzle-box problem-solving test (Figure 2). This test has been proposed as an indicator for deficits in executive functions related to schizophrenia (Abdallah et al., 2011). I found a subtle impairment in selected trials compared to wild-type littermates, but *GluA3*$^{-/-}$ did not differ from controls in most tasks. Particularly, *GluA3*$^{-/-}$ mice had difficulties achieving the improvement observed in wild types after subsequent trials, for example, in the 'underpass' task 2. *GluA3*$^{-/-}$ mice were also impaired when presented with new problems, as in the first trial of task 3 (digging) and 4 (plug), and after subsequent trials they did not differ from the controls anymore. However, *GluA3*$^{-/-}$ mice had no general impairment of their digging abilities or motivation to dig.

This is especially interesting in light of the discovery of several mutations of the GRIA3 gene that codes for the GluA3 subunit, which lead to moderate to severe cases of mental retardation in humans (see below). Moreover, a neurological child disease involving epilepsy, hemiplegia, dementia and inflammation of the brain known as Rasmussen's encephalitis has been linked to an autoimmune response against the body's own GluA3 subunits (Rogers et al., 1994). An X-chromosome translocation within the GRIA3 gene was first reported in a patient with bipolar disorder and mental

retardation (Gécz et al., 1999). Later, several missense mutations and one deletion in the GRIA3 gene were linked to different degrees of mental retardation and these mutations were shown to cause misfolding and reduction in GluA3 (Wu et al., 2007). Also, two partial tandem duplication of GRIA3 running in two different families of patients have been linked in to mental retardation (Bonnet et al., 2009; Chiyonobu et al., 2007).

GluA1$^{-/-}$ mice have already previously been analyzed in the same testing protocol (Abdallah et al., 2011). That study showed that *GluA1*$^{-/-}$ mice also had selected impairment of some tasks, in particular, in the short-term improvement after subsequent trials, normally exhibited by controls. *GluA1*$^{-/-}$ mice have been proposed as an animal model of schizophrenia (Wiedholz et al., 2008).

Together, the results presented in this thesis, as well as those obtained by Abdallah and colleagues, signal that the behavioral phenotype resulting from knocking out GluA1 or GluA3 subunits does not cause generalized cognitive impairment, but rather a specific deficit in problem solving, and might have important applications as a model of schizophrenia and moderate mental retardation. More refined testing protocols are required for this type of analysis. GluA1 and GluA3 knockout mice are important tools for the establishment of such behavioral tests.

3.1.2. GluA1-containing AMPARs and short-term fear memory

I analyzed two different mouse lines with altered populations of GluA1-containing AMPARs. One of them with a global depletion of the subunit, *GluA1*$^{-/-}$ (Zamanillo et al., 1999); the other one with a point mutation, *GluA1*$^{R/R}$ (Vekovischeva et al., 2001). I found that both of this manipulations resulted in a severely impaired expression of fear during the acquisition phase of cued fear conditioning, nevertheless, with evidence for the formation of long-term memory (Figure 5 and 6).

Little is known about the processes occurring *during* the acquisition protocol in fear conditioning. However, a general observation is that wild-type animals show immediate expression of fear after a US (foot shock) presentation. Therefore, the particular phenotype observed in *GluA1*$^{-/-}$ and *GluA1*$^{R/R}$ mice, in

which they do not increase their fear response, even after three US presentations, is of special interest. Several explanations could be given to this phenomenon.

First, the global knockout of normal AMPARs produces general synaptic transmission deficiencies in several regions of the brain important for the physiological manifestations of fear, including the CeA, hypothalamus, and brain stem; for this reason, these mice are unable to express fear. However, this hypothesis is not in line with the small but significant increase in immobility in response to the CS observed when testing the animals 24 h later. Therefore, the expression of fear in the form of immobility is possible in *GluA1*$^{-/-}$ and *GluA1*$^{R/R}$ mice.

Second, the global knockout of normal AMPARs affects brain regions responsible for motor initiation and/or coordination—e.g. cerebellum, substantia nigra, ventral tegmental area, and striatum—thus rendering these mice highly hyperactive and reducing the capacity to detect immobile states by the experimenters. This hypothesis is supported by the fact that *GluA1*$^{-/-}$ and *GluA1*$^{R/R}$ mice have higher exploratory activity in the open field test (Bannerman et al., 2004; Vekovischeva et al., 2001). However, it does not explain the increase in immobility during the cued retrieval test 24 h later, since mouse hyperactivity would mask the fear response in all of the testing phases and not only during acquisition.

Third, there is a specific impairment of fear expression during the acquisition phase, which does not affect the fear response in a subsequent test after 24 h. I propose that it is this hypothesis that better explains the phenotype observed in *GluA1*$^{-/-}$ and *GluA1*$^{R/R}$ mice. The supporting evidence for this affirmation goes back to studies in spatial memory, where a similar interpretation can be made.

Previous studies have shown that *GluA1*$^{-/-}$ mice are strongly impaired in solving spatial working memory component in the elevated T-maze (Reisel et al., 2002) or the six-arm radial maze (Schmitt et al., 2003). In these tests, mice must be able to recall events that occurred seconds to minutes before the decision point. In strong contrast, spatial reference memory is normal in these

mice, for example, in the Morris water maze (Reisel et al., 2002; Zamanillo et al., 1999) or in the Y-maze (Reisel et al., 2002); in the reference memory tasks, learning occurs during a long period of time involving training for several days. Therefore, it has been proposed that GluA1 knockout unravels the dissociation of short-term and long-term memory processes (Sanderson et al., 2009).

There is a likely parallel between the spatial memory and fear memory phenotypes of GluA1 mutant mice. In both cases, a short-term component, relying on recently visited spatial locations or recently experienced noxious stimuli, is heavily impaired; whereas a long-term component, based on retrieval of associations after one or several days, is normal or only slightly affected. The fact that a similar phenotype in emotional memory was observed for *GluA1*$^{-/-}$ and *GluA1*$^{R/R}$ mice shows that there is a requirement for this AMPAR population for short-term memory.

Sanderson and colleagues (Sanderson et al., 2008) have proposed that the dissociation of short and long-term spatial memory processes could be explained by a model elaborated by Wagner three decades ago (Wagner, 1981). This SOP model (accounting both for *Standard Operating Procedures* in Memory and *Sometimes-Opponent Process*) is based on the hypothesis that memory "nodes" (e.g. stimuli) consist of elements (e.g. different characteristics of each stimulus) that can be in one of three possible states: an inactive state (I), and two active states, A1 at the focus of attention, and A2 as in marginal working memory. The different relationships of the three states are shown in the following scheme taken from Wagner (1981):

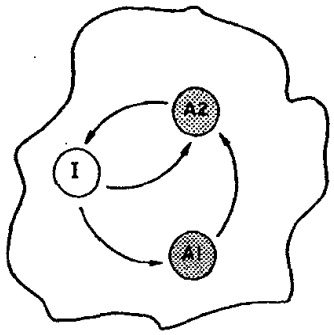

The SOP model has the advantage that it predicts the occurrence of priming of short-term memory. The presentation of a stimulus leads many of its elements to move from inactivity into the active state A1, after which these

elements will decay to A2, before finally decaying back to I. When the stimulus is presented again after a short-enough time period, at which most of its elements are still in A2, there will be fewer elements available to enter the A1 state and the stimulus will be less likely to become the focus of attention the second time it is presented. The direct passage from I to A2 is assumed to occur only by activation of another 'node' that has a positive association with the node in the scheme.

Under this model, the impairment of *GluA1*$^{-/-}$ mice in spatial working memory tasks could be interpreted as an increase of the rate of passage from A2 to I, so that a stimulus that has just been presented quickly abandons the active state. In the T-maze, for example, when wild-type mice visit one arm, the representation of this arm remains in the active state A2 for a sufficient amount of time as to be less interesting when presented for a second time after a few seconds or minutes; thus resulting in the mice exploring the more interesting alternative arm. For *GluA1*$^{-/-}$ mice, on the other hand, the representation of the visited arm would quickly go back to the inactive state, so that the same arm would be just as interesting during the second visit. Likewise, in the case of fear conditioning acquisition, an increased rate of passage of the US (foot shock) representation from A2 to inactive in *GluA1*$^{-/-}$ mice could explain why these mice do not express fear during this training, since their marginal working memory would be impaired. An alternative possibility is that the transfer of information from A1 to A2 is too slow in *GluA1*$^{-/-}$ mice and the marginal working memory is not established at a time when the recall is necessary—e.g. in the second run in the T-maze. This slow transfer might also explain the lack of fear response during the three shocks observed in *GluA1*$^{-/-}$ and *GluA1*$^{R/R}$ mice.

Nevertheless, what makes the SOP model particularly interesting in the light of the experimental data regarding *GluA1*$^{-/-}$ is that, according to this model, the formation of long-term memories is not a direct and sequentially subordinated consequence of short-term working memory performance, that is, of the maintenance of an active representation of a stimulus in the A2 state. But rather, Wagner proposed that long-term positive or "excitatory" associations

arise from the simultaneous activation of two stimuli in the A1 state—in the focus of attention. This would explain, why *GluA1*$^{-/-}$ mice are able to acquire spatial reference memory, even though their spatial working memory is impaired. It would also explain why *GluA1*$^{-/-}$ and *GluA1*$^{R/R}$ mice are able to form a CS/US association, as evidenced in the retrieval test, even though they are unable to maintain a working memory representation of the shock—and express fear—during the acquisition of fear conditioning. Moreover, this particular requirement of GluA1-containing AMPARs in short-term memory processes seems to be specific for this receptor population. GluA3-containing AMPARs do not seem to be necessary for the maintenance of the A2 active state of mental representations of stimuli, since no working memory impairment is observed in *GluA3*$^{-/-}$ mice in the fear-conditioning acquisition.

In conclusion, my data support the hypothesis that memory does not necessarily go through a short-term working memory state, before becoming stable on the long-term, but that these two dissociated processes occur in parallel.

3.1.3. GluA3- and GluA1-containing AMPARs in long-term fear memory

In a first experiment, testing the behavior of *GluA3*$^{-/-}$ mice in the passive avoidance task, substantial retrieval of the avoidance memory was observed, which was evidenced for as long as 67 d, whereas wild-type mice showed a significant decrease in their avoidance response already after 37 d (Figure 4). The analysis of *GluA1*$^{-/-}$ mice in the same paradigm yielded similar results (Figure 7), showing significant recall of the avoidance memory in knockout mice for up to 23 d, while wild-type mice already exhibited decrease in fear memory at this time point. These results suggested that the knockout of each of the dominant AMPAR populations in excitatory neurons had a strong effect in the retention of long-term fear memories in the passive avoidance task. However, in both of these experiments, the mice used were not naïve and had already been trained in classical fear conditioning followed by cued fear extinction. This pre-exposure to shock stimuli could have interfered with the

formation of the passive avoidance memories, in which shocks are also used as US. Therefore, confirmation of these results was necessary to be able to draw appropriate conclusions.

For this reason, a further experiment was performed in which naïve *GluA1*$^{-/-}$ and *GluA3*$^{-/-}$ mice were analyzed in parallel in the same passive avoidance task and repeatedly tested at different time points from acquisition to assess changes in the strength of memory with the passage of time (Figure 8). These results confirmed the initial observations relating the long-term avoidance memory. That is, also in naïve mice an enhancement in the retention time of passive avoidance fear memory was observed, indicating that both knockout of GluA1 and of GluA3 had an important positive effect in long-term memory.

Strikingly, in the case of *GluA1*$^{-/-}$ mice, a remarkably similar situation has been reported for habituation of spatial memory in the novelty preference test in the Y-maze (Sanderson et al., 2009). In an elegant experimental design, Sanderson and colleagues showed strong evidence for an apparently paradoxical short-term "working" memory impairment in *GluA1*$^{-/-}$ mice accompanied by a long-term memory enhancement under conditions in which wild-type animals performed badly. For this, they showed that short (1 min) inter-trial intervals (ITIs) during training improved learning in wild-type mice but impaired learning in *GluA1*$^{-/-}$ mice, whereas long ITIs did exactly the opposite. This has been interpreted as evidence for a dissociation between short-term (non-associative) GluA1-dependent memory and long-term (associative) memory, which in certain occasions could even compete with one another (Sanderson and Bannerman, 2010).

However, it must be noted that the short-term memory deficit reported here was observed in a three-shock acquisition protocol for fear conditioning, while the long-term memory enhancement was evidenced in a different paradigm—passive avoidance. This was due to two factors. First, a three-shock acquisition protocol in passive avoidance is not practicable, since this paradigm is designed to produce learning resulting from one single trial. Second, long-term memory analysis of fear-conditioning memories in *GluA1*$^{-/-}$ is difficult,

since the measure of fear in this paradigm is based on freezing behavior, which can be partially masked by their hyperactive phenotype, making the passive avoidance protocol more appropriate.

The remarkable observation that the *GluA1*$^{-/-}$ memory phenotype is comparable in two types of learning components in spatial and emotional learning, supports the view that the short-term/long-term dissociation could be a general principle followed by memory systems involving different regions of the brain.

This reasoning can be extended to explain, at least partially, the emotional memory phenotype of *GluA3*$^{-/-}$ mice. In this case, only the enhancement of long-term fear memory was observed, but not short-term memory impairment, and this was supported by data from passive avoidance learning (Figure 8) as well as from cued fear conditioning (Figure 9). This is not in conflict with the model discussed above, since it is possible that the short-term working memory processes in fear conditioning acquisition do not rely on GluA3-containing AMPARs, while the long-term memory processes do. This different involvement of GluA1- and GluA3-containing AMPARs is most likely related to the different roles of these two receptor populations in synaptic transmission and plasticity. This is best exemplified by LTP at different input synapses in the amygdaloid system: thamalo-amygdala LTP and intra-BLA LTP both depend on GluA1, whereas cortico-amygdala LTP depends both on GluA1 and GluA3 (Humeau et al., 2007). Interestingly, from lesion studies it is known that it is the cortico-amygdala pathway that is necessary for maintaining auditory cued fear memories (Boatman and Kim, 2006), while either pathway supports their initial learning (Romanski and LeDoux, 1992). Therefore, the discrepancies in the roles of GluA1 and GluA3 in conditioned short-term and long-term memory can be best explained by different AMPAR subunit compositions in distinct synapses of the amygdaloid complex.

3.2. rAAV-mediated gene delivery into the BLA and manipulation of fear memories

There is only a limited number of available references for the successful use of viral vectors for the modification of gene expression in the amygdala to study memory processes, either using rAAVs (Glass et al., 2008; Rumpel et al., 2005) or other viral tools, e.g. herpes simplex virus (Han et al., 2009; Zhou et al., 2009). Therefore, one of the goals of this thesis was to test whether rAAV-mediated expression of gene products that alter neuronal activity could be used to modify behavior in mice. For this purpose, TTLC was expressed by injecting rAAVs into the amygdaloid complex.

I found that rAAV could successfully infect neurons in the amygdala without causing cell-death and without altering the general behavioral performance, as shown in the open field and elevated plus-maze tests (Figure 11). In emotional learning, amygdala neuron silencing by TTLC was enough to disturb the performance in memory retrieval tests (Figure 12), both on the short- and long-term. However, it is not clear whether this impairment is due to an alteration in consolidation processes that occur after acquisition or to the inability to retrieve the memory during the tests. The deficit was not paradigm-specific, as a similar deficit was found in another amygdala-dependent learning test—passive avoidance (Figure 13). These results were consistent with the critical involvement of the amygdaloid complex in both of these tasks revealed by lesion studies (Russo et al., 1976; Swartzwelder, 1981; Weiskrantz, 1956; Zola-Morgan et al., 1991).

Nevertheless, the whole potential of this novel technical approach for silencing amygdala neurons has still to be exploited. Importantly, the advantage of the reversibility given by the doxycycline-controlled induction can be of great use in order to assess, for example, the role of synaptic transmission through the BLA in learning phases posterior to initial acquisition, such as retrieval, reconsolidation and extinction.

3.3.Involvement of NMDARs in post-acquisition memory processes

3.3.1. Methodological considerations of the experimental design

I have shown that knockout of NMDARs in the BLA starting 7 d after acquisition of cued fear conditioning strongly impairs cued recall of a 35-d-old fear memory (**Figure 16**).

The design for this experiment was conceived with the purpose of sparing consolidation- and reconsolidation-related processes that occur after acquisition and reactivation of a memory, respectively (Figure 15). First of all, animals were left undisturbed for 2 d after acquisition of fear conditioning before being re-exposed to the training context during the first contextual test. Re-exposure to the CS (tone) did not occur until the third day. A great amount of evidence shows that manipulations as diverse as protein synthesis inhibition, NMDAR or AMPAR blockage, electroconvulsive shock, and hypothermia do not disturb memory when applied at time points later than 24 h (Kandel, 2001; McGaugh, 2000). Furthermore, reactivation of fear memory, by short re-exposure to the context or the CS, by itself does not produce an impairment of memory tested at later time intervals (Suzuki et al., 2004). Therefore, it is safe to assume that the retrieval tests performed at this stage, which were normal for all mouse groups, did not have a negative effect on further tests. Additionally, the CS-reexposure during the first cued test was limited to 3 min, with the goal of avoiding the possibility of triggering extinction of memory with too long a reactivation trial (Pedreira and Maldonado, 2003).

Moreover, the Dox treatment for the induction of Cre recombinase expression was started 7 d after initial acquisition, i.e. 4 d after the first cued test. The choice of this time point for the beginning of the NMDAR and AMPAR knockout induction allows two things. First, to rule out effects of the knockout on the initial time-window of susceptibility after fear learning, which lasts 1–2 d. Second, to rule out that later results from memory testing are due to a direct effect of the gene knockout on fear reconsolidation, in the sense of the processes that occur after memory reactivation by a short re-exposure to the CS.

The Dox administration was carried out during 23 d for all mice

including controls, to exclude an unspecific effect of the drug alone on general body homeostasis that could influence performance on behavioral testing. What is more, it has not been reported that Dox treatment by itself can cause major alterations in behavior. Nevertheless, since the acquisition of the fear memory was performed under no-Dox conditions, the Dox treatment was stopped after 23 d and the mice were allowed a 5 d drug-free period before further memory tests were performed. This was done in order to exclude state-dependent effects on the second round of memory tests (Sara, 2000a).

Altogether, these methodological considerations allow the conclusion that the memory outcome of the second cued and context tests are due to the knockout of the GluN1 or GluA1 genes.

3.3.2. Memory retrieval impairment after GluN1 knockout in the BLA

The most remarkable results were obtained in the 35 d cued retrieval test (**Figure 16**). *GluN1*$^{\Delta BLA}$ mice showed a clear impairment in their ability to recall the CS-US association in contrast to wild types, which had undiminished recall of the cued fear memory. The advantage of this study is, however, that it enables an intra-subject analysis of memory performance. The quantification of the relative change in freezing before and after gene knockout showed that NMDAR-knockout had a significant effect on cued memory recall.

This kind of analysis also proved very useful for understanding the *GluA1*$^{\Delta BLA}$ phenotype. For these mice, the comparison between the freezing levels during the 35 d cued test did not yield differences compared to the wild types, suggesting that they were not impaired in their ability to recall the fear association. Nevertheless, the comparison of the total freezing levels before and after the Dox treatment (**Figure 16**g) and the intra-subject relative change in freezing (**Figure 16**h) show that *GluA1*$^{\Delta BLA}$ mice have a tendency to reduce the freezing response after the knockout has taken place. This trend was not significant, though, which is likely due to the small sample size (n = 5) for this group. Therefore, the role of GluA1-containing receptors in the amygdala for memory recall after 35 d remains inconclusive.

The extinction protocol performed 13 d after the second cued test showed that the immobility levels in response to the tone remained low in *GluN1*$^{\Delta BLA}$ mice, and decreased in *GluA1*$^{\Delta BLA}$ and control mice (Figure 17). The effect of the NMDAR knockout on extinction cannot be assessed from this experiment, since the fear levels were already low during the first extinction trial. GluA1-containing AMPAR knockout on the other hand, did not have a significant effect on this extinction protocol. Therefore, the following discussion will be limited to the first retrieval tests after gene knockout.

The impairment observed in the 35 d retrieval test for the cued memory after NMDAR knockout in the BLA must be analyzed in two contexts: the pharmacological evidence for a non-requirement of NMDARs in retrieval, and other long-term NMDAR knockout experiments that follow a similar design of post-acquisition manipulations (Cui et al., 2004; Shimizu et al., 2000).

One of the possible explanations for the retrieval deficit in *GluN1*$^{\Delta BLA}$ mice could be that these mice simply were unable to express fear in the form of freezing due to the NMDAR knockout, rather than due to direct effects on the fear association itself. However, this reasoning is unlikely in light of the vast experimental evidence obtained from pharmacological experiments in which NMDAR antagonists were injected into the BLA shortly before the retrieval tests without impairing the recall ability for different fear memory paradigms, in different model organisms, and with several pharmacological agents (Ben Mamou et al., 2006; Lee et al., 2006; Myskiw et al., 2010; Torras-Garcia et al., 2005; Walker et al., 2002; Zimmerman and Maren, 2010). Thus, it can be concluded that if NMDAR activation is not required for successful retrieval of fear memories during a recall test, then, the impairment observed in *GluN1*$^{\Delta BLA}$ mice is likely related to a specific effect on the fear association itself, which has been diminished or erased.

Different to the previous studies, I used a genetic approach in which the GluN1 subunit was knocked out in the BLA starting on day 7 after initial acquisition. Therefore, there is an important difference from the pharmacological studies, in that NMDARs are completely absent from the infected neurons after the induction with Dox, and are not just transiently

inactivated.

There are three other studies in which an inducible genetic approach was applied to study NMDAR function in long-term memory. In the first one (Shimizu et al., 2000), a Dox-inducible and reversible forebrain-specific knockout of GluN1 was used to study long-term memory of hippocampus-dependent tasks. Shimizu and colleagues found that contextual fear conditioning—but not cued—could be disrupted if GluN1 was knocked out for the first 14 d after acquisition, when memory was tested at 29 d. If the knockout took place during the last 8 d before the memory test, there was no effect on the contextual or on the cued recall, further supporting the view that NMDAR activity and expression is not necessary for fear expression during a retrieval test. The authors found similar results for spatial memory in the Morris water maze. This study was the first to propose that a mechanism of synaptic reentry reinforcement (SRR) could be necessary for consolidation of long-term memories, but, due to the genetic model, this hypothesis was restricted to the hippocampus and other regions of the forebrain.

A second study by the Tsien lab used a similar genetic approach, but restricting the knockout to hippocampus, cortex and striatum (Cui et al., 2004). They were able to show that retrieval of a 9-month-old contextual and cued fear memory was impaired when NMDARs were knocked out during a 1-month period 6 months after the initial acquisition, but not if the knockout occurred only for one week. They hypothesized that a SRR mechanism relying on NMDAR periodic reactivation was necessary for the maintenance and stabilization of long-term memories.

A third study by the same group extended the SRR hypothesis to non-declarative taste memory in the conditioned taste aversion task (Cui et al., 2005). Now they showed that NMDAR knockout in cortex, hippocampus and striatum during the first two weeks following the training session to develop aversion to a particular taste disrupted this memory when the animals were tested after 1 month. The same results were obtained when the knockout took place during the two weeks prior to the retrieval test, but not when it occurred for only 5 days before the recall test. Since conditioned taste aversion does not

require the hippocampus and the striatum (Yamamoto et al., 1995), Cui and colleagues concluded that cortical NMDAR reactivation during the post-training consolidation period is necessary for memory stabilization for long-term storage.

Taken together, the pharmacological and transgenic studies presented above support the conclusion that the memory impairment observed in the 35 d cued test in my *GluN1*$^{\Delta BLA}$ mouse cohort arises from a disruption of the fear association rather than from inhibited fear expression. In other words, NMDAR expression in neurons of the BLA is required for the stabilization of cued fear memory for long-term retrieval.

The experiments in this thesis have the advantage of the stereotaxic rAAV-mediated high anatomical restriction of the NMDAR knockout to the BLA, which is so far not possible by transgenic methods. Also, by using the rtTA/Dox system the start of the knockout can also be temporally delimited, thus allowing to exclude an intervention on the initial 1–2 d consolidation lability period. One limitation, however, is the inability to completely infect and express Cre recombinase in all neurons of the BLA. It is important to take this into account for the interpretation of the contextual retrieval tests. There were no differences in the retrieval of the contextual component before and after gene knockout either for *GluN1*$^{\Delta BLA}$ or *GluA1*$^{\Delta BLA}$ mice. Contextual fear memory is dependent on hippocampal function; the role of the amygdaloid complex in purely contextual fear is disputed (Phillips and LeDoux, 1992; Vazdarjanova and McGaugh, 1998). In my experiments, the hippocampus was left intact, which, combined with the remaining subsets of uninfected BLA-neurons that still expressed GluN1 and/or GluA1, could explain that no abnormal phenotype was observed for the contextual component of the fear memory.

3.3.3. A role of NMDARs in the BLA for offline memory reactivation

My results point towards a requirement of NMDARs in the BLA for stabilization of memory for long-term retrieval and are compatible with the SRR hypothesis (Shimizu et al., 2000; Wittenberg and Tsien, 2002). In this sense,

it is likely that periodic reactivation of NMDARs could serve as a synapse-stabilizing mechanism that would allow the long-term storage of associations, and that this would be a global process not limited to the hippocampus or the cortex, but also including the BLA and probably other brain regions. Such a mechanism would be said to occur offline, since no direct stimulation is applied to elicit recall of the fear memory. The clearest example of learning-related offline processes is sleep, but there is no reason to think that these reactivation processes do not occur during the awake state. During sleep, sensory input is greatly diminished, yet there is strong evidence that there is reactivation of memory traces from previous experiences (Sutherland and McNaughton, 2000). Therefore, much elaboration has been done for more than a decade on the role of sleep in memory consolidation (Buzsáki, 1998). Moreover, there is electrophysiological evidence that NMDARs are necessary for some of these reactivation events, e.g. for the ensemble spontaneous firing in the striatum during sleep in rats, and could be involved in the offline information flow during habit formation in rats (Pomata et al., 2008). Further evidence comes from human studies in which glutamatergic signaling through NMDARs during sleep has been shown to be necessary for visual discrimination memory enhancement (Gais et al., 2008), in a process related to memory consolidation. Memory offline reactivation, in principle, does not have to be limited to sleep. For example, 45 min after conditioned taste aversion learning in rats, there is release of glutamate in the insular cortex in the absence of stimulation, which does not occur in the absence of training, and which could be blocked by NMDAR antagonists (Guzmán-Ramos et al., 2010).

Together, these offline reactivation events could be seen as conscious or unconscious episodes of memory recall, which occur periodically, even in the absence of external cues or stimulation, and which would help to stabilize memories over time. It could be hypothesized that such reactivation episodes could trigger reconsolidation processes, in a similar way as reconsolidation is triggered by short re-exposure to a CS, weeks after fear conditioning. NMDARs are essential for memory reconsolidation and antagonists or agonists can impair or potentiate it, respectively (Ben Mamou et al., 2006; Lee et al., 2006).

In light of these studies, the memory impairment observed in *GluN1*$^{\Delta BLA}$ mice could be interpreted as a result of the periodic offline reactivation of the cued fear memory in the absence of NMDARs, which would disrupt reconsolidation and reinforcement of the fear association. At least one study has shown contextual memory impairment after chronic inhibition of NMDARs by daily systemic ketamine injections for two weeks after learning (Amann et al., 2009). Interestingly, repeated episodes of short reactivation immediately followed by MK-801 treatment have been shown to disrupt reconsolidation and decrease memory strength of amphetamine-induced conditioned place preference (Sadler et al., 2007). Similar results have been obtained for cue-induced alcohol self-administration, for which the alcohol-seeking behavior was strongly reduced in rats after several reactivation sessions coupled with NMDAR antagonist treatment (Wouda et al., 2010). In a different study, this effect was seen even after one reactivation session (von der Goltz et al., 2009). Although the reactivation events in that study were induced and therefore not offline, they indicate that even complex and strong memories of addiction can be disrupted by manipulations affecting reconsolidation.

Finally, through further analysis of the mouse cohort used in this experiment, I was able to show that these mice were not essentially impaired in their exploratory behavior (Figure 18) or in the ability to make simple cued associations in the visual swim task (Figure 19), supporting the view that the phenotype observed was specific to fear conditioning.

In conclusion, NMDARs in the BLA are necessary after memory consolidation for successful retrieval of the fear memory 35 d later. This effect was not due to disruption of the initial 1–2 d consolidation window, or the expression of fear during the retrieval test, but was the result of disruption of the CS/US association. I hypothesize that this impairment arises from the disruption of reconsolidation occurring after periodic events of offline (sleep or awake) reactivation of the fear memory. The involvement of AMPARs in these processes remains inconclusive.

3.4.Remarks on rAAV-mediated and transgenic gene manipulation

One distinctive aspect of this thesis is the combined experimental work with two different methods for gene manipulation in the mouse brain. In the first part of my analyses, I studied the behavior of complete knockout mice for the AMPAR subunits GluA1 and GluA3. In the second part, I used stereotaxic rAAV-delivery to modify gene expression in BLA neurons. Both approaches can be successfully used to answer appropriate questions.

The generation of global knockout and transgenic mouse models revolutionized the study of the functions of single genes on behavior. It became possible to modify the expression of specific genes, in specific brain areas—forebrain (Shimshek et al., 2006), hippocampus (Niewoehner et al., 2007)—and in specific cell populations such as interneurons (Fuchs et al., 2007) or dopaminergic neurons (Lemberger et al., 2007). The generation of brain region-specific or cell-type-specific mouse lines is time-consuming and expensive, and the availability of such lines is still limited. Moreover, several different mouse lines typically need to be crossed, involving several generations, to be able to define the extent of a gene manipulation. For example, Cui and colleagues (2004) used four different lines for their reversible GluN1 forebrain knockout. The number of animals that need to be killed in such experiments is high. However, the reproducibility of the transgenic expression patterns is unprecedented with very low variability from animal to animal—a highly desirable property for behavioral analyses. Nevertheless, the most important drawbacks of the transgenic approaches in solving questions in neuroscience are whether the necessary mouse lines are available, and whether the mouse is the appropriate animal model for those questions.

Viruses manipulate their host cells in order to express genes that are important for their propagation. Therefore, they are logical candidates for use in molecular biology and neuroscience. However, most of the available recombinant viral vectors suffer from the toxic nature of their natural counterparts—e.g. lenti-, rabies, herpes virus. For this reason, rAAVs are an exceptional tool for gene manipulation in the brain, since they do not elicit toxic or inflammatory responses (Peel and Klein, 2000; Tenenbaum et al., 2004). A

great advantage of the use of rAAVs is the specificity of infection in the brain that can be achieved just by defining the stereotaxic coordinates of delivery (Cetin et al., 2006). Moreover, the number of animals required for a behavioral experiment is greatly reduced, since several rAAV vectors can be injected simultaneously, as I have shown in this thesis. Using select promoters to drive gene expression can further restrict the specificity of infection. The availability of such cell-type-specific promoters is a limiting factor, but the contents of the rAAV vector can be easily modified by molecular biology methods. The potential development of tissue-specific promoters for rAAV is further discussed in part II of this thesis. However, the ~4.7 kb packaging limit restricts the amount of genetic information that can be packed into one rAAV.

Another significant advantage of rAAV-based approaches with respect to transgenic methods is that rAAVs can be used to modify gene expression in different species, such as rats (Noordmans et al., 2004), macaques (Ciron et al., 2009), and humans (LeWitt et al., 2011), increasing the number of scientific questions that can be addressed. Nevertheless, rAAV-mediated gene delivery suffers from an important drawback, which is the high degree of inter-subject variability (see Appendix Figure 33). The quality and amount of virus injected plays an important role in determining this variation, since the spread of rAAV particles could result in anatomically adjacent brain areas being infected. In animal experiments, behavioral readout can be influenced by variables, such as the age and life history of the animals, and the testing context (Crabbe et al., 1999; Mandillo et al., 2008; McIlwain et al., 2001). Thus, the variability of infection from subject to subject is an important factor to be considered, but it can also provide valuable information as to what degree of correlation there is between the strength of a given manipulation and the behavioral outcome.

As more transgenic and viral tools become available and their limitations become clear, the combination of different methods will continue to provide more powerful applications in brain research.

Part Two:
An endogenous neuronal promoter for use in rAAV

4. Introduction

The mechanisms by which gene expression is regulated in different regions of the brain remain mostly unknown due to the highly complex nature of the processes involved. Despite this fact, the regulatory sequences present at the promoter regions of genes have long been exploited as an invaluable tool to drive expression of proteins in brain research. This approach has been of particular use in the generation of tissue-specific transgenic mice, with several limited examples available: forebrain (Mayford et al., 1996; Mayford et al., 1995), dentate gyrus (McHugh et al., 2007; Niewoehner et al., 2007), or CA1 and dentate gyrus (von Engelhardt et al., 2008). To exploit the transgenic use for the entire set of brain-specific promoters, the GENSAT project was founded. GENSAT generated hundreds of independent transgenic lines, which express the indicator protein GFP under the endogenous promoter of genes carried on recombinant BACs (Gong et al., 2003). This approach revealed several promoters that have highly specific expression patterns. However, it still requires expensive and time-consuming studies before it convincingly demonstrates that the GENSAT patterns can be reproduced in different constructs that rely on the very same BAC. Furthermore, a temporal control of gene expression is not possible, since most of the brain-specific genes are expressed already at early embryonic stages or start expressing in the first three postnatal weeks.

The use of rAAV-mediated gene delivery bypasses several of these problems by enabling expression of the genes of interest in a way that depends on the site and time of injection, which can be controlled. Use of rAAV vectors has been proven not to be toxic (Tenenbaum et al., 2004) and to produce a long-lasting expression of the delivered gene without triggering immune responses (Peel and Klein, 2000). Moreover, rAAV vectors do not integrate into the chromosomes of mice or do it with a very low frequency, reducing possible effects on the host cells due to integration (Nakai et al., 2001).

However, only a small number of promoters might be useful in the rAAV system due to the DNA-size packaging limit of around 5 kb. For this reason, cell-type-specificity remains an issue that needs considerable experimental investigation. The analysis of the conserved regulatory sequences of genes with particular expression patterns could lead to the finding of new promoter elements for use in rAAV vectors. This study proposes the *lynx2* promoter as a potential candidate for cell-type specific expression in the mouse.

4.1.Lynx2 as a member of the Ly-6/neurotoxin superfamily

Lynx2 belongs to the Ly-6/neurotoxin superfamily of proteins, which includes the snake venom neurotoxins and the mammalian ly-6 immune system genes (Gumley et al., 1995). Lynx2 was identified from embryonic ventral spinal cord cDNA and shares the same gene structure, sequence similarity and cystine-rich motif of the other members of the Ly-6/neurotoxin superfamily (Dessaud et al., 2006). The *lynx2* gene consists of 3 exons encoding a 141-amino acid protein with an N-terminal secretory signal sequence and a hydrophobic C-terminus with a glycosyl-phosphatidyl inositol anchor site (Udenfriend and Kodukula, 1995). Both mouse and human Lynx2 mature proteins have identical sequences.

In mice, *lynx2* mRNA is detected from embryonal day 9.5 in discrete neuronal populations along hindbrain and spinal cord and in specific brain structures after birth, namely, the CA1 region and the DG of the hippocampus and in some cells of the cerebellar granular layer and the cortical layers IV and V (Dessaud et al., 2006). In adults, there is also a strong expression in the lateral amygdala and the prefrontal cortex (Figure 22a, b, *stjudebgem.org*; *allenbrainatlas.org*). Previous efforts to generate BACs using *lynx2* by the GENSAT project (Figure 22c,d) and in our lab (Verena Bosch, Figure 22e) produced variable expression patterns. I used the rAAV approach to test if this variability, which is likely due to the different integration site of each BAC, could be eliminated.

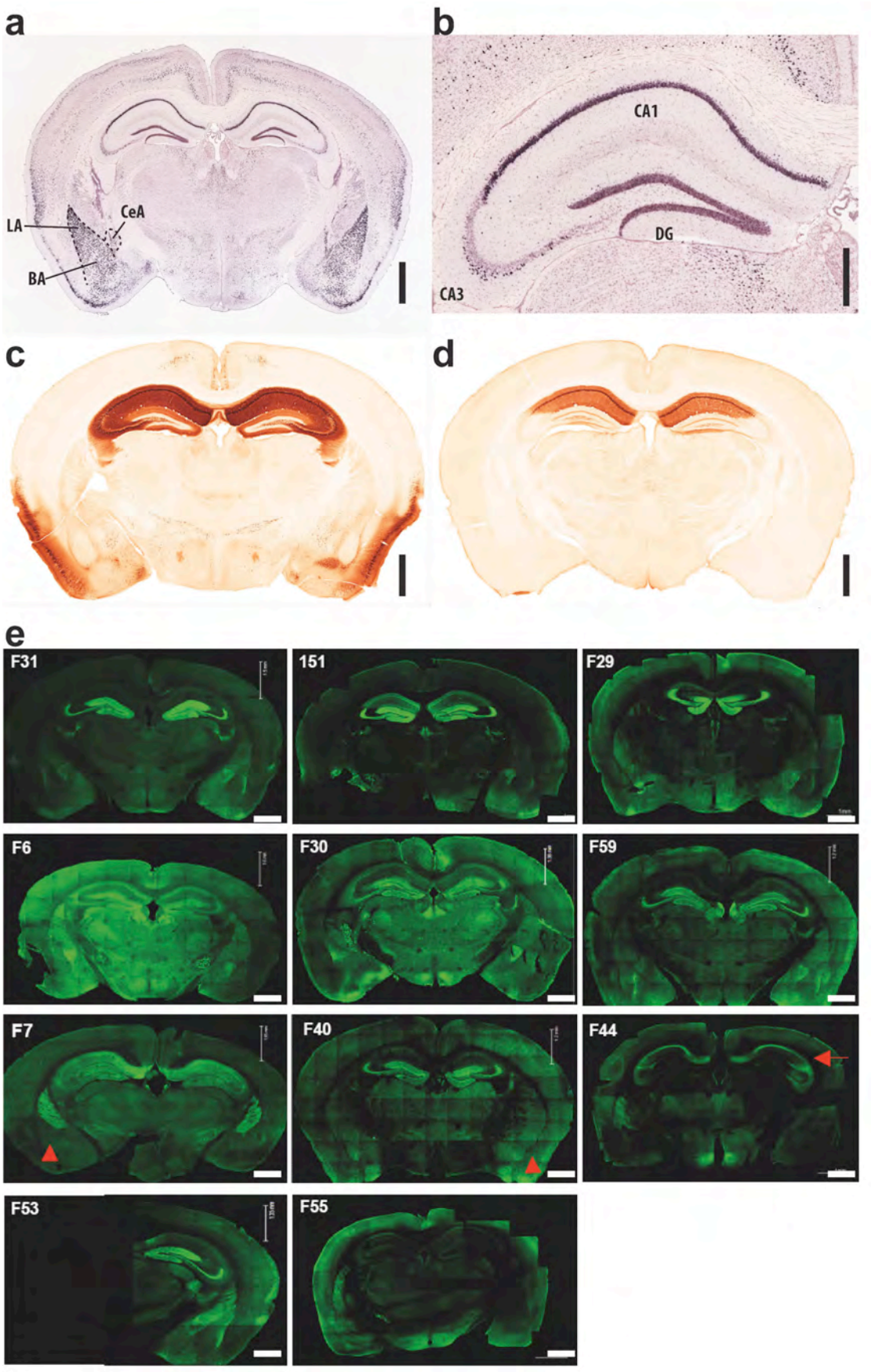

Figure 22. Endogenous expression of *lynx2* in the adult mouse brain as shown by *in situ* hybridization and examples of *lynx2* BAC expression studies

a, Coronal view of *lynx2* mRNA expression by non-radioactive *in situ* hybridization showing high levels in the lateral amygdala (LA), defined cortical layers and hippocampus. Scale bar, 1 mm. **b,** In the hippocampus, *lynx2* mRNA expression is limited to the dentate gyrus (DG) granule cells and the CA1 neurons. In CA3 only few cells are positive for *lynx2* mRNA signal. Scale bar, 500 µm. **c,** Cre immunostaining of *lynx2* BAC-Cre line NR149-CRE showing strong Cre expression in piriform cortex, CA1 and CA3, but not in DG or amygdala. Scale bar, 1 mm. **d,** Cre immunostaining of *lynx2* BAC-Cre line NR151-CRE with restricted Cre expression in CA1. Scale bar, 1 mm. **e,** GFP immunostaining of eleven *lynx2* BAC-GFP founder mice illustrating high variation of GFP expression. Scale bar, 1 mm. (a and b: adapted from the Allen Brain Atlas, *allenbrainatlas.org*; c and d: adapted from the GENSAT project, *gensat.org*; e: adapted from Verena Bosch, Inaugural Dissertation 2008).

Regarding the physiological role, Lynx2 binds and modulates nicotinic acetylcholine (ACh) receptors (nAChRs) *in vitro* by increasing receptor desensitization and decreasing ACh binding affinity (Tekinay et al., 2009). Knockout of Lynx2 is linked to increased anxiety behavior evidenced by fewer entries and time spent in the light compartment of a light-dark box and less time spent in the open arms of the elevated plus maze (Tekinay et al., 2009). Fear learning, as well, is strengthened in the passive avoidance task, and whereas contextual fear conditioning is normal, freezing levels in cued fear conditioning are higher in the knockout (Tekinay et al., 2009).

4.2. The lynx2 *promoter*

The murine *lynx2* gene is about 40 kb long and is located on chromosome 1, being antisense to an orphan G-protein associated receptor gene called GPR39 with a partially overlapping exon (exon 3 of *lynx2*). Interestingly, these two genes have seemingly mutually-excluding expression (Egerod et al., 2007). In order to identify the promoter region of the *lynx2* gene, I inserted a 1547bp fragment around the first exon into a rAAV vector in order to drive EGFP expression. For a quantitative analysis of different fragments of this promoter, I inserted upstream and downstream fragments of the exon into a luciferase-expressing construct (Nordeen, 1988) to quantify expression strength in HEK293 cells and rat hippocampal primary neurons. I further inserted the *lynx2* promoter into a rAAV for simultaneous expression of Cre recombinase and the fluorescent protein Venus linked by the self-cleaving 2A-peptide.

5. Results

The *lynx2* gene is localized on chromosome 1 of the mouse. It is an antisense gene with its first exon 1422 bp downstream from the first exon of the Nap5 gene (Figure 23a). Thus, we hypothesized that the promoter region should be at least in part contained within this intergenic region. Furthermore, the first exon of the *lynx2* gene mostly consists of an untranslated sequence with relatively high conservation among mammals (UCSC Genome Browser *genome.ucsc.edu*). Based on this, we hypothesized a 1547bp region around exon 1 as the promoter region for this gene (Figure 23b).

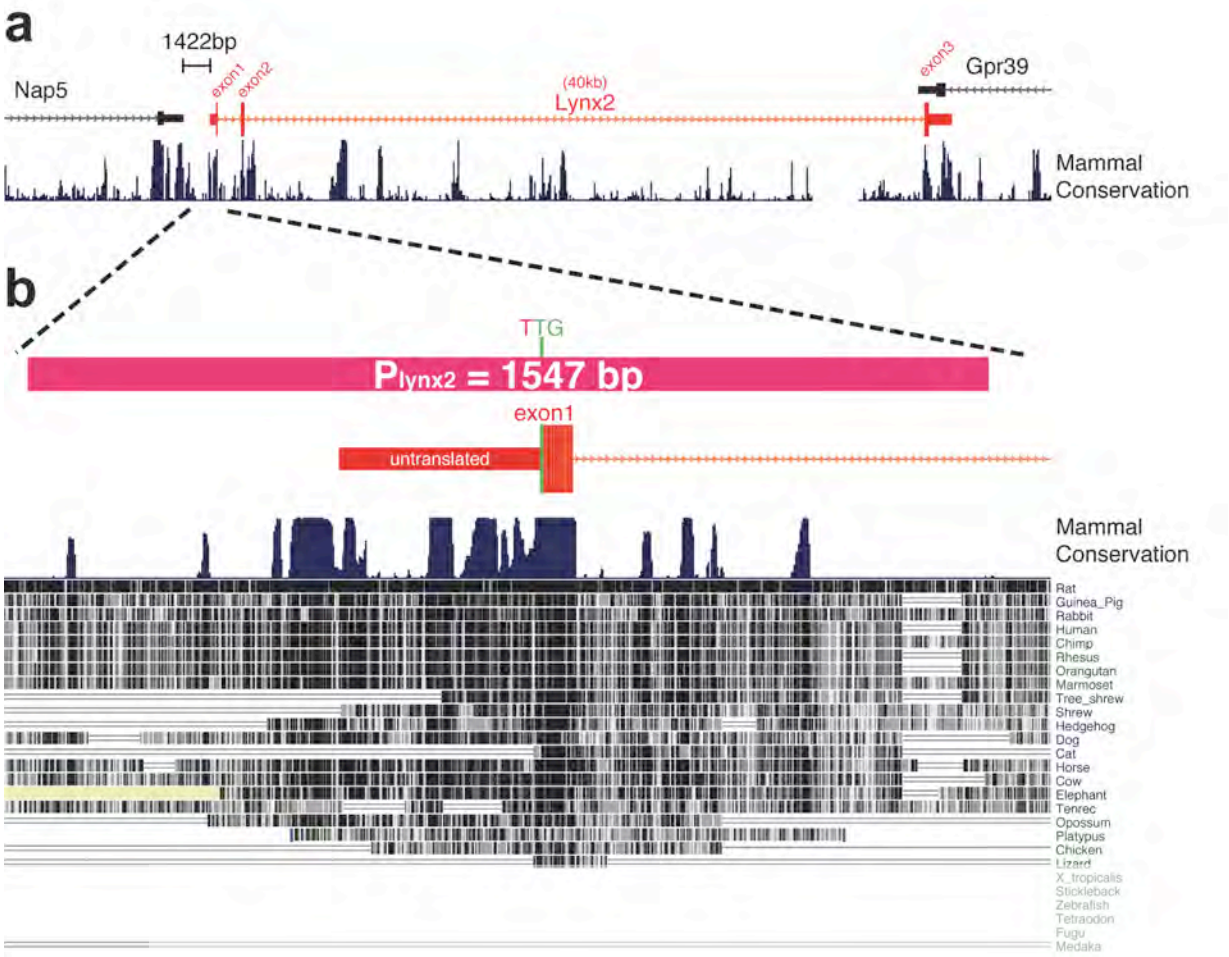

Figure 23. Scaled schematic representation of the *lynx2* gene neighborhood
a, The *lynx2* gene is an antisense gene located between the Gpr39 and the Nap5 genes. The three exons are indicated by the bold bars and the intronic regions in orange. A 1422 bp intergenic region precedes exon 1. Conservation across mammals is indicated below. **b,** Region of 1547 bp around the first exon of the *lynx2* gene proposed as the

promoter region. The mutated transcription initiation codon (TTG) is indicated. The 30-way mammal conservation analysis for this region is shown below (adapted from the UCSC Genome Browser *genome.ucsc.edu*).

5.1. Characterization of the lynx2 *promoter by rAAV delivery*

The 1547 bp *lynx2* promoter with mutated start codon (ATG to TTG) was cloned into an rAAV construct into the pAAV-6A-SEWB plasmid to drive the expression of EGFP (Figure 24a). Successful purification was evidenced by the presence of only three protein bands in an SDS-polyacrylamide gel, corresponding to the three capsid proteins VP1, VP2 and VP3 (Figure 24b). The virus was successfully tested in hippocampal primary neurons and an infectious titer of 4494 ± 606 neurons / µl was achieved (Figure 24c).

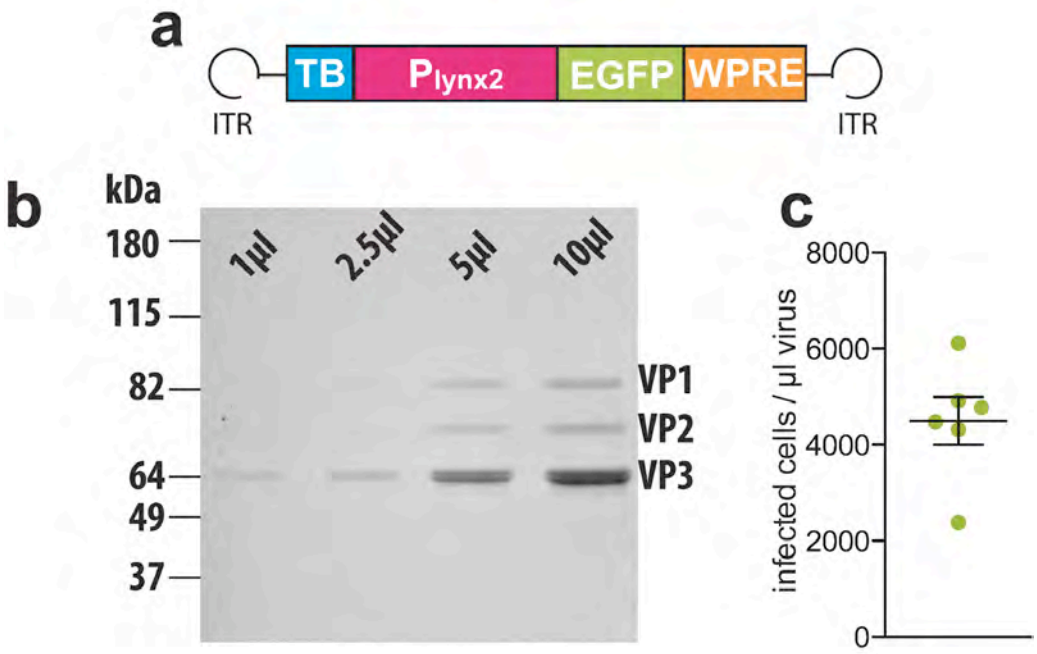

Figure 24. Characterization of rAAV-P$_{lynx2}$-EGFP
a, Scheme of the rAAV-P$_{lynx2}$-EGFP construct. Two inverted terminal repeats (ITRs) flank the packaged retion. A transcription block (TB) element precedes the promoter. The Woodchuck hepatitis virus post-transcriptional regulatory element (WPRE) was used to increase expression (Xu et al., 2001). **b,** SDS protein gel showing the three major bands corresponding to the rAAV packaging proteins in the purified preparation (VP1, VP2, VP3); the loaded volume is indicated. **c,** Mean infectious titer for the rAAV preparation of 4494 ± 606 infected primary neurons per microliter of virus. Scale bar, 200 µm.

Then, rAAV-P*lynx2*-EGFP was injected into the lateral ventricles and both hippocampi of P0 mice to achieve global brain infection and be able to test whether the presence of the *lynx2* promoter gives any specificity to the expression of EGFP. Examination of the brains of the injected pups at day P21 showed a marked specificity of EGFP fluorescence in the DG of the hippocampus as well as in a defined region of the neocortex corresponding to layer VI (Figure 25a, b). However, scattered cells also expressed EGFP in area CA1 of the hippocampus and other layers of the cortex. In the DG, EGFP was expressed throughout its dorso-ventral axis (Figure 25d). In cortical layer VI, the whole antero-posterior axis showed expression of EGFP (Figure 25c, d).

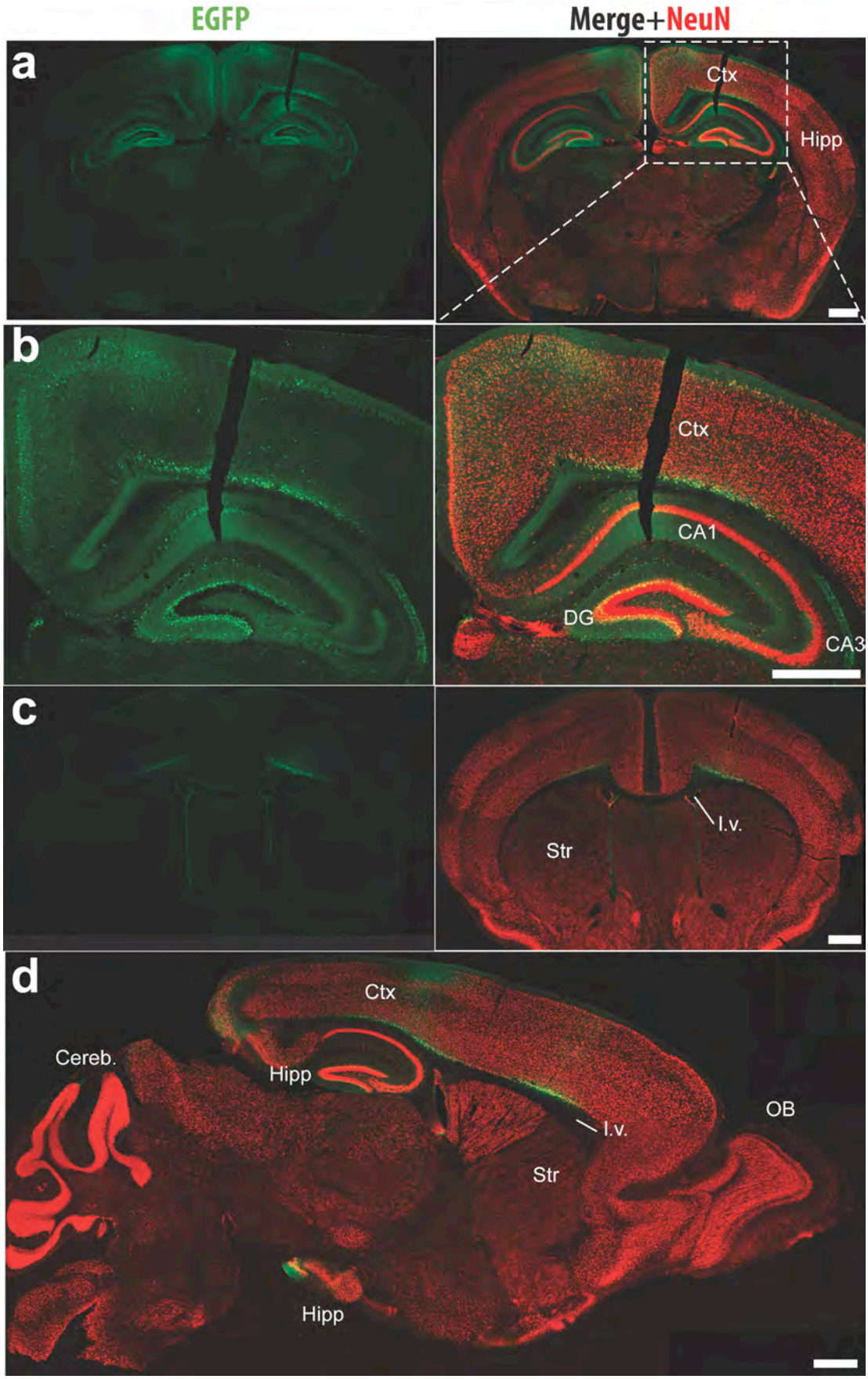

Figure 25. EGFP expression pattern driven by the *lynx2* promoter after P0 brain injection in mice analyzed at P21

a, Coronal slicing revealed strongest EGFP expression in DG as well as in cortical layer VI. **b,** Detailed view showing main expression in DG granule cells and cortical layer VI, as well as sparse neurons in other cortical layers, and regions CA1 and CA3 of the hippocampus. **c,** Cortical slicing at the level of the lateral ventricles reveals EGFP expression lining the ventricle walls and the cortical layer VI. **d,** Sagittal slicing showing EGFP expression in hippocampal DG and in cortical layer VI along the whole antero-posterior length. Ctx: cortex; Hipp: hippocampus; Cereb: cerebellum; Str: striatum; l.v.: lateral ventricle; OB: olfactory bulb. DG: dentate gyrus. All scale bars, 1mm.

To test the tissue specificity of rAAV-P$_{lynx2}$-EGFP in the adult mice, 10-week-old males were injected unilaterally into DG, CA1 regions and cortex (Figure 26a). At post-injection day 14 (PId14), EGFP expression was strongest for DG granule cells and layer VI. Otherwise, scattered single neurons were fluorescent in several regions of the cortex and hippocampal CA1 region. DG granule cell labeling was strong enough to conspicuously label mossy fibers and terminals at the CA1 region more ipsilaterally but also contralaterally. Interestingly, after intra-amygdala injection, a strong expression in the lateral amygdala (LA) could not be observed, on the contrary, the EGFP expression was lower in LA than in the adjacent piriform cortex or central amygdala (Figure 26b).

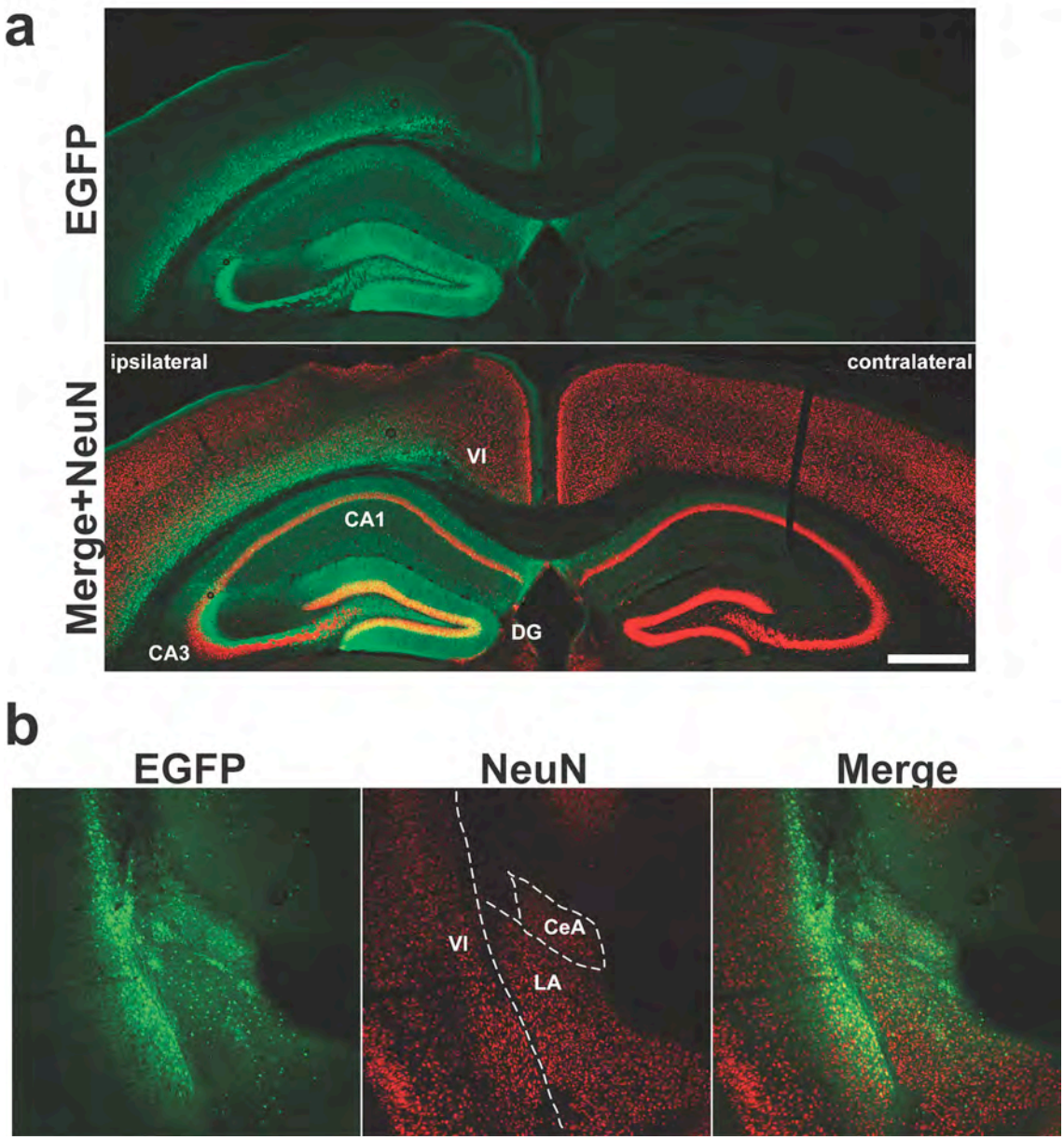

Figure 26. EGFP expression after unilateral rAAV injection in adult mice analyzed at PId14

a, After intra-hippocampal and intra-cortical rAAV-P_{lynx2}-EGFP injection, robust EGFP expression is evidenced in the DG granule cells as well as in cortical layer VI (VI). EGFP fluorescence is also strongly seen in the mossy fibers. Fluorescence is also seen more weakly in fibers of the contralateral uninjected hippocampus. **b,** Intra-amygdala injection of rAAV-P_{lynx2}-EGFP showed no specific expression of EGFP in the lateral amygdala (LA). In the amygdaloid complex, best expression was found in the central amygdala (CeA). Scale bar, 1mm.

To assess whether neural types other than neurons were also infected by rAAV-P$_{lynx2}$-EGFP, immunostaining against the glial cell marker glial fibrillary acidic protein (GFAP) was performed, revealing no colocalization with EGFP-expressing cells, which were only positive for the neuronal marker NeuN (Figure 27a, b). This holds true for all injection sites tested.

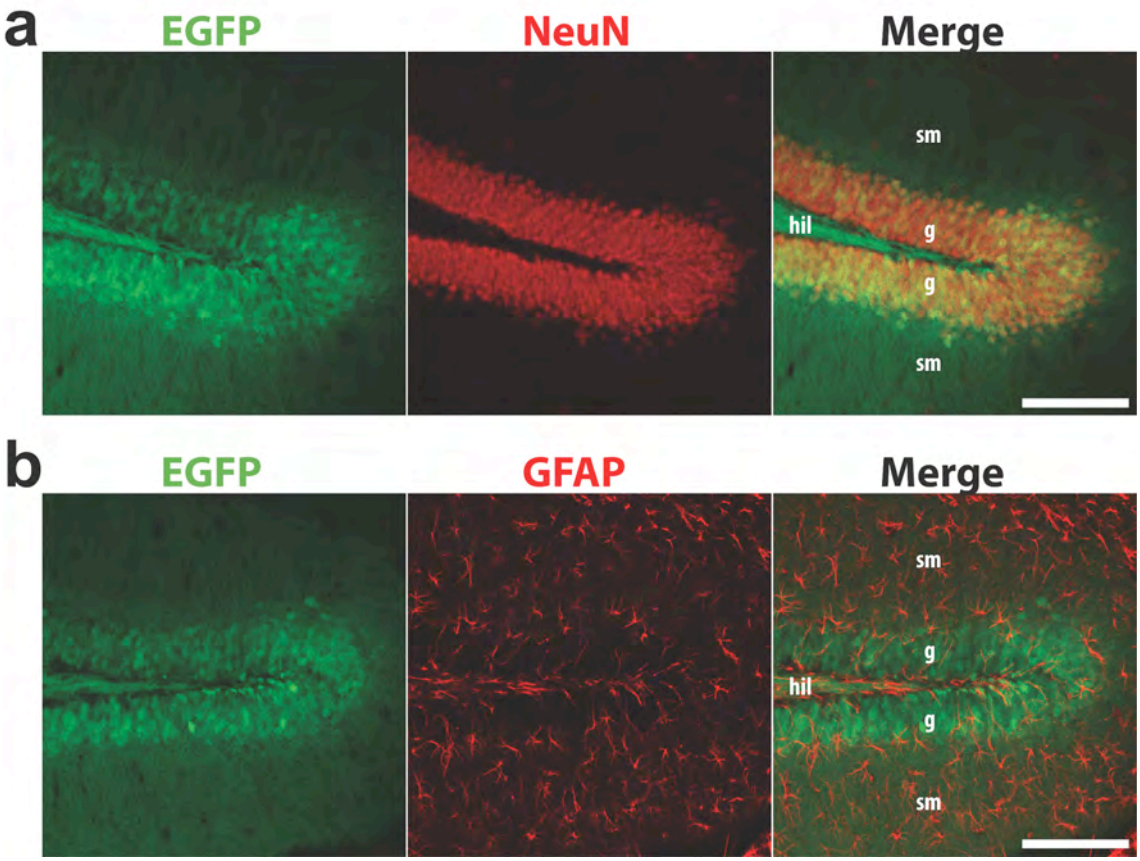

Figure 27. The *lynx2* promoter drives expression of EGFP in neurons but not in astrocytes in the DG
a, Only NeuN-positive cells show expression of EGFP driven by the *lynx2* promoter in the DG. **b,** GFAP-positive cells do not express EGFP under the *lynx2* promoter in the DG. The pictures correspond to adult-injected mice analyzed at PId14. sm: Stratum moleculare; g: granule cell layer; hil: hilus. Scale bars, 200 µm.

Further analysis revealed no major colocalization of infected neurons with the interneuronal marker parvalbumin, neither in P0 nor in adult injected mice (Figure 28a, b). Calbindin-positive EGFP-expressing neurons were only present in the DG as expected, since mature granule cells are known to express this marker (Rami et al., 1987). Remarkably, in P0-injected mice, only the superficial layers of the DG granule cells showed EGFP expression at P21, with the inner layers showing no green fluorescence. In contrast, in adult mice,

nearly all mature calbindin-positive neurons expressed EGFP at PId14. For layer VI neurons, no obvious difference was observed between P0- and adult-injected mice.

In conclusion, the *lynx2* promoter is able to drive rAAV-mediated EGFP expression in mature principal neurons located primarily in DG (granule cells) or layer VI of the neocortex.

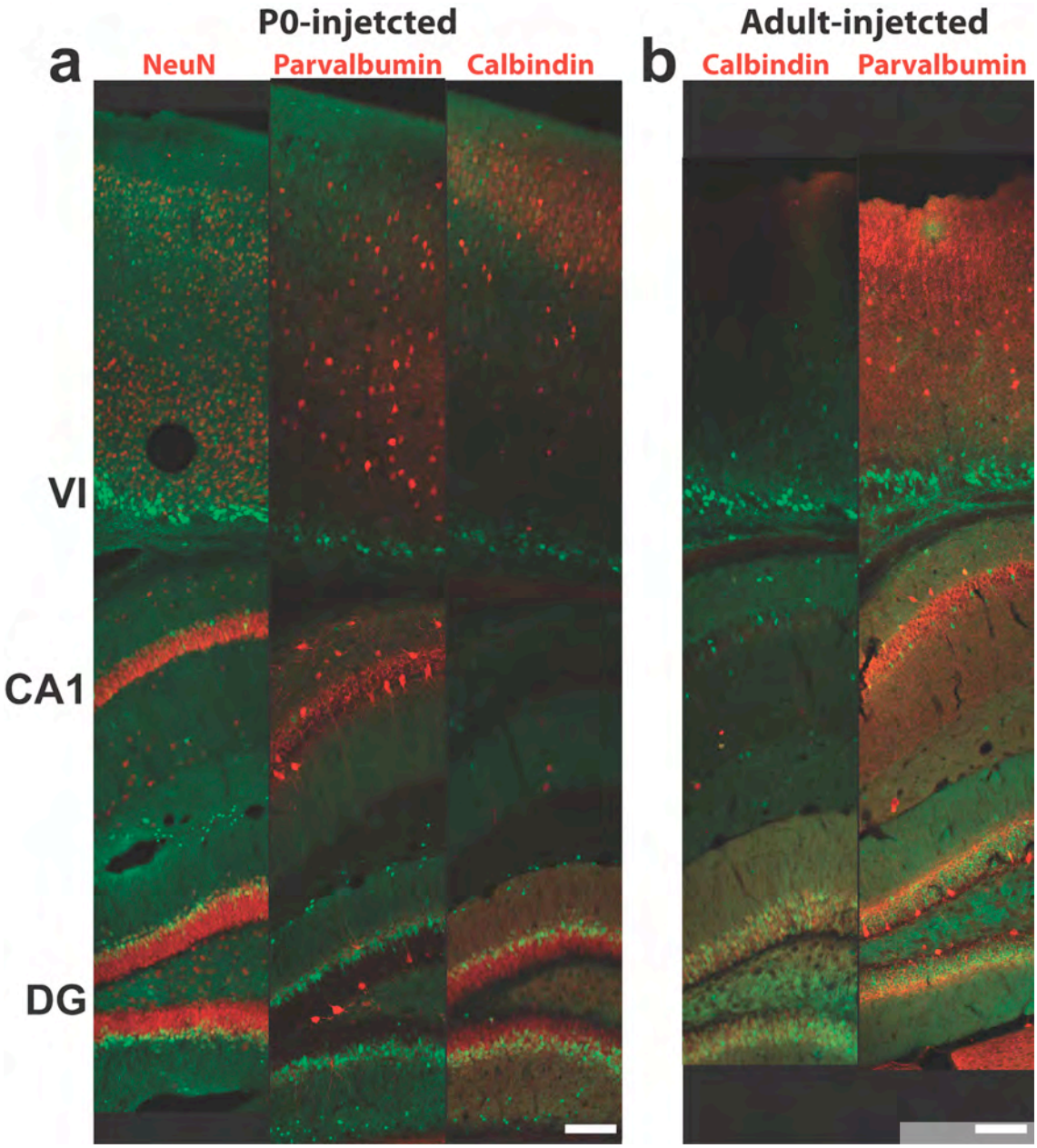

Figure 28. Neuronal and interneuronal marker immunostaining after rAAV-P$_{lynx2}$-EGFP infection in DG, CA1 and cortex
a, EGFP expression (green) and immunostaining (red) against the neuronal marker NeuN and the interneuronal markers parvalbumin and calbindin of P0-injected mice analyzed at P21. **b,** Calbindin and parvalbumin immunostaining of adult-injected mice analyzed at PId14. Scale bar, 200 µm

5.2. Quantification of gene expression under the **lynx2** *promoter*

In order to quantify the amount of expressed protein under the *lynx2* promoter and to test whether the promoter length can be reduced without losing neuronal specificity, a dual luciferase assay was performed. The 1547bp *lynx2* promoter was cloned into a firefly luciferase-expressing plasmid pXP1 or pXP2 (Nordeen, 1988). Additionally, a version of the *lynx2* promoter with an intact start codon (1547 bp +ATG) in which expression of EGFP should be disrupted, as well as three different fragments of the total length of the promoter (800 bp, 500 bp, 700 bp), was also cloned into the pXP1 or pXP2 promoter canning vectors (Figure 29a). Moreover, CMV-firefly luciferase and Syn-firefly luciferase plasmids were also used for comparison as examples of strong promoters.

Cotransfection of each of the constructs with a CMV-*Renilla* luciferase plasmid in HEK293 cells and hippocampal primary neurons was used to normalize the effects of transfection efficiency by calculating a firefly-to-*Renilla* luciferase activity ratio (Figure 29b). In HEK293 cells, all tested promoters were less than 1% as strong as the CMV promoter, whereas in hippocampal primary neurons, both the Syn and the CMV promoter had comparable activity levels. A closer look to luciferase activity in HEK293 cells shows that the 1547 bp *lynx2* promoter is very weakly expressed in these cells, with similar levels as the ATG-truncated version and the promoter-less pXP1 vector. However, all three *lynx2* promoter 800 bp, 500 bp and 700 bp fragments produced higher levels of luciferase expression, which in the case of the 800 bp fragment were as high as for Syn. Very similar results were obtained in hippocampal primary neurons, where the *lynx2* promoter fragments produced luciferase activity levels between three and ten times higher than the complete 1547 bp *lynx2* promoter or all other constructs compared. In conclusion, the use of fragments smaller than the initially hypothesized *lynx2* promoter decreases the specificity by enhancing expression in cultured cells without tissue properties.

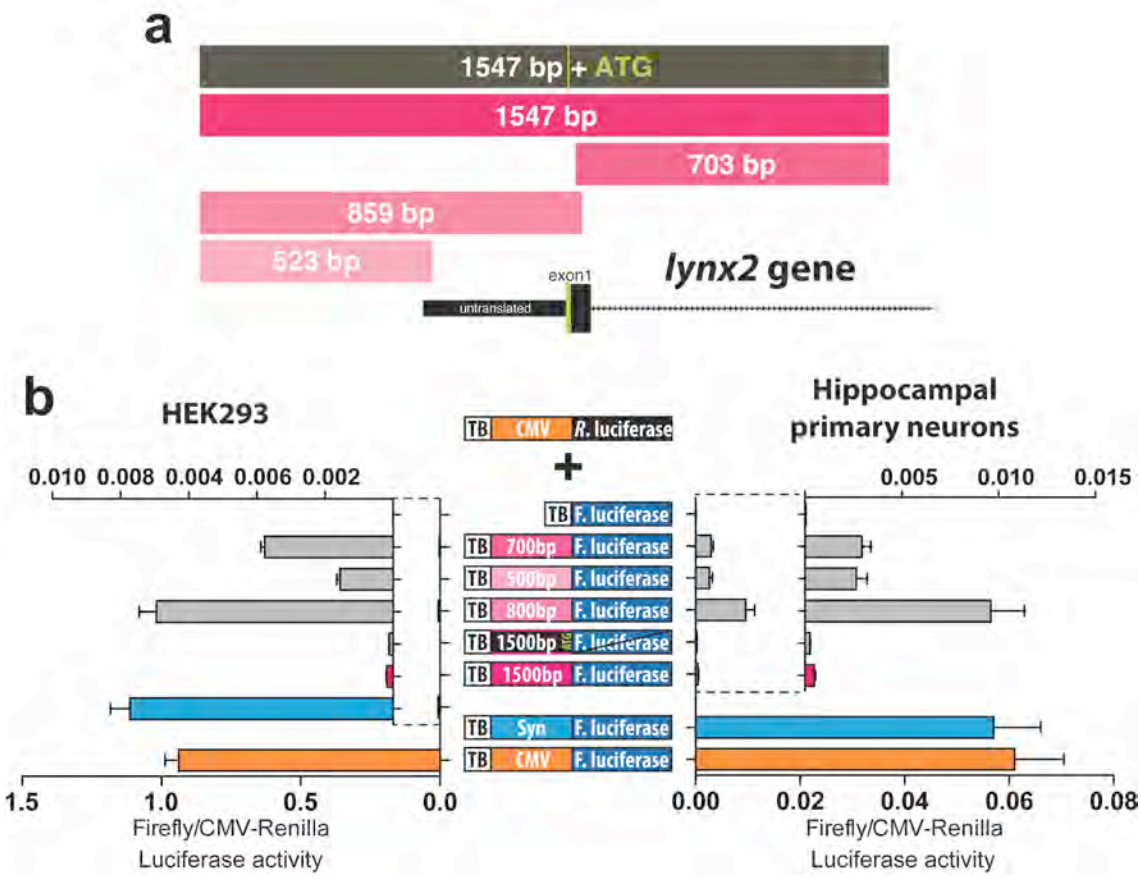

Figure 29. Quantification of protein expression under different fragments of the *lynx2* promoter by dual luciferase assay
a, Scheme of the 1547 bp P_{lynx2} and its different fragments cloned, as well as the truncated version of the promoter with intact ATG (in green). The relative position of the first exon of the *lynx2* gene is shown below. **b,** Firefly-to-*Renilla* luciferase activity ratio in HEK293 cells or hippocampal primary neurons transfected with different promoter constructs. Cells were cotransfected with a CMV-*Renilla* luciferase plasmid and one construct for Firefly luciferase expression under a number of different promoters including CMV, Syn, P_{lynx2} or fragments from it, or a promoter-less pXP1 construct.

5.3. *Expression of Cre recombinase under the* lynx2 *promoter*

The Cre-loxP system allows for great flexibility to genetically modify mice in a controlled manner. Therefore, a rAAV construct for expression of Cre recombinase was cloned under the promoter of the *lynx2* gene: rAAV-P_{lynx2}-iCre2A-Venus. To test if this virus could be used to induce recombination, rAAV-P_{lynx2}-iCre2A-Venus was injected into the hippocampus and amygdala of 12-week-old Cre indicator mice (*Rosa26-lacZ*$^{2lox/2lox}$; Soriano, 1999). After successful recombination, the cells of these mice express beta-galactosidase, an enzyme that catalyzes the hydrolysis of X-gal to yield a blue

product, which can be detected with high sensitivity. The results of the analysis at PId21 show that the highest expression of Cre occurs in the DG, correlating with the expression of Venus, which is linked to Cre by the 2A peptide (Figure 30a). In the CA1 and cortical areas, Cre was only weakly expressed, but these low levels were sufficient to drive full recombination of the loxP sites and expression of beta-galactosidase, as evidenced by immunostaining (Figure 30b) and by X-gal staining (Figure 30c). Additionally, injection of this AAV into the amygdala triggered recombination in amygdala neurons as well as in adjacent cortical and striatal areas.

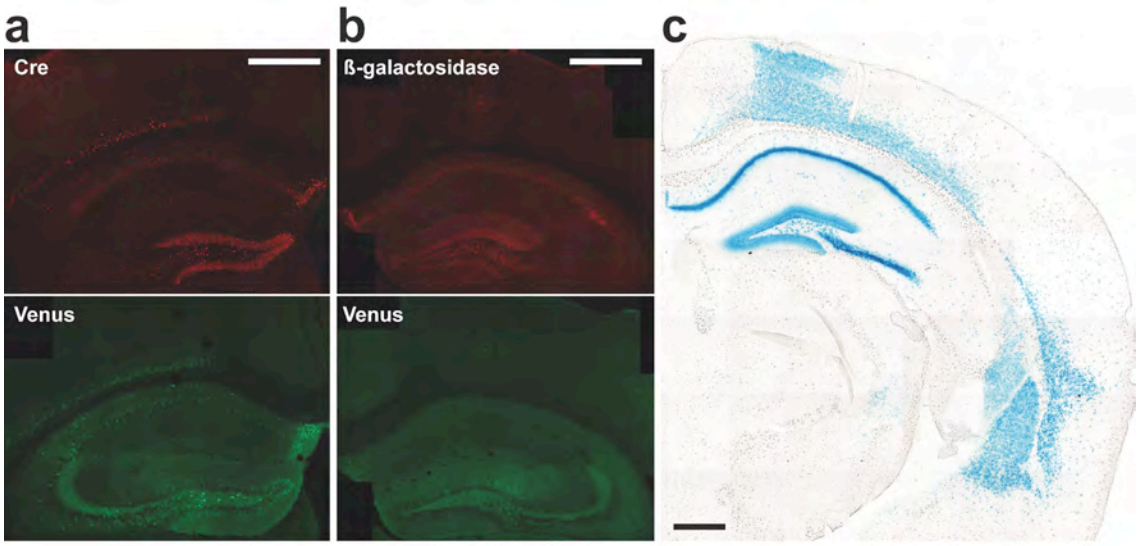

Figure 30. Expression profile induced by rAAV-P$_{lynx2}$-iCre2A-Venus in *Rosa26-lacZ*$^{2lox/2llox}$ mice analyzed at PId21
a, Immunostaining against Cre recombinase shows that the highest levels of expression occur in the DG, with weaker and more sparse expression in CA1 and cortex. **b,** immunostaining of beta-galactosidase reveals higher expression in the DG than in other areas. **c,** X-gal staining shows that both regions with high and low expression of Cre under the *lynx2* promoter show complete recombination. Scale bars, 500 µm.

6. Discussion

The regulation of gene expression is a highly complex process that occurs at different cellular levels. At the level of DNA, promoters play a significant role in driving expression of genes by acting as binding sites for transcription factors (Smale and Kadonaga, 2003), or sites of epigenetic regulation by DNA methylases (Bird, 2002). However, little is known about the properties of neuronal specific promoters and their cell-type specificity. In the present work, I attempted to use the promoter region of a CNS-specific gene to generate a rAAV vector with specific expression in the BLA.

The *lynx2* promoter was chosen because *in situ* hybridization studies (Allen Brain Atlas, *allenbrainatlas.org,* Figure 22) of the expression of *lynx2* mRNA in mice have shown that this gene is highly expressed in the BLA, in addition to the hippocampal dentate gyrus and CA1 region (Dessaud et al., 2006). Surprisingly, when a ~1.5 kb region was cloned for use as a promoter of a gene of interest in a rAAV vector, the specificity of the expression was restricted to the hippocampus, and in particular, the dentate gyrus. First, I will elaborate on the general characteristics of the cloned P_{lynx2}.

The promoter activity of the *lynx2* gene fragment cloned was confirmed by the successful expression of EGFP by rAAV-mediated delivery to primary cultured neurons (Figure 24). Transcription of the gene of interest depends on the binding of the RNA polymerase and a series of transcription factors that are essential for this process (Smale and Kadonaga, 2003). Therefore, the evidence of expression under the cloned *lynx2* gene region supports our speculation that promoter activity is present within the ~1.5 kb sequence.

The first remarkable property of the *lynx2* promoter is its neuronal specificity (Figure 27, Figure 28). This was evident in all injected mice and was independent of the virus preparation. Few rAAV-promoters are known to have specific neuronal expression. Among these, the synapsin promoter is the most widely used, and although it has the advantage of driving strong levels of expression in neurons, it lacks any brain-region specificity in rAAV vectors.

Other promoters, such as CMV, elongation factor 1α (EF1α), or CAG, also drive expression in glial cells in addition to neurons (Alexopoulou et al., 2008; Kuroda et al., 2008). Therefore, the neuron specificity of P_{lynx2} indicates that it preserves some of the native properties of the complete *lynx2* endogenous promoter.

The injection of rAAV-P_{lynx2}-EGFP into the brains of newborn mice was used as a means of testing in which brain regions there was expression driven by the promoter, when a broad volume of the brain was exposed to infectious rAAV particles. Previous studies have shown that bilateral injection into the lateral ventricles with rAAVs can produce widespread infection extending to the olfactory bulb and the cerebellum (Pilpel et al., 2009). P_{lynx2}-driven EGFP expression was limited almost exclusively to the hippocampus and deeper layers of the neocortex (Figure 25). In particular, DG granule cells showed strong fluorescence, while only a small portion of the CA1 closest to the site of injection showed EGFP expression. This is a stringent test of brain region specificity showing evidence of the hippocampus-linked expression driven by P_{lynx2}. On the other hand, no EGFP expression was found in the BLA, which was the original region of interest for gene manipulation by rAAVs.

In order to test whether this expression pattern was the same in adult mice, rAAV-P_{lynx2}-EGFP was injected into the hippocampus and the BLA showing that, indeed, there is a preferential expression in DG granule cells (Figure 26). In the BLA, the fluorescent signal was observed in an unspecific way in neurons of the injected area, being higher in areas surrounding the BLA, in a pattern different from the endogenous mRNA expression of the *lynx2* gene. This surprising fact suggests that the transcription factors that drive the specific expression of *lynx2* in BLA neurons do not bind to the ~1.5 kb sequence cloned as P_{lynx2}. It is likely that there are other upstream or downstream intergenic or intronic sequences that are responsible for regulating expression of *lynx2* in the BLA. This is in line with the presence of highly conserved intronic regions for this gene in different species. The engineering of additional versions of P_{lynx2} containing additional conserved regions could help to identify the factors behind expression in the BLA.

Remarkably, the comparison of P0 and adult-injected mice showed that the number of neurons that showed Plynx2-driven EGFP expression was different (Figure 28). In P0-injected mice, only the outer layers of the DG were EGFP-positive when analyzed at P21. In a pattern coinciding with that of granule cell neurogenesis (Zhao et al., 2008), it can be postulated that only the younger DG neurons did not express EGFP. It can be inferred that at the time of injection, rAAV-P_{lynx2}-EGFP was only able to transduce mature neurons in the DG, whereas immature neuronal precursors, which constitute the inner border of the granule cell layer were either not infected or did not express EGFP. In adult-injected mice, after 14 d post-injection, nearly all mature (calbindin-positive) granule cells are EGFP-positive. This is in line with the view that only mature neurons can be manipulated by rAAVs, because DG granule cell neurogenesis occur at a much lower turnover rate as age increases (Lazic, 2011), being fastest in newborn mice. This could have important applications in systematic studies of the rate of DG neurogenesis.

By using a luciferase assay to quantify the expression driven by P_{lynx2}, as well as several promoter fragments of smaller size, I found that the entire ~1.5 kb sequence was necessary to retain tissue-specificity (Figure 29). Smaller fragments of the promoter in plasmids also gave rise to the expression in dissociated neuron cultures and in non-neuronal HEK293 cells. This could be explained by the hypothesis that the smaller fragments all have promoter activity, in the sense that they can help transcription initiation, but they correspond to binding sites for ubiquitous transcription factors required for generalized expression.

The DG-specificity of expression driven by P_{lynx2} is not exclusive and a lower EGFP signal was also observed in some neurons of the CA1 or cortical regions. Therefore, a rAAV for P_{lynx2}-driven expression of Cre and Venus was tested in *Rosa-lacZ*$^{2lox/wt}$ mice (Soriano, 1999). Recombination was observed in the hippocampus, cortex and amygdala, without regional specificity (Figure 30). Due to the enzymatic reaction that lacZ detection relies on, the sensitivity of the staining is higher than that of fluorescent reporter proteins. Furthermore, since the triggered expression of beta-galactosidase is an 'all-or-none' effect,

low- and high-expressing cells are detected by the same lacZ staining intensity, revealing the maximal population of cells expressing the virally transduced P_{lynx2}-driven gene. In contrast, when the effects of the gene of interest depend on the amount of expression, P_{lynx2} is an excellent candidate for specific targeting of DG, since the expression in granule cells is higher than in surrounding regions. Thus, genes for fluorescent proteins or with dominant negative mutations can be directed specifically to the DG.

Nevertheless, not only the base pair sequence in a promoter region determines the levels of gene expression. Epigenetic modifications, such as DNA methylation can also determine whether a gene is expressed or not. There is increasing evidence that rapid changes in DNA methylation occur during the adult life, for example during learning (Miller and Sweatt, 2007). Therefore, it is a factor that should be kept in mind when working with endogenous promoters, in particular, for gene-transfer vectors that integrate into the genome, such as those based on lenti- and retroviruses. However, it is not resolved yet, whether extrachromosomal gene copies of rAAVs are targets for DNA modifying enzymes. Moreover, beyond the DNA sequence within the virus, the serotype of the rAAV greatly influences the infectivity, and is always discussed as an important factor controlling the specificity of infection (Sin et al., 2005). In addition, virus titer and the purification procedure can influence the specificity of infection. The impact of both variables, serotype and purification method, on the cell-type specificity in rAAV gene-transfer studies remains to be investigated on a systematic level.

7. Materials and Methods

7.1.Materials

7.1.1. Laboratory equipment and materials

Table 3. List of reagents and manufacturers

Chemicals, reagents, media	Manufacturer
Acetic acid	Sigma
Acrylamide	BioRad
Agarose	Invitrogen
Ammonium persulfate	Sigma
Ampicilline	Sigma
Aqua Polymount	Polysciences
B27 supplement	Gibco
BCA solution	Sigma
Benchmark Pre-Stained Protein Ladder	Invitrogen
Beta-mercaptoethanol	Sigma
Bovine serum albumin	Sigma
Bradford solution	BioRad
Brilliant blue (Coomassie)	Serva
Bromo-chloro-indolyl-galactopyranoside, X-gal	Gerbu
Bromophenol blue	IBI
Chloramphenicol	Roche
Copper (II) sulfate solution	Sigma
Cytosine arabinoside	Sigma
D-Glucose	Roth
DAPI	Sigma
Diaminobenzidin	Fluka
Diphtheria toxin	Sigma
Doxycycline hyclate	Sigma (D9891)
Ethanol	Sigma
Ethidium bromide	Serva
Formamide	Fluka
Glycerol	Roth
Glycine	Gerbu
HEPES	Gerbu
Horse serum	Gibco
Hydrogen peroxide	Sigma
Isoflurane	Baxter
Isopropanol	Merck
Kanamycine	Sigma
Ketamine (Ketavet®)	Inversa
Kumasi brilliant blue	Serva

Licain, lidocaine	Delta Select
Lipofectamine2000	Invitrogen
Magnesium chloride	Merck
Methanol	Merck
Minimum essential medium	Gibco
Neurobasal medium	Gibco
Nitrocellulose membrane	Whatman, Protran
Normal goat serum	Vector
Paraformaldehyde 37 %	Merck
Passive lysis buffer	Promega
Penicillin/Streptomycin	Gibco
Poly-L-lysine	Sigma
Potassium chloride	Roth
Potassium ferricyanide	Sigma
Potassium ferrocyanide	Sigma
Protein standard	BioRad
Regenerated cellulose filter	Amicon, Millipore
SDS	Merck
Sodium acetate	Merck
Sodium azide	Merck
Sodium chloride	Merck
Sodium deoxycholate	Sigma
Sucrose	Sigma
TEMED	BioRad
Tetracycline	Sigma
Tris-HCl	Roth
Triton X-100	Sigma
Trizma base	Sigma
Xylazine (Rompun®)	Bayer

Enzymes	**Manufacturer**
Benzonase	Sigma
Escherichia coli Klenow DNA polymerase I	Roche
Phusion DNA polymerase	NEB
Proteinase K	Roche
Restriction endonucleases	NEB/Fermentas
T4 DNA ligase	Roche
Taq DNA polymerase	Gibco BRL

Bacterial cells	**Manufacturer**
TOP10	Invitrogen
SURE® 2 supercompetent cells	Stratagene

Antibodies	**Manufacturer**
Mouse monoclonal antibody against NeuN	Chemicon, 1:1000
Rabbit polyclonal antibody against Cre recombinase	Covance, 1:1000
Rabbit polyclonal antibody against GluA1, ab31232	Abcam, 1:500
Rabbit polyclonal antibody against GFAP	Dako, 1:600
Rabbit polyclonal antibody against beta-Galactosidase	Cappel, 1:500
Peroxidase-coupled goat anti-rabbit antibody	Vector Laboratories, 1:600
FITC/Cy3-coupled goat anti-mouse antibody	Jackson ImmunoResearch, 1:250
FITC/Cy3-coupled goat anti-rabbit antibody	Jackson ImmunoResearch, 1:250

Virus purification equipment	**Manufacturer**
Heparin columns	Amersham
Sepharose columns	Amersham
ÄKTAprime plus HPLC setup	General Electric
Amicon Ultra Concentrator	Millipore

Kits	**Manufacturer**
HiSpeed® Plasmid Maxi kit	QIAGEN
Dual-Luciferase® reporter 1000 assay system	Promega
QIAprep® Spin Miniprep kit	QIAGEN
QIAquick® Gel Extraction and PCR purification kit	QIAGEN
QuantiPro™ BCA assay kit	Sigma
Zero Blunt TOPO PCR cloning kit	Invitrogen

Laboratory equipment	**Manufacturer**
Avanti™ J-25 Centrifuge	Beckman
BioFix® Lumi-10 luminometer	Macherey-Nagel
Coverslips	Roth
Fear-conditioning system 303410-BOX-MAU	TSE
LAS-3000 intelligent dark box	Fujifilm
Milli-Q water purification device	Millipore
Passive-avoidance tower 256005M	TSE
Stereotaxic Apparatus	Kopf
Veriti 96 well thermal cycler	Applied Biosystems
Versamax tunable microplate reader	Molecular Devices
Vibratome VT1000S	Leica

Microscopy equipment	Manufacturer
Zeiss Axio Imager M1	Carl Zeiss
Zeiss LSM5 PASCAL	Carl Zeiss
Argon laser (457, 476, 488, 514 nm), Helium Neon laser (543 nm)	Lasos Lasertechnik

Software	Manufacturer
A plasmid Editor	M. Wayne Davis
Gene Construction Kit	Textco BioSoftware
Illustrator CS4	Adobe
ImageJ	National Institutes of Health
Leica Confocal Software	Leica
MATLAB	Mathworks
Photoshop CS4	Adobe
Prism v5.0c	GraphPad Software Inc.
R	The R Foundation for Statistical Computing
VideoMot 2	TSE

7.1.2. Buffer compositions

Table 4. List of components and concentrations of the buffers used in this work.

10x DNA loading buffer	30% glycerol, 0.25% bromophenol blue, 0.25% Xylencyanol, 25 mM EDTA
5x Laemmli buffer	60 mM Tris-HCl pH 6.8, 2% SDS, 10% glycerol, 5% beta-mercaptoethanol, 0.01% bromophenol blue
Growth medium	Neurobasal Medium, 2% B27 Supplement, 0.25% L-Glutamine, 1% Penicillin/Streptomycin
PBS	137 mM NaCl, 2.7 mM KCl, 1.4 mM KH_2PO_4, 4.3 mM NaH_2PO_4, pH7.4
PBS-MK	1 mM $MgCl_2$, 2.5 mM KCl, 1x PBS
PBS/Hepes/Glucose	30 mM HEPES, 33 mM Glucose, 1x PBS
Plating medium	Minimum Essential Medium with Earl's salt, 10% Fetal Bovine Serum, 0.5% Glucose, 100 mM Sodium pyruvate, 1% Penicillin/Streptomycin, 0.11% L-Glutamate
Resolving gel	375 mM Tris-HCl pH 8.8, 8% acrylamide, 0.1% SDS, 0.06% TEMED, 0.06% Ammonium persulfate
Stacking gel	125 mM Tris-HCl pH 6.8, 3.9% acrylamide, 0.1% SDS, 0.12% TEMED, 0.06% Ammonium persulfate
TAE buffer	40 mM Tris, 5 mM sodium acetate, 2 mM EDTA, pH 8.3
TENS Buffer	100 mM Tris-HCl pH 8.0, 5 mM EDTA, 200 mM NaCl, 0.5% SDS
TNT buffer	20 mM Tris, 150 mM NaCl, 1% TritonX-100, 10 mM $MgCl_2$ (pH 7.5)

7.2. *Animals*

7.2.1. Legal aspects

All procedures were performed in accordance with the Tierschutzgesetz, 25.05.1998, last change 21.06.2005: the national German law for protection of animals that also regulates experiments with animals Az: G56/05.

7.2.2. Housing

Mice were housed individually or in groups of 2–6 subjects in Makrolon type IIA cages. Room temperature was 21-23 ºC and humidity 90%. A circadian rhythm of 12 h / 12 h was maintained with light phase starting at 8 a.m. All experiments were performed during the light phase. Food and water were available *ad libitum* unless otherwise indicated.

Table 5. List of mouse lines analyzed in this thesis including reference.

Mouse line	Reference / Provider
C57Bl/6N	Charles River
GluA1$^{-/-}$	Zamanillo et al., 1999
GluA1$^{2lox/2lox}$	Zamanillo et al., 1999
GluA1$^{R/R}$	Vekovischeva et al., 2001
GluA3$^{-/-}$	(Sanchis-Segura et al., 2006)
GluN1$^{2lox/2lox}$	Niewoehner et al., 2007
Rosa26-lacZ$^{2lox/2lox}$	Soriano et al., 1999

7.3. *Basic molecular biology*

Standard methods for cloning of plasmids, bacteria cultures, transformation of competent *Escherichia coli*, transfection of HEK293 cells, SDS-PAGE and PCR techniques, were adapted from classical protocols (Ausubel, 2000; Sambrook and Russell, 2001).

For amplification of DNA, Luria-Bertani, Standard I, and TBA/B medium were used to culture *E. coli* cells at 37ºC. Plasmid DNA was purified using QIAprep Spin Miniprep / Maxiprep Kits. For DNA extraction from agarose gels or PCR, the QIAquick Gel Extraction or PCR purification kits were used. DNA sequencing was performed by GATC Biotech AG (Konstanz,

Germany). Oligonucleotides and primers were synthesized by Thermo Fisher Scientific GmbH (Ulm, Germany). Restriction enzymes were purchased from New England Biolabs (Ipswich, MA, USA) or Fermentas GmbH (Germany).

7.3.1. Genotyping

Mouse tails were digested with Proteinase K (1 mg/ml) in TENS-buffer at 55 °C for 8–12 h. Genomic DNA was precipitated by adding one volume of isopropanol and washed with 70% ethanol. After adding distilled water, genotyping PCRs were performed in 10 µl reactions containing 1x PCR buffer, 2 mM $MgCl_2$, 0.2 mM per nucleotide dNTPs, sense- and antisense primers 0.4 µM each, 0.4 U Taq polymerase, water and 1 µl template DNA.

7.3.2. Cloning of the *lynx2* promoter

The *lynx2* promoter was first cloned using the following primers: 5'ccggatccAGTGAGGTGGGTTTCTCTCAGG, 5'GCAAAAgcTTGCTGCGATGC CGAGAACCCACAaCCTCCCGG; 5'GCAGCAAgcTTTTGCGGATTGTTCTGG CTTCC, 5'gcctcgagTGTGCGCGTCTGCTTAGGGAC, into plasmid pCR®-Blunt II-TOPO® to be used for further cloning between the ApaI and NheI sites of plasmid pAAV-6A-SEWB to generate plasmid pAAV-P_{lynx2}-EGFP. From this construct, the region containing the promoter was cloned between the MluI and EcoRI sites of plasmid pAAV-syn-iCre2A-Venus (Tang et al., 2009) to generate plasmid pAAV-P_{lynx2}-iCre2A-Venus. Venus is a modified version of YFP (Nagai et al., 2002). For luciferase expression analysis, the *lynx2* promoter or fragments of it were cloned using the BamHI, XhoI, HindIII sites of plasmid pXP1. The synapsin promoter was cloned between the XhoI and BglII sites of plasmid pXP2.

7.4. *Cell culture*

7.4.1. HEK293 cell transfection

HEK293 cells and primary hippocampal neurons were transfected with Lipofectamine2000 by standard methods (Dalby et al., 2004).

7.4.2. Hippocampal primary neurons

Pregnant rats were killed by isoflurane overdose and the uterus was surgically removed. The rat embryos were decapitated at embryonic day 18, the hippocampi were dissected in PBS/Hepes/Glucose buffer and tripsinized at 37 ^{o}C for 10 min. Dissociated cells were plated at a concentration of 50000 per 13-mm coverslip on poly-L-lysine-coated glass coverslips in plating medium. After 24 h, the plating medium was replaced with growth medium, followed by a further renewal of half of the medium volume and addition of 4 µm Ara-C after three days. Further manipulations of the primary neuron culture (infection, transfection) were performed at least seven days after plating.

7.4.3. Dual luciferase assay

HEK293 and hippocampal primary neurons were cotransfected with one of the firefly luciferase-expressing plasmids and a CMV-*Renilla* luciferase construct. Two days after transfection, cells in a well of a 24-well plate were lysed with 100 µl passive lysis buffer. From the lysate, 20 µl were used for firefly luciferase and *Renilla* luciferase activity measurement using the Dual-Luciferase® reporter 1000 assay system. Luciferase activity was quantified with a BioFix® Lumi-10 luminometer 15 s after addition of substrate.

7.5. *rAAV production*

7.5.1. Sepharose column HPLC purification

Plasmids corresponding to rAAV constructs were cotransfected with plasmid pFdelta6 (containing helper Adenovirus genes), pRV1 (rep1 and cap1 genes), and pH21 in HEK293 cells in a 5:18:5:5 weight ratio. Forty-eight hours after

transfection, the cells were pelleted at 800 rpm and lysed by resuspension in TNT buffer (20 mM Tris, 150 mM NaCl, 1% TritonX-100, 10 mM $MgCl_2$, pH 7.5) for 10 min at room temperature. Unpackaged DNA was degraded by incubating the lysate with benzonase (40 U / ml). Packaged viruses were purified through 5 ml Sepharose columns and eluted in 50 mM Glycine pH 2.7. Viral fractions were neutralized by adding Tris-HCl pH 8.0 to a concentration of 100 mM. Finally, rAAVs were washed with PBS (pH 7.5) and concentrated in a regenerated Amicon ultra cellulose concentrator.

7.5.2. Purification with heparin column

This method was used for viruses rAAV-syn-tTA, rAAV-syn-rtTA, rAAV-P_{tetbi}-TTLC-tdTomato, and rAAV-P_{tetbi}-iCre-tdTomato. Plasmids corresponding to the rAAV constructs were cotransfected with pDP1 and pDP2 helper plasmids in HEK293 cells. Forty-eight hours after transfection, HEK293 cells were collected and lysed by resuspension in 20 mM Tris 150 mM NaCl buffer (pH 8.0), repeated freeze-thaw cycles in liquid nitrogen and 0.5% sodium deoxycholate treatment. Unpackaged DNA was degraded with 40 U/ml Benzonase. Packaged viruses were purified through 5 ml Heparin columns and concentrated in a regenerated Amicon ultra cellulose concentrator.

7.5.3. Infectious titer determination

Primary hippocampal neurons in 24-well plates were infected at day 4 in vitro with different volumes of rAAV. Fourteen days later, the highest dilution at which fluorescent cells were present was used for counting. Six 10x magnification fields were photographed and the number of fluorescent neurons was determined. This number was multiplied by ratio of the total well surface area to the 10x field area and divided by the volume of virus applied to yield the number of neurons infected per microliter of virus.

7.5.4. Sources of rAAVs

A detailed list of the rAAV construct references as well as the sources of the purified viral preparations is given in the following table:

Table 6. List of rAAVs used in this study including source or reference.

rAAV	Source/Reference
rAAV-syn-tTA	Zhu et al., 2007
rAAV-syn-rtTA	Mazahir T. Hasan
rAAV-P_{tetbi}-iCre-tdTomato	Godwin Dogbevia/ Mazahir T. Hasan
rAAV-P_{tetbi}-TTLC-tdTomato	Godwin Dogbevia/ Mazahir T. Hasan
rAAV-6A-SEWB	Shevtsova et al., 2005
rAAV-syn-iCre-2A-Venus	Tang et al., 2009
rAAV-P_{lynx2}-EGFP	Own
rAAV-P_{lynx2}-iCre-2A-Venus	Own

7.6. Protein analysis

7.6.1. Cell lysis for SDS-PAGE

The medium was removed from the cell culture and gentle washing with PBS was performed. Cultured cells were resuspended in 1x passive lysis buffer and shaken for 15 min.

7.6.2. Protein concentration determination

To determine the concentration of protein in a lysate, absorbance measurements after Bradford (595 nm) or BCA assay were performed and linear regression to an appropriate bovine serum albumin standard curve was calculated.

7.6.3. SDS-PAGE

Protein samples (2–10 µg) were boiled in 1x protein loading buffer and loaded on a stacking gel at 90 mV and 400 mA. After reaching the resolving gel, samples were run at 150 mV and 400 mA.

7.6.4. Coomassie staining

For total protein visualization, the SDS-PAG was incubated in Coomassie (also Kumasi) staining solution (0.6 g/L brilliant blue, 50% methanol, 10% acetic acid in water) for 30 min. Next, the gel was washed at least three times in destaining solution (50% methanol, 7,5% acetic acid in water).

7.7. Stereotaxic rAAV delivery

7.7.1. Newborn mice

Postnatal day 0 (P0) mice were rendered immobile by cooling on ice and injected with 1 µl of rAAV per point at coordinates relative to bregma: anteroposterior -2.00 mm, lateral ±1.00 mm, dorsoventral from skin -1.00 mm for hippocampus; and anterioposterior -1.00 mm, lateral ±0.7 mm, dorsoventral from skin -1.00 mm for lateral ventricle.

7.7.2. Adult mice

Adult mice were injected using a well established method (Cetin et al., 2006). Mice were anesthetized with an intraperitoneal injection of Rompun® (20 mg / kg) and Ketavet® (100 mg / kg) and secured in a Kopf stereotaxic apparatus. The coordinates relative to bregma used for the hippocampus were: anteroposterior (AP) -2.00 mm; mediolateral (ML) ±1.5 mm; dorsoventral (DV) from pial surface -1.55 mm for dentate gyrus, -1.05 mm for CA1, -0.35 mm for cortex (Paxinos and Franklin, 2001). For targeting the complete amygdala, following coordinates were used AP -1.50 mm, ML ±3.35 mm, DV -3.70 mm. For the BLA only, the coordinates were: AP -1.80 mm, ML ±3.60 mm, DV -3.75 mm.

7.8. Immunohistochemistry

Mice were anesthetized by isoflurane inhalation and transcardially perfused with ice-cold PBS (pH 7.5) and ice-cold 4% paraformaldehyde in PBS. Brains were post-fixed overnight in the same fixative and sliced to 50 µm-thick sections using a vibratome. Slices were stored in PBS with penicillin/streptomycin (100 U/ml and 100 µg/ml respectively) and 0.01% sodium azide at 4 ^{o}C.

7.8.1. Fluorescence immunostaining

Free-floating immunostaining was performed in 24-well plates. Sections were first blocked (3% normal goat serum and 1% TritonX-100 in PBS) for 1 h, and

then incubated for 24 h at 4ºC with the appropriate primary antibodies diluted in 1% serum, 0.3% TritonX-100 in PBS. Afterwards, three washes in the same diluent were performed, followed by incubation with the appropriate fluorescence-coupled secondary antibodies for 2 h at room temperature. Finally, the sections were treated with DAPI and then mounted, dehydrated, and coverslipped with Aquamount.

7.8.2. Peroxidase immunostaining

Endogenous peroxidase activity in the brain slices was saturated with 3% H_2O_2 for 15 min and blocked for 1 h. The slices were incubated with the primary antibody for 24 h at 4ºC, then washed, and incubated with peroxidase-coupled secondary antibody for 1 h at room temperature. After washing, slices were developed in DAB solution (0.35 mg/ml DAB, 0.0075% H_2O_2 in PBS) for 5–30 min. Repeated washing in PBS stopped the reaction and the slices were cleared in xylol for 5 min, before being mounted with Aquamount.

7.8.3. X-gal staining

Brain slices were incubated in 5 mM $K_4Fe(CN)_6$, 5 mM $K_3Fe(CN)_6$, 2 mM $MgCl_2$, 2 mg/ml X-Gal in 1x Dimethylformamid/PBS solution at room temperature for 5–60 min or overnight. Afterwards, slices were washed in PBS, immersed in 10 mM Tris-HCl pH 7.5, and mounted with Aquamount.

7.9.Drug treatments

7.9.1. Doxycycline

Doxycycline was diluted in water and administered intra-peritoneally at 100 µg/g body weight. Oral administration was at a concentration of 2 mg/ml in drinking water with 5% sucrose.

7.10. Behavioral tests

7.10.1. Handling prior to behavioral testing

Three to seven days before start of behavioral experiments, mice were taken out of their cages and manipulated for 5 min in order for them to get accustomed to human contact.

7.10.2. Open-field test

Mice were placed on the center of a 50 cm x 50 cm square gray opaque plastic arena illuminated with 1000 lux and allowed to explore for 5–15 min. A video tracking system monitoring the arena from the top was used to measure the distance traveled by the mice in 1 min bins, as well as the percentage of time spent exploring the central 25 cm x 25 cm area of the arena.

7.10.3. Light-dark box

Mice were kept under dark conditions for 30 min before the start of the experiment. The apparatus consisted of a plastic box (40 cm long, 30 cm wide, 36 cm high) consisting of two symmetrical compartments communicated by a small opening (3.5 cm wide, 3 cm high): one of them with white walls and brightly lit with 1000 lux; the other with black walls and a black lid to create a dark interior. Mice were first placed in the light compartment and the amount of time spent exploring each of the two chambers was measured during 5 min, as well as the number of entries into the dark compartment.

7.10.4. Elevated plus maze

The apparatus consisted of a plus-shaped platform elevated 1 m from the ground with 38 cm long arms and a 3.5 cm x 3.5 cm intersection. Two opposed arms were flanked by 3 cm high walls that protected the mice from falling, while the other two arms were open. The mice were placed on the central intersection of the maze and the amount of time spent in the closed arms and the number of entries into the closed arms were measured during 10 min. The central area of the cross was considered part of the closed arms.

7.10.5.Puzzle box

A previously published detailed protocol was used (Abdallah et al., 2011). The apparatus used was identical: a plastic white arena with two compartments, divided by a removable barrier. The start zone was a brightly lit area (58 cm long, 28 cm wide). The goal zone was a smaller area closed with a black lid (15 cm long, 28 cm wide). Mice were trained in a series of trials that started with the mouse being placed in the start zone and allowing exploration until the mouse found the entrance (~4 cm wide) to the goal zone. The latency to enter the goal area with all four paws was measured. In the first task, there was one only trial in which the entrance to the goal zone was an open door, which could be easily crossed by the mouse. The second task consisted of three trials, in which the entrance was an underpass, through which the mouse had to crawl. The third task had three trials and mice had to dig their way through sawdust embedding blocking the underpass. The fourth task consisted of three trials in which mice had to remove a cardboard plug. Tasks 1, 2 and 3 were limited to 3 min, after which the experiment was stopped and animals that did not cross were gently pushed through the entrance to the goal zone. Task 4 was limited to 4 min. For tasks 2, 3 and 4 the first and second trials were performed on the same day, trial 3 was carried out on the following day.

7.10.6.Fear-conditioning acquisition

Mice were placed into the fear-conditioning box (TSE; 25 cm wide, 25 cm long, 35 cm high) with a metallic grid floor, transparent plexiglass walls, 70% ethanol smell, and 800 lux illumination (Context I). The conditioning box contains a frame with 16 infrared sensors (1.5 cm spacing) for each axis—x,y,z—to monitor the position and speed of the animals. Mice were allowed to explore for 6 or 3 min, after which a 30 s 80 dB 7.5 kHz tone was presented. The last 2 s of the tone coincided with a 0.4 mA foot shock. The tone (CS) and shock (US) presentation was repeated two more times with 2 min intervals between tone presentations and a final 2 min exploration period after the last shock. In the case of the one-shock protocol, only one CS/US pairing was presented followed by a 1 min exploration period.

7.10.7. Contextual fear test

The contextual retrieval test was performed by placing the mice in context I and monitoring freezing during a 3 or 8 min period.

7.10.8. Cued fear test

The cued retrieval test was performed by placing the mice in a different box with gray plastic floor, black plastic walls, 1 % acetic acid smell and 400 lux illumination (Context II). Mice were allowed to explore for 3 or 6 min, after which the CS was presented continuously for 3 min or 8 min.

7.10.9. Extinction of cued fear

The extinction training consisted in performing a daily cued test every 24 h for several consecutive days.

7.10.10. Fear conditioning evaluation

MatLab (Mathworks, Germany) was used to create a continuous time-line for the immobility of the mice in 10 s intervals. Immobility was considered when mice moved less than 1 cm/s. The percentage of time mice spent immobile was calculated for 1 min or 30 s bins. In some cases, freezing was quantified by observation of video recordings with a time-sampling procedure. Freezing was assessed every 5 s and defined as the absence of visible movement, except for respiration (Blanchard and Blanchard, 1969). The percentage of freezing was calculated for 1 min or 30 s bins.

7.10.11. Passive avoidance

The passive avoidance apparatus consisted of a dark chamber with a metallic grid floor placed on top of a tower. The chamber has an entrance that leads to a small platform, which is elevated 1 m above the ground and illuminated with 1000 lux from the top. When indicated, a habituation session was conducted, in which the mice were placed on the platform and allowed to enter the dark chamber and explore for 3 min. In the acquisition phase, mice were placed on the platform and allowed to explore for 1 min. If they did not enter within this time, mice were returned to the home cage and the procedure was repeated

after 5 min. The latency to enter was measured and, once the mouse was inside, the entrance was blocked and a 2 s 0.7 mA foot shock was administered, after which mice remained an additional 1 min inside before returning to their home cage. In the test session, mice were again placed on the open platform and the latency to enter the dark chamber was measured.

7.10.12. Visual-association swimming task

The protocol used was modified from Prusky and colleagues (2000). The apparatus consisted of a small trapezoidal pool (36 cm and 24 cm sides, 137 cm long, 50 cm high) and a large trapezoidal pool (70 cm and 24 cm sides, 137 cm long) filled with water at a depth of 15 cm, in which a 14 cm high platform could be completely submerged. The water temperature was constantly kept at 21ºC.

7.11. Statistics

All results are presented in the form Mean ± Standard Error of the Mean (s.e.m.) unless otherwise indicated. Data were tested for normality using the D'Agostino-Pearson or the Shapiro-Wilk tests. For one-factor comparisons between two independent groups, two-tailed Student's *t*-test was performed to compare the means. For comparing more than two groups and/or more than one factor, one- or two-way —repeated-measures, when applicable— analysis of variance (ANOVA) were run. When the data was not normally distributed, the Mann-Whitney *U* test was performed to compare two groups. For comparison of 'survival' curves, a censored-subject analysis using the log-rank Mantel-Cox test was carried out. When significant differences were found, post hoc pairwise two-tailed *t*-statistic comparisons were performed with Bonferroni correction for type I error minimization. Unless otherwise indicated, the significance value used was always $\alpha = 0.05$.

8. Appendix

8.1. Tables of results and statistical analyses

This section corresponds to the raw data analyzed from the different behavioral experiments and the respective statistical analysis. In all cases an $\alpha = 0.05$ was used for significance tests. Test results are summarized as $*p < 0.05$, $**p < 0.01$, $***p < 0.001$, or 'ns' as not significant. t is the value of the Student's statistic. When necessary, the Bonferroni-corrected α is shown. Sum.: summary.

Appendix Table 7. Open field test for *GluA3*$^{-/-}$ mice during a 6 min observation period.

	***GluA3*$^{-/-}$**	**Wild type**
Total traveled distance (m)	25.50 ± 1.719	34.46 ± 1.565
Time in center (%)	3.177 ± 0.6844	5.757 ± 1.542

Appendix Table 8. Median latency to enter the dark chamber in the puzzle-box test for *GluA3*$^{-/-}$ mice.

Log-rank Mantel-Cox C^2 and p value for comparisons by genotype. The Bonferroni-corrected α is presented for comparisons of tasks with multiple trials.

Task.trial	***GluA3*$^{-/-}$**	**Wild type**	$C^2_{1,N=24}$	p	**Bonferroni α**
1	94	94	0.1175	0.7317	0.05
2.1	46	48	2.597	0.1070	0.016
2.2	35.00	10.00	11.49	**0.0007**	0.016
2.3	99	62	0.001273	0.9715	0.016
3.1	180	143	6.961	**0.0083**	0.016
3.2	180	81	4.478	0.0343	0.016
3.3	180	180	3.918	0.0478	0.016
4.1	240	160	5.929	**0.0149**	0.016
4.2	240	144	3.116	0.0775	0.016
4.3	240	163	2.055	0.1517	0.016

Appendix Table 9. Mean immobility percentage in a minute-by-minute basis for *GluA3*$^{-/-}$ mice during the acquisition protocol and 24 h later in a cued retrieval test.
Student's *t* statistics and *p* value with Bonferroni-corrected α for 16 comparisons.

Acquisition						
Minute	CS/US	*GluA3*$^{-/-}$	Wild type	*t*	*p*	Summary
1	-	0.7692	0.0	0.1486	P > 0.05	ns
2	-	2.564	0.6061	0.3783	P > 0.05	ns
3	-	4.231	0.9091	0.6418	P > 0.05	ns
4	-	5.641	2.121	0.6801	P > 0.05	ns
5	-	5.513	4.242	0.2455	P > 0.05	ns
6	-	7.821	3.939	0.7499	P > 0.05	ns
6.5	Tone/Shock	11.03	2.727	1.603	P > 0.05	ns
7.5	-	18.08	10.15	1.531	P > 0.05	ns
8.5	-	23.33	18.48	0.9369	P > 0.05	ns
9	Tone/Shock	32.56	9.697	4.419	P<0.001	***
10	-	29.36	14.55	2.862	P > 0.05	ns
11	-	35.77	20.45	2.959	P < 0.05	*
11.5	Tone/Shock	42.05	15.45	5.139	P<0.001	***
12.5	-	40.77	21.67	3.691	P<0.01	**
13.5	-	39.87	21.06	3.635	P<0.01	**
Cued retrieval test						
Minute	CS	*GluA3*$^{-/-}$	Wild type	t	p	Summary
1	-	12.05	7.879	0.5502	P > 0.05	ns
2	-	15.90	5.606	1.357	P > 0.05	ns
3	-	18.46	6.212	1.615	P > 0.05	ns
4	-	27.05	6.818	2.668	P > 0.05	ns
5	-	18.21	6.364	1.561	P > 0.05	ns
6	-	15.51	6.061	1.246	P > 0.05	ns
7	Tone	55.26	30.30	3.290	P < 0.05	*
8	Tone	59.23	25.30	4.474	P<0.001	***
9	Tone	65.13	22.42	5.631	P<0.001	***
10	Tone	51.92	19.70	4.249	P<0.001	***
11	Tone	52.31	21.36	4.080	P<0.001	***
12	Tone	45.90	17.27	3.774	P<0.01	**
13	Tone	37.69	23.03	1.933	P > 0.05	ns
14	Tone	35.26	19.85	2.032	P > 0.05	ns

Appendix Table 10. Mean total immobility levels before and during tone presentation in the 24 h cued retrieval test for *GluA3*$^{-/-}$ mice.
Student's *t* pairwise comparisons.

	GluA3$^{-/-}$	Wild type	*t*	*p*	Summary
Before tone	17.86	8.864	1.558	>0.05	ns
Tone	50.34	29.71	3.570	<0.01	**
t	6.858	3.979			
p	<0.0001	0.0026			
Summary	***	**			

Appendix Table 11. Mean total immobility levels by infrared sensor readings during the tone presentation in five consecutive extinction trials for *GluA3*$^{-/-}$ mice.
Bonferroni-corrected Student's *t* pairwise comparisons between genotypes and experimental conditions.

	GluA3$^{-/-}$		Wild type		Tone *GluA3*$^{-/-}$ vs. Wild type		
Trial	Before	Tone	Before	Tone	*t*	*p*	Summary
E1	17.86	50.34	8.864	29.71	4.176	P<0.001	***
E2	18.78	43.86	16.24	25.95	3.627	P<0.01	**
E3	19.62	31.65	17.05	22.61	1.830	P > 0.05	ns
E4	16.79	22.21	17.53	17.52	0.9501	P > 0.05	ns
E5	15.85	21.39	16.72	16.12	1.068	P > 0.05	ns

	Before/Tone			Before/Tone		
	t	*p*	Summary	*t*	*p*	Summary
E1	6.867	P<0.001	***	4.055	P<0.001	***
E2	5.304	P<0.001	***	1.889	P > 0.05	ns
E3	2.545	P > 0.05	ns	1.083	P > 0.05	ns
E4	1.145	P > 0.05	ns	0.001228	P > 0.05	ns
E5	1.171	P > 0.05	ns	0.1167	P > 0.05	ns

Appendix Table 12. Mean total freezing levels by direct observation during the tone presentation in five consecutive extinction trials for *GluA3*$^{-/-}$ mice.
Bonferroni-corrected Student's *t* pairwise comparisons between genotypes and experimental conditions.

	***GluA3*$^{-/-}$**		**Wild type**		**Tone *GluA3*$^{-/-}$ vs. Wild type**		
Trial	**Before**	**Tone**	**Before**	**Tone**	***t***	***p***	**Summary**
E1	17.00	70.00	3.788	30.68	6.858	P<0.001	***
E2	19.00	57.00	12.12	28.41	4.987	P<0.001	***
E3	6.000	33.00	5.303	14.39	3.245	P<0.01	**
E4	7.000	9.000	0.7576	8.333	0.1163	P > 0.05	ns
E5	5.000	6.000	3.788	4.545	0.2537	P > 0.05	ns

	Before/Tone			**Before/Tone**		
	t	***p***	**Summary**	***t***	***p***	**Summary**
E1	8.882	P<0.001	***	4.900	P<0.001	***
E2	6.368	P<0.001	***	2.967	P < 0.05	*
E3	4.525	P<0.001	***	1.656	P > 0.05	ns
E4	0.3352	P > 0.05	ns	1.380	P > 0.05	ns
E5	0.1676	P > 0.05	ns	0.1380	P > 0.05	ns

Appendix Table 13. Median latency to enter the dark compartment in the passive avoidance test for *GluA3*$^{-/-}$ mice.
Log-rank Mantel-Cox C^2 and p value for comparisons with Bonferroni-corrected α for multiple comparisons.

Phase	*GluA3*$^{-/-}$	Wild type	$C^2_{1,N=24}$	p	Bonferroni α
Acquisition	3	3	0.37860	0.5384	0.01
24 h	40	35	0.35380	0.5520	0.01
7 d	42	27	0.02142	0.8836	0.01
37 d	60	14	9.03800	**0.0026**	0.01
67 d	168.5	6	16.89000	**0.0001**	0.01

Comparison		$C^2_{1,N=24}$	p	$C^2_{1,N=24}$	p	Bonferroni α
Acq.	24 h	22.02	**<0.0001**	14.88	**0.0001**	0.0125
Acq.	7 d	22.07	**<0.0001**	16.71	**<0.0001**	0.0125
Acq.	37 d	17.56	**<0.0001**	7.845	**0.0051**	0.0125
Acq.	67 d	27.1	**<0.0001**	4.778	0.0288	0.0125

Appendix Table 14. Mean immobility percentage of *GluA1*$^{R/R}$ and C57Bl/6N mice in fear conditioning.
Bonferroni-corrected multiple pairwise Student's t comparisons.

Acquisition

Minute	CS/US	*GluA1*$^{R/R}$	Wild type	t	p	Summary
1	-	0.1852	0.3704	0.04854	P > 0.05	ns
2	-	0.0	1.481	0.3883	P > 0.05	ns
3	-	0.0	1.481	0.3883	P > 0.05	ns
4	-	0.3704	1.481	0.2912	P > 0.05	ns
5	-	0.1852	2.963	0.7280	P > 0.05	ns
6	-	0.7407	3.519	0.7280	P > 0.05	ns
6.5	Tone/Shock	1.852	2.963	0.2912	P > 0.05	ns
7.5	-	0.3704	7.407	1.844	P > 0.05	ns
8.5	-	0.1852	16.11	4.174	P<0.001	***
9	Tone/Shock	0.0	14.44	3.786	P<0.01	**
10	-	0.0	19.44	5.096	P<0.001	***
11	-	0.5556	35.00	9.028	P<0.001	***
11.5	Tone/Shock	0.0	39.26	10.29	P<0.001	***
12.5	-	0.1852	31.67	8.251	P<0.001	***
13.5	-	0.3704	51.11	13.30	P<0.001	***

Cued retrieval test

Minute	CS	*GluA1*$^{R/R}$	Wild type	t	p	Summary
1	-	1.296	27.04	3.269	P < 0.05	*
2	-	2.222	28.52	3.340	P < 0.05	*
3	-	0.3704	31.48	3.951	P<0.01	**
4	-	1.667	37.96	4.609	P<0.001	***
5	-	1.296	36.85	4.515	P<0.001	***
6	-	1.667	29.07	3.481	P<0.01	**
7	Tone	15.37	42.04	3.387	P < 0.05	*
8	Tone	16.67	47.41	3.904	P<0.01	**
9	Tone	14.81	47.78	4.186	P<0.001	***
10	Tone	12.78	51.30	4.892	P<0.001	***

11	Tone	11.85	56.67	5.691	P<0.001	***
12	Tone	8.333	51.48	5.480	P<0.001	***
13	Tone	13.15	43.89	3.904	P<0.01	**
14	Tone	10.19	34.44	3.081	P < 0.05	*

Context retrieval test

Minute	CS	*GluA1*$^{R/R}$	Wild type	*t*	*p*	Summary
1	Context	3.519	24.63	2.679	P > 0.05	ns
2	Context	5.926	36.48	3.877	P<0.01	**
3	Context	3.704	31.85	3.572	P<0.01	**
4	Context	5.556	21.67	2.044	P > 0.05	ns
5	Context	5.926	22.59	2.115	P > 0.05	ns
6	Context	7.593	24.81	2.185	P > 0.05	ns
7	Context	7.037	23.89	2.138	P > 0.05	ns
8	Context	6.667	27.96	2.702	P > 0.05	ns

Appendix Table 15. Mean immobility percentage by infrared sensor readings in fear conditioning of *GluA1*$^{-/-}$ mice.

Acquisition

Minute	CS/US	*GluA1*$^{-/-}$	Wild type	*t*	*p*	Summary
1	-	1.458	2.778	0.2816	P > 0.05	ns
2	-	1.458	3.889	0.5188	P > 0.05	ns
3	-	0.8333	5.370	0.9683	P > 0.05	ns
4	-	0.4167	3.333	0.6225	P > 0.05	ns
5	-	0.4167	2.963	0.5435	P > 0.05	ns
6	-	0.2083	3.333	0.6670	P > 0.05	ns
6.5	Tone/Shock	3.333	7.778	0.9486	P > 0.05	ns
7.5	-	2.708	20.74	3.849	P<0.01	**
8.5	-	0.8333	18.33	3.735	P<0.01	**
9	Tone/Shock	0.4167	24.07	5.049	P<0.001	***
10	-	0.8333	45.37	9.506	P<0.001	***
11	-	2.083	50.37	10.31	P<0.001	***
11.5	Tone/Shock	0.8333	37.41	7.806	P<0.001	***
12.5	-	2.708	51.11	10.33	P<0.001	***
13.5	-	0.4167	62.59	13.27	P<0.001	***

Cued retrieval test

Minute	CS	*GluA1*$^{-/-}$	Wild type	*t*	*p*	Summary
1	-	5.208	25.93	2.860	P > 0.05	ns
2	-	5.417	21.67	2.243	P > 0.05	ns
3	-	3.958	27.59	3.263	P < 0.05	*
4	-	4.375	18.89	2.004	P > 0.05	ns
5	-	4.167	13.15	1.240	P > 0.05	ns
6	-	2.500	15.56	1.802	P > 0.05	ns
7	Tone	17.08	51.85	4.800	P<0.001	***
8	Tone	11.04	56.85	6.324	P<0.001	***
9	Tone	9.375	62.96	7.398	P<0.001	***
10	Tone	6.667	47.04	5.573	P<0.001	***

11	Tone	6.042	45.37	5.429	P<0.001	***
12	Tone	5.417	40.56	4.851	P<0.001	***
13	Tone	8.125	50.37	5.832	P<0.001	***
14	Tone	11.46	41.67	4.170	P<0.001	***

Appendix Table 16. Mean total immobility levels before and during tone presentation in the 24 h cued retrieval test for *GluA1*$^{-/-}$ mice.
Student's *t* pairwise comparisons.

	GluA1$^{-/-}$	Wild type	t_7	*p*	Summary
Before tone	4.271	20.46	5.055	0.0015	**
Tone	9.401	49.58	6.810	0.0003	***
t_{14}	2.391	5.277			
p	0.0314	0.0007			
Summary	*	***			

Appendix Table 17. Mean total immobility levels by infrared sensor readings during the tone presentation in five consecutive extinction trials *GluA1*$^{-/-}$ mice.
Bonferroni-corrected Student's *t* pairwise comparisons between genotypes and experimental conditions.

	GluA1$^{-/-}$		Wild type		Tone *GluA1*$^{-/-}$ vs. Wild type		
Trial	Before	Tone	Before	Tone	*t*	*p*	Summary
E1	4.271	9.401	20.46	49.58	6.204	P<0.001	***
E2	10.03	13.36	27.35	38.54	3.888	P<0.001	***
E3	15.24	8.438	21.17	32.75	3.754	P<0.01	**
E4	14.25	8.423	17.56	24.70	2.423	P > 0.05	ns

	Before/Tone			Before/Tone		
	t_7	*p*	Summary	t_8	*p*	Summary
E1	3.136	0.0165	*	5.277	0.0007	***
E2	0.1856	0.1059	ns	3.648	0.0065	**
E3	3.320	0.0128	*	4.303	0.0026	**
E4	1.772	0.1269	ns	2,355	0.0463	*

Appendix Table 18. Median latency to enter the dark compartment in the passive avoidance test for *GluA1*$^{-/-}$ mice.
Log-rank Mantel-Cox C^2 and *p* value for comparisons with Bonferroni-corrected α for multiple comparisons.

Phase		***GluA3*$^{-/-}$**		**Wild type**		$C^2_{1,N=17}$	*p*	**Bonferroni α**
Acquisition		14.5		3		5.127	0.0236	0.0125
24 h		600		115		1.479	0.2239	0.0125
7 d		600		88		3.496	0.0615	0.0125
23 d		600		200		7.726	**0.0054**	0.0125
Comparison		$C^2_{1,N=8}$	*p*	$C^2_{1,N=9}$	*p*	**Bonferroni α**		
Acq.	24 h	8.59	**0.0034**	8.824	**0.0030**	0.0166		
Acq.	7 d	7.576	**0.0059**	6.235	**0.0125**	0.0166		
Acq.	23 d	13.5	**0.0002**	8.330	**0.0039**	0.0166		

Appendix Table 19. Median latency to enter the dark compartment in the passive avoidance test for *GluA1*$^{-/-}$ and *GluA3*$^{-/-}$ mice.

Phase	*GluA1*$^{-/-}$	*GluA3*$^{-/-}$	*GluA1*$^{+/+}$	*GluA3*$^{+/+}$	Wild types (merged)
Acquisition	10	6.5	3	3	3
24 h	600	324	44	20.5	29
7 d	600	600	536	56	93.5
37 d	600	600	270	89.5	200
67 d	600	600	595	84.5	197.5
161 d	600	399.5	86.5	79	86.5

Appendix Table 20. Log-rank Mantel-Cox comparison of the latency to enter the dark compartment in the passive avoidance test between wild-type *GluA1*$^{+/+}$ and *GluA3*$^{+/+}$ mice.

	GluA1$^{+/+}$ vs. *GluA3*$^{+/+}$		
Phase	$C^2_{1,N=16}$	*p*	**Summary**
Acquisition	0.1328	0.7155	ns
24 h	1.147	0.2841	ns
7 d	1.848	0.1740	ns
37 d	2.152	0.1423	ns
67 d	3.079	0.0793	ns
161 d	1.134	0.2870	ns

Appendix Table 21. Median latency to enter the dark compartment in the passive avoidance test for *GluA1*$^{-/-}$ and *GluA3*$^{-/-}$ mice.
Log-rank Mantel-Cox C^2 and *p* value for comparisons with Bonferroni-corrected α for multiple comparisons.

	GluA1$^{-/-}$ vs. Wild type			*GluA3*$^{-/-}$ vs. Wild type			*GluA1*$^{-/-}$ vs. *GluA3*$^{-/-}$			
Phase	$C^2_{1,N=16}$	*p*	**Sum.**	$C^2_{1,N=16}$	*p*	**Sum.**	$C^2_{1,N=16}$	*p*	**Sum.**	α
Acquisition	7.849	0.0051	*	3.162	0.0754	ns	2.193	0.1387	ns	0.0167
24 h	4.101	0.0429	ns	1.576	0.2093	ns	0.5069	0.4765	ns	0.0167
7 d	6.218	0.0126	*	6.218	0.0126	*	0.0022	0.9624	ns	0.0167
37 d	7.631	0.0057	*	10.07	0.0015	**	1.00	0.3173	ns	0.0167
67 d	6.416	0.0113	*	8.607	0.0033	**	1.00	0.3173	ns	0.0167
161 d	6.919	0.0085	*	2.352	0.1251	ns	3.142	0.0763	ns	0.0167

		GluA1$^{-/-}$			*GluA3*$^{-/-}$			Wild type			
Comparison		$C^2_{1,N=16}$	*p*	**Sum.**	$C^2_{1,N=16}$	*p*	**Sum.**	$C^2_{1,N=16}$	*p*	**Sum.**	α
Acq.	24 h	13.08	0.0003	***	14.94	0.0001	***	17.00	<0.0001	***	0.01
	7 d	17.06	<0.0001	***	16.75	<0.0001	***	15.81	<0.0001	***	0.01
	37 d	17.06	<0.0001	***	16.75	<0.0001	***	34.35	<0.0001	***	0.01
	67 d	17.06	<0.0001	***	27.08	<0.0001	***	28.43	<0.0001	***	0.01
	161 d	13.99	0.0002	***	16.75	<0.0001	***	33.15	<0.0001	***	0.01
		GluA1$^{-/-}$			*GluA3*$^{-/-}$			Wild type			
Comparison		$C^2_{1,N=16}$	*p*	**Sum.**	$C^2_{1,N=16}$	*p*	**Sum.**	$C^2_{1,N=16}$	*p*	**Sum.**	α
24 h	Acq.	13.08	0.0003	***	14.94	0.0001	***	17.00	<0.0001	***	0.01
	7 d	1.518	0.2179	ns	3.568	0.0589	ns	0.4739	0.4912	ns	
	37 d	1.518	0.2179	ns	6.929	0.0085	*	1.302	0.2539	ns	
	67 d	1.518	0.2179	ns	6.929	0.0085	*	1.562	0.2113	ns	
	161 d	0.0270	0.8694	ns	0.3263	0.5678	ns	0.1021	0.7494	ns	

		GluA1$^{-/-}$			*GluA3*$^{-/-}$			Wild type			
Comparison		$C^2_{1,N=16}$	*p*	**Sum.**	$C^2_{1,N=16}$	*p*	**Sum.**	$C^2_{1,N=16}$	*p*	**Sum.**	**α**
7 d	Acq.	17.06	<0.0001	***	16.75	<0.0001	***	15.81	<0.0001	***	0.01
	24 h	1.518	0.2179	ns	3.568	0.0589	ns	0.4739	0.4912	ns	
	37 d	0.0022	0.9624	ns	1.00	0.3173	ns	0.0192	0.8897	ns	
	67 d	0.0022	0.9624	ns	1.00	0.3173	ns	0.1433	0.7050	ns	
	161 d	1.317	0.2511	ns	7.660	0.0056	*	0.7068	0.4005	ns	

Appendix Table 22. Mean immobility percentage by infrared sensor readings in fear conditioning of *GluA3*$^{-/-}$ and *GluA1*$^{+/-}$ mice during the acquisition phase.

						Acquisition					
Min.	CS/US	*GluA3*$^{-/-}$	**Control**	*t*	*p*	Sum.	*GluA3*$^{-/-}$ *A1*$^{+/-}$	*GluA1*$^{+/-}$	*t*	*p*	Sum.
1	-	1.026	0.0	0.1452	>0.05	ns	0.5128	0.2381	0.04745	>0.05	ns
2	-	5.128	0.8333	0.6082	>0.05	ns	0.2564	1.905	0.2847	>0.05	ns
3	-	3.205	5.000	0.2542	>0.05	ns	0.5128	3.333	0.4871	>0.05	ns
4	-	3.590	1.250	0.3313	>0.05	ns	0.7692	0.9524	0.03163	>0.05	ns
5	-	5.641	3.333	0.3268	>0.05	ns	1.026	0.7143	0.05378	>0.05	ns
6	-	7.949	6.250	0.2406	>0.05	ns	0.3846	3.333	0.5093	>0.05	ns
6.5	CS/US	8.718	8.333	0.05447	>0.05	ns	1.538	2.857	0.2278	>0.05	ns
7.5	-	14.87	13.75	0.1589	>0.05	ns	2.051	3.810	0.3037	>0.05	ns
8.5	-	26.79	30.00	0.4539	>0.05	ns	3.846	4.286	0.07592	>0.05	ns
9	CS/US	36.41	19.17	2.442	>0.05	ns	10.51	13.33	0.4871	>0.05	ns
10	-	32.44	36.25	0.5401	>0.05	ns	11.03	13.57	0.4397	>0.05	ns
11	-	46.15	43.33	0.3994	>0.05	ns	11.67	22.14	1.809	>0.05	ns
11.5	CS/US	48.46	34.17	2.024	>0.05	ns	33.33	31.43	0.3290	>0.05	ns
12.5	-	36.92	50.00	1.852	>0.05	ns	21.03	19.52	0.2594	>0.05	ns
13.5	-	53.46	45.00	1.198	>0.05	ns	30.26	35.00	0.8193	>0.05	ns
Min.	CS/US	*GluA3*$^{-/-}$	*GluA3*$^{-/-}$ *A1*$^{+/-}$	*t*	*p*	Sum.	***Control***	*GluA1*$^{+/-}$	*t*	*p*	Sum.
1	-	1.026	0.5128	0.1059	>0.05	ns	0.0	0.2381	0.03076	>0.05	ns
2	-	5.128	0.2564	1.006	>0.05	ns	0.8333	1.905	0.1384	>0.05	ns
3	-	3.205	0.5128	0.5558	>0.05	ns	5.000	3.333	0.2153	>0.05	ns
4	-	3.590	0.7692	0.5823	>0.05	ns	1.250	0.9524	0.03845	>0.05	ns
5	-	5.641	1.026	0.9528	>0.05	ns	3.333	0.7143	0.3383	>0.05	ns
6	-	7.949	0.3846	1.562	>0.05	ns	6.250	3.333	0.3768	>0.05	ns
6.5	CS/US	8.718	1.538	1.482	>0.05	ns	8.333	2.857	0.7074	>0.05	ns
7.5	-	14.87	2.051	2.647	>0.05	ns	13.75	3.810	1.284	>0.05	ns
8.5	-	26.79	3.846	4.737	<0.001	***	30.00	4.286	3.322	<0.05	*
9	CS/US	36.41	10.51	5.346	<0.001	***	19.17	13.33	0.7536	>0.05	ns
10	-	32.44	11.03	4.420	<0.001	***	36.25	13.57	2.930	>0.05	ns
11	-	46.15	11.67	7.119	<0.001	***	43.33	22.14	2.737	>0.05	ns
11.5	CS/US	48.46	33.33	3.123	<0.05	*	34.17	31.43	0.3537	>0.05	ns
12.5	-	36.92	21.03	3.282	<0.05	*	50.00	19.52	3.937	<0.01	**
13.5	-	53.46	30.26	4.790	<0.001	***	45.00	35.00	1.292	>0.05	ns

Appendix Table 23. Mean immobility percentage by infrared sensor readings in fear conditioning of *GluA3*$^{-/-}$ and *GluA1*$^{+/-}$ mice during the cued retrieval tests.

		Cued test									
		24 h					31 d				
Min.	CS	*GluA3*$^{-/-}$ *A1*$^{+/-}$	*GluA1*$^{+/-}$	*t*	*p*	Sum.	*GluA3*$^{-/-}$ *A1*$^{+/-}$	*GluA1*$^{+/-}$	*t*	*p*	Sum.
1	-	17.56	10.24	0.8529	>0.05	ns	24.74	29.76	0.5549	>0.05	ns
2	-	22.69	18.81	0.4520	>0.05	ns	28.59	28.81	0.02430	>0.05	ns
3	-	24.23	12.62	1.352	>0.05	ns	32.82	19.05	1.523	>0.05	ns
4	-	24.87	13.57	1.316	>0.05	ns	22.69	18.81	0.4294	>0.05	ns
5	-	27.95	11.67	1.895	>0.05	ns	28.46	13.57	1.647	>0.05	ns
6	-	34.23	15.95	2.128	>0.05	ns	35.38	20.71	1.622	>0.05	ns
7	CS	70.77	48.81	2.556	>0.05	ns	57.95	39.05	2.090	>0.05	ns
8	CS	54.87	39.52	1.787	>0.05	ns	43.85	32.62	1.241	>0.05	ns
9	CS	58.08	38.81	2.243	>0.05	ns	52.31	32.14	2.230	>0.05	ns
10	CS	51.67	42.86	1.026	>0.05	ns	47.56	31.19	1.811	>0.05	ns
11	CS	53.97	44.76	1.072	>0.05	ns	49.36	14.52	3.852	<0.01	**
12	CS	41.67	28.10	1.580	>0.05	ns	37.69	12.14	2.825	>0.05	ns
13	CS	43.59	20.48	2.691	>0.05	ns	41.41	23.10	2.025	>0.05	ns
14	CS	37.05	24.05	1.514	>0.05	ns	33.97	33.10	0.09721	>0.05	ns

		Cued test 31 d				
Min.	CS/US	*GluA3*$^{-/-}$	Control	*t*	*p*	Sum.
1	-	21.54	45.83	2.175	>0.05	ns
2	-	38.21	34.17	0.3615	>0.05	ns
3	-	36.15	21.67	1.297	>0.05	ns
4	-	36.79	20.83	1.429	>0.05	ns
5	-	31.28	15.42	1.420	>0.05	ns
6	-	34.36	17.92	1.472	>0.05	ns
7	CS	46.79	44.58	0.1980	>0.05	ns
8	CS	47.05	58.75	1.047	>0.05	ns
9	CS	54.74	36.67	1.618	>0.05	ns
10	CS	47.95	35.42	1.122	>0.05	ns
11	CS	50.00	29.17	1.865	>0.05	ns
12	CS	39.23	17.92	1.908	>0.05	ns
13	CS	41.03	18.75	1.994	>0.05	ns
14	CS	40.90	17.50	2.094	>0.05	ns

Appendix Table 24. Mean total immobility levels before and during tone presentation in the 24 h and 31 d cued retrieval tests for *GluA3*$^{-/-}$ and *GluA1*$^{+/-}$ mice. Student's *t* pairwise before/tone comparisons.

	24 h		31 d			
	GluA3$^{-/-}$ *A1*$^{+/-}$	*GluA1*$^{+/-}$	*GluA3*$^{-/-}$ *A1*$^{+/-}$	*GluA1*$^{+/-}$	*GluA3*$^{-/-}$	Control
Before tone	25.26	13.81	28.78	21.79	33.06	25.97
Tone	51.46	35.92	45.51	27.23	45.96	32.34
t	6.189	3.833	3.952	0.944	3.048	0.8348
p	<0.001	<0.01	<0.01	>0.05	<0.05	>0.05
Summary	***	**	**	ns	*	ns

Appendix Table 25. Open field, light dark box and elevated plus maze tests for amygdala-silenced TTLC mice.

Test		TTLC	Control			
Open Field Total Distance (cm)	Minute 1	418.1	351.1			
	Minute 2	378.6	349.6			
	Minute 3	378.3	313.2			
	Minute 4	310.5	323.1			
	Minute 5	289.9	290.7			
	Minute 6	277.1	242.7			
	Minute 7	267.4	256.6			
	Minute 8	258.6	334.6			
	Minute 9	257.2	323.8			
	Minute 10	225.8	287.6	***t***	***p***	**Sum.**
Light-dark box	Time in the dark (%)	73.53±4.52	69.17±2.15	0.7394	0.4808	ns
	Entries into the dark	14.00±1.06	14.75±3.06	0.2713	0.7930	ns
Elevated plus maze	Time in closed arm	83.72±15.09	89.67±3.94	0.3811	0.7188	ns

Appendix Table 26. Mean immobility percentage of amygdala-silenced TTLC and C57Bl/6N mice in fear conditioning.

Context retrieval test 24 h						
Minute	CS	TTLC	Control	*t*	*p*	Summary
1	Context	13.06	39.58	3.255	<0.05	*
2	Context	27.50	25.83	0.2045	>0.05	ns
3	Context	8.611	16.67	0.9884	>0.05	Ns
4	Context	9.444	20.00	1.295	>0.05	ns
5	Context	7.778	16.67	1.091	>0.05	ns
Context retrieval test 41 d						
Minute	CS	TTLC	Control	*t*	*p*	Summary
1	Context	31.67	45.42	1.472	>0.05	ns
2	Context	33.06	37.08	0.4311	>0.05	ns
3	Context	24.17	24.17	0.000	>0.05	ns
4	Context	13.89	21.25	0.7878	>0.05	ns
5	Context	18.89	33.75	1.591	>0.05	ns
Cued retrieval test 48 h						
Minute	CS	TTLC	Control	*t*	*p*	Summary
1	-	5.278	25.83	2.868	<0.05	*
2	-	12.22	24.58	1.725	>0.05	ns
3	-	7.500	23.33	2.209	>0.05	ns
12	Tone	12.50	39.17	3.721	<0.01	**
13	Tone	14.72	34.58	2.771	<0.05	*
14	Tone	23.33	30.83	1.046	>0.05	ns
Cued retrieval test 42 d						
Minute	CS	TTLC	Control	*t*	*p*	Summary
1	-	14.44	23.75	1.329	>0.05	ns
2	-	16.11	26.25	1.448	>0.05	ns
3	-	9.444	24.17	2.103	>0.05	ns
12	Tone	15.56	45.00	4.206	<0.001	***
13	Tone	16.11	22.08	0.8532	>0.05	ns
14	Tone	12.22	23.75	1.647	>0.05	ns

Appendix Table 27. Mean total freezing levels before and during tone presentation in the 24 h cued retrieval test for TTLC mice.
Student's *t* pairwise comparisons.

Time point	Test	TTLC	Control	*t*	*p*	Summary
24 h	Context	23.15	56.94	2.755	0.0248	*
41 d	Context	18.33	41.67	2.842	0.0218	*
48 h	Before tone	14.81	25.00	1.629	0.1421	ns
48 h	Tone	11.11	52.78	6.852	0.0001	***
42 d	Before tone	12.960	48.61	4.142	0.0032	**
42 d	Tone	7.407	29.17	4.937	0.0011	**

Appendix Table 28. Median latency to enter dark chamber in the passive avoidance task for amygdala-silenced TTLC mice.

Phase	**TTLC**	**Wild type**	$C^2_{1,N=10}$	***p***	**Bonferroni α**
Acquisition	8	13.5	0.2765	0.5990	0.025
24 h test	12.5	182.5	1.825	0.1767	0.025
24 h (w/o outlier)	11	182.5	7.914	0.0049	0.025

Comparison		$C^2_{1,N=6}$	***p***	$C^2_{1,N=4}$	***p***	**Bonferroni α**
Acq.	24 h	0.7239	0.3949	7.344	**0.0067**	0.05

Appendix Table 29. Mean immobility percentage by infrared sensor readings in fear conditioning of *GluA1*$^{\Delta BLA}$ and *GluN1*$^{\Delta BLA}$ mice during the acquisition phase.

		Acquisition								
Min.	CS/US	**Control**	***GluA1***$^{\Delta BLA}$	*t*	*p*	Sum.	***GluN1***$^{\Delta BLA}$	*t*	*p*	Sum.
1	-	2.407	0.3333	0.2530	>0.05	ns	2.083	0.04538	>0.05	ns
2	-	4.259	2.000	0.2756	>0.05	ns	3.542	0.1005	>0.05	ns
3	-	6.111	1.333	0.5829	>0.05	ns	5.208	0.1264	>0.05	ns
4	-	2.593	3.000	0.04970	>0.05	ns	6.458	0.5414	>0.05	ns
5	-	2.222	5.667	0.4202	>0.05	ns	5.833	0.5057	>0.05	ns
6	-	5.000	6.000	0.1220	>0.05	ns	5.625	0.08752	>0.05	ns
6.5	CS/US	3.333	4.667	0.1627	>0.05	ns	6.667	0.4668	>0.05	ns
7.5	-	12.59	20.67	0.9850	>0.05	ns	29.58	2.379	>0.05	ns
8.5	-	13.52	20.67	0.8721	>0.05	ns	23.75	1.433	>0.05	ns
9	CS/US	22.96	28.67	0.6958	>0.05	ns	22.08	0.1232	>0.05	ns
10	-	30.19	42.00	1.441	>0.05	ns	32.50	0.3242	>0.05	ns
11	-	35.93	52.00	1.961	>0.05	ns	43.75	1.096	>0.05	ns
11.5	CS/US	41.48	42.00	0.06326	>0.05	ns	34.58	0.9660	>0.05	ns
12.5	-	38.89	42.33	0.4202	>0.05	ns	52.08	1.848	>0.05	ns
13.5	-	37.78	31.33	0.7862	>0.05	ns	55.63	2.499	>0.05	ns

Appendix Table 30. Mean freezing percentage by direct observation in fear conditioning of *GluA1*$^{\Delta BLA}$ and *GluN1*$^{\Delta BLA}$ mice during the acquisition phase

Context test before DOX										
Min.	CS/US	**Control**	***GluA1*$^{\Delta BLA}$**	*t*	*p*	Sum.	***GluN1*$^{\Delta BLA}$**	*t*	*p*	Sum.
1	Context	12.96	16.67	0.2903	>0.05	ns	22.92	0.8955	>0.05	ns
2	Context	16.67	33.33	1.306	>0.05	ns	14.58	0.1874	>0.05	ns
3	Context	11.11	40.00	2.264	>0.05	ns	10.42	0.06247	>0.05	ns
Cued test before DOX										
Min.	CS/US	**Control**	***GluA1*$^{\Delta BLA}$**	*t*	*p*	Sum.	***GluN1*$^{\Delta BLA}$**	*t*	*p*	Sum.
1	-	0.0	3.333	0.5113	>0.05	ns	2.083	0.3668	>0.05	ns
2	-	0.9259	1.667	0.1136	>0.05	ns	0.0	0.1630	>0.05	ns
3	-	0.0	1.667	0.2557	>0.05	ns	0.0	0.0	>0.05	ns
4	CS	36.11	48.33	1.875	>0.05	ns	39.58	0.6114	>0.05	ns
5	CS	30.56	45.00	2.216	>0.05	ns	40.63	1.773	>0.05	ns
6	CS	25.00	43.33	2.812	<0.05	*	21.88	0.5503	>0.05	ns
Cued test after DOX										
Min.	CS/US	**Control**	***GluA1*$^{\Delta BLA}$**	*t*	*p*	Sum.	***GluN1*$^{\Delta BLA}$**	*t*	*p*	Sum.
1	-	4.630	3.333	0.2103	>0.05	ns	4.167	0.08623	>0.05	ns
2	-	5.556	5.000	0.09015	>0.05	ns	6.250	0.1293	>0.05	ns
3	-	2.778	3.333	0.09015	>0.05	ns	3.125	0.06467	>0.05	ns
4	CS	39.81	41.67	0.3005	>0.05	ns	20.83	3.535	<0.01	**
5	CS	25.93	23.33	0.4207	>0.05	ns	6.250	3.665	<0.01	**
6	CS	20.37	21.67	0.2103	>0.05	ns	11.46	1.660	>0.05	ns
7	CS	7.407	30.00	3.666	<0.01	**	8.333	0.1725	>0.05	ns
8	CS	8.333	16.67	1.352	>0.05	ns	4.167	0.7761	>0.05	ns
9	CS	9.259	16.67	1.202	>0.05	ns	4.167	0.9485	>0.05	ns
10	CS	1.852	13.33	1.863	>0.05	ns	3.125	0.2371	>0.05	ns
11	CS	0.9259	6.667	0.9315	>0.05	ns	1.042	0.02156	>0.05	ns

Appendix Table 31. Mean immobility percentage by infrared sensor readings in fear conditioning of *GluA1*$^{\Delta BLA}$ and *GluN1*$^{\Delta BLA}$ mice during the acquisition phase.

Context test before DOX										
Min.	CS/US	**Control**	***GluA1*$^{\Delta BLA}$**	*t*	*p*	Sum.	***GluN1*$^{\Delta BLA}$**	*t*	*p*	Sum.
1	Context	14.44	11.00	0.5036	>0.05	ns	18.33	0.6527	>0.05	ns
2	Context	19.26	21.33	0.3033	>0.05	ns	17.92	0.2253	>0.05	ns
3	Context	18.15	31.33	1.928	>0.05	ns	14.38	0.6333	>0.05	ns
Cued test before DOX										
Min.	CS/US	**Control**	***GluA1*$^{\Delta BLA}$**	*t*	*p*	Sum.	***GluN1*$^{\Delta BLA}$**	*t*	*p*	Sum.
1	-	7.407	7.667	0.03411	>0.05	ns	5.833	0.2377	>0.05	ns
2	-	14.81	13.33	0.1949	>0.05	ns	10.63	0.6328	>0.05	ns
3	-	12.41	11.67	0.09746	>0.05	ns	7.917	0.6783	>0.05	ns
4	CS	41.30	49.00	1.014	>0.05	ns	30.63	1.612	>0.05	ns
5	CS	30.56	46.67	2.120	>0.05	ns	33.96	0.5139	>0.05	ns
6	CS	33.15	49.67	2.173	>0.05	ns	29.58	0.5384	>0.05	ns

		Cued test after DOX								
Min.	CS/US	**Control**	***GluA1*$^{\Delta BLA}$**	*t*	*p*	Sum.	***GluN1*$^{\Delta BLA}$**	*t*	*p*	Sum.
1	-	21.85	36.67	1.548	>0.05	ns	24.17	0.2777	>0.05	ns
2	-	23.70	33.00	0.9717	>0.05	ns	25.63	0.2305	>0.05	ns
3	-	20.37	17.67	0.2826	>0.05	ns	14.79	0.6693	>0.05	ns
4	CS	51.30	43.33	0.8323	>0.05	ns	29.58	2.605	>0.05	ns
5	CS	34.26	28.00	0.6542	>0.05	ns	22.50	1.411	>0.05	ns
6	CS	24.81	25.67	0.08904	>0.05	ns	20.63	0.5027	>0.05	ns
7	CS	22.41	34.00	1.212	>0.05	ns	23.33	0.1111	>0.05	ns
8	CS	27.96	33.33	0.5613	>0.05	ns	31.88	0.4694	>0.05	ns
9	CS	32.96	27.00	0.6233	>0.05	ns	30.83	0.2555	>0.05	ns
10	CS	23.89	27.33	0.3600	>0.05	ns	16.25	0.9165	>0.05	ns
11	CS	19.26	32.33	1.367	>0.05	ns	23.96	0.5638	>0.05	ns
		Context test after DOX								
Min.	CS/US	**Control**	***GluA1*$^{\Delta BLA}$**	*t*	*p*	Sum.	***GluN1*$^{\Delta BLA}$**	*t*	*p*	Sum.
1	Context	19.44	16.67	0.2969	>0.05	ns	16.67	0.3408	>0.05	ns
2	Context	27.59	22.33	0.5622	>0.05	ns	26.46	0.1392	>0.05	ns
3	Context	24.63	41.00	1.750	>0.05	ns	21.88	0.3380	>0.05	ns
4	Context	25.19	23.67	0.1623	>0.05	ns	11.25	1.710	>0.05	ns
5	Context	20.00	20.67	0.07126	>0.05	ns	22.29	0.2812	>0.05	ns
6	Context	17.41	32.33	1.596	>0.05	ns	28.75	1.392	>0.05	ns
7	Context	18.89	21.00	0.2257	>0.05	ns	16.67	0.2727	>0.05	ns
8	Context	8.333	33.33	2.672	>0.05	ns	16.67	1.023	>0.05	ns

Appendix Table 32. Mean total freezing levels before and after Dox treatment during the first 3 min of tone presentation of the cued retrieval tests for *GluA1*$^{\Delta BLA}$ and *GluN1*$^{\Delta BLA}$ mice

Student's *t* pairwise before Dox/after Dox comparisons.

	Control	***GluA1*$^{\Delta BLA}$**	***GluN1*$^{\Delta BLA}$**
Before Dox	45.56	30.56	34.03
After Dox	28.89	28.70	12.85
t	2.77	0.4129	4.452
p	<0.05	>0.05	<0.001
Summary	*	ns	***

Appendix Table 33. Mean relative change in freezing before and after Dox treatment in *GluA1*$^{\Delta BLA}$ and *GluN1*$^{\Delta BLA}$ mice

Student's *t* pairwise comparisons with Control.

	Control	***GluA1*$^{\Delta BLA}$**	***GluN1*$^{\Delta BLA}$**
Mean	-0.3660	0.005727	-0.6092
s.e.m.	0.1002	0.1661	0.1122
	t	1.708	3.245
	p	>0.05	<0.05
	Summary	ns	*

8.2. Supplementary data on GluN1$^{\Delta BLA}$ and GluA1$^{\Delta BLA}$ mice

The following data correspond to experiments performed after the extinction protocol in *GluN1$^{\Delta BLA}$* and *GluA1$^{\Delta BLA}$* mice. However, the interpretation of these results is masked by possible interference of the previous behavioral manipulations (fear conditioning, retrieval tests, extinction) on the outcome of further tests of this cohort of mice.

8.2.1. Passive avoidance after GluN1 and GluA1 knockout in the BLA

In order to test whether a new fear-related task could be acquired after GluN1 or GluA1 knockout in the BLA, mice were trained in the passive avoidance. In short, the latency to enter a dark compartment is measured, after this had been associated with a foot shock. The acquisition phase for this paradigm was performed 63 d after the start of the previous fear conditioning. A retrieval test was performed after 24 h (Appendix Figure 31a). The statistical analysis did not reveal significant differences between the groups (Log-rank Mantel-Cox, $c^2_{2,N=22} = 0.2376$, $p = 0.8880$). A closer look at the latencies showed a high variation for all groups of mice (Appendix Figure 31b). Even in the control group, mice ranged from immediately entering the dark compartment, even though they had experienced a foot shock in it before, to not entering within 5 min. Therefore, no straightforward conclusions could be drawn from this test regarding the ability to acquire a new fear association in *GluN1$^{\Delta BLA}$* and *GluA1$^{\Delta BLA}$* mice, since the test protocol, in this case, was not reliable.

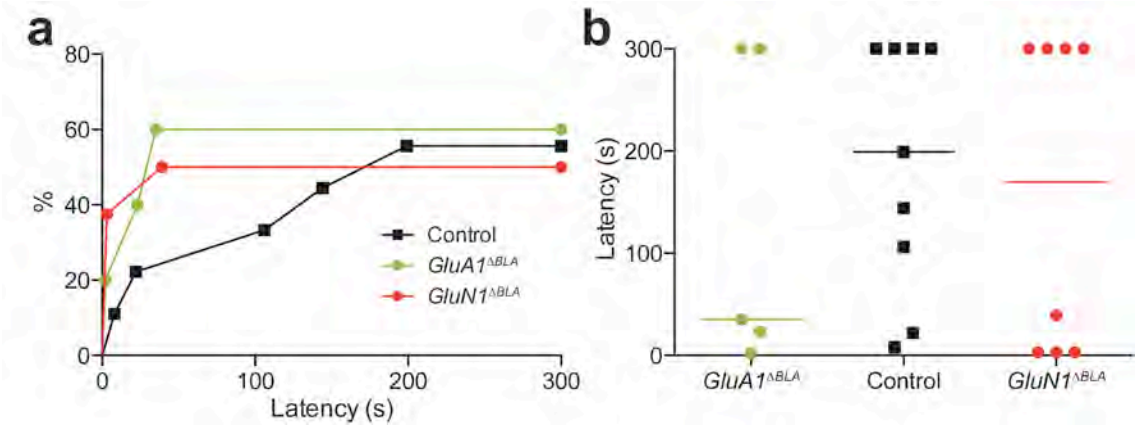

Appendix Figure 31. Retrieval after 24 h of the passive avoidance task in *GluN1*$^{\Delta BLA}$ and *GluA1*$^{\Delta BLA}$ mice
a, 'Survival' analysis of the latency to enter the dark compartment during the 24 h retrieval test. No significant differences between the curves. **b,** Scatter plot of the latency to enter dark chamber including censored mice. The horizontal lines indicate the medians.

8.2.2. Reacquisition of cued fear after GluN1 and GluA1 knockout in the BLA

A final test in the fear-conditioning paradigm was performed in order to test if GluN1$^{\Delta BLA}$ mice were altogether unable to show expression of fear. Mice were subjected to a second acquisition protocol (re-acquisition), consisting of three tone-shock pairings, after which immobility levels to the context and the tone were immediately assessed (Appendix Figure 32a). All three groups of mice showed comparable levels of freezing when evaluated immediately after the three-shock administration and during the final 3 min of tone presentation (genotype $F_{2,19}$ = 0.3333, p = 0.7206; time $F_{11,19}$ = 4.187, p < 0.0001; interaction $F_{22,19}$ = 0.7602, p = 0.7717). A further cued retrieval test, 9 d after re-acquisition showed that there no longer were any significant differences between the three groups (Appendix Figure 32b; genotype $F_{2,19}$ = 1.088, p = 0.3570; time $F_{5,19}$ = 2.179, p < 0.0629; interaction $F_{10,19}$ = 0.6707, p = 0.7488). These results indicate that *GluN1*$^{\Delta BLA}$ mice, as well as controls and *GluA1*$^{\Delta BLA}$ mice, were able to express fear in an acute protocol, suggesting that the central nucleus of the amygdala, responsible for fear expression, remained functional.

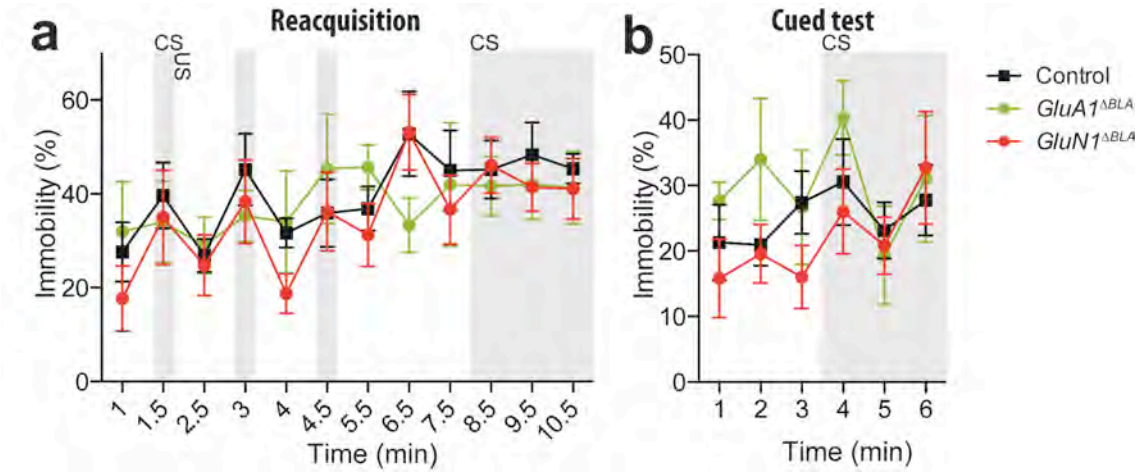

Appendix Figure 32. Reacquisition of fear conditioning in *GluN1*$^{\Delta BLA}$ and *GluA1*$^{\Delta BLA}$ mice
a, Reacquisition of fear conditioning by a three-shock protocol, followed by immediate assessment of contextual and cued fear. No significant differences between the genotypes were observed. **b,** Cued retrieval test 9 d after reacquisition.

8.2.3. Post-mortem analysis after GluN1 and GluA1 knockout in the BLA

Appendix Figure 33. Fluorescence immunostaining against Cre recombinase in brains of *GluN1*$^{\Delta BLA}$ and *GluA1*$^{\Delta BLA}$ mice (next page)
a, Schematic representation of the coronal section levels showed in (b), indicating the localization of the BLA, CeA, striatum and piriform cortex. **b,** Examples of Cre immunostaining shown in green and DAPI nuclear staining in blue for *GluN1*$^{\Delta BLA}$ and *GluA1*$^{\Delta BLA}$ mice. Scale bar, 1 mm.

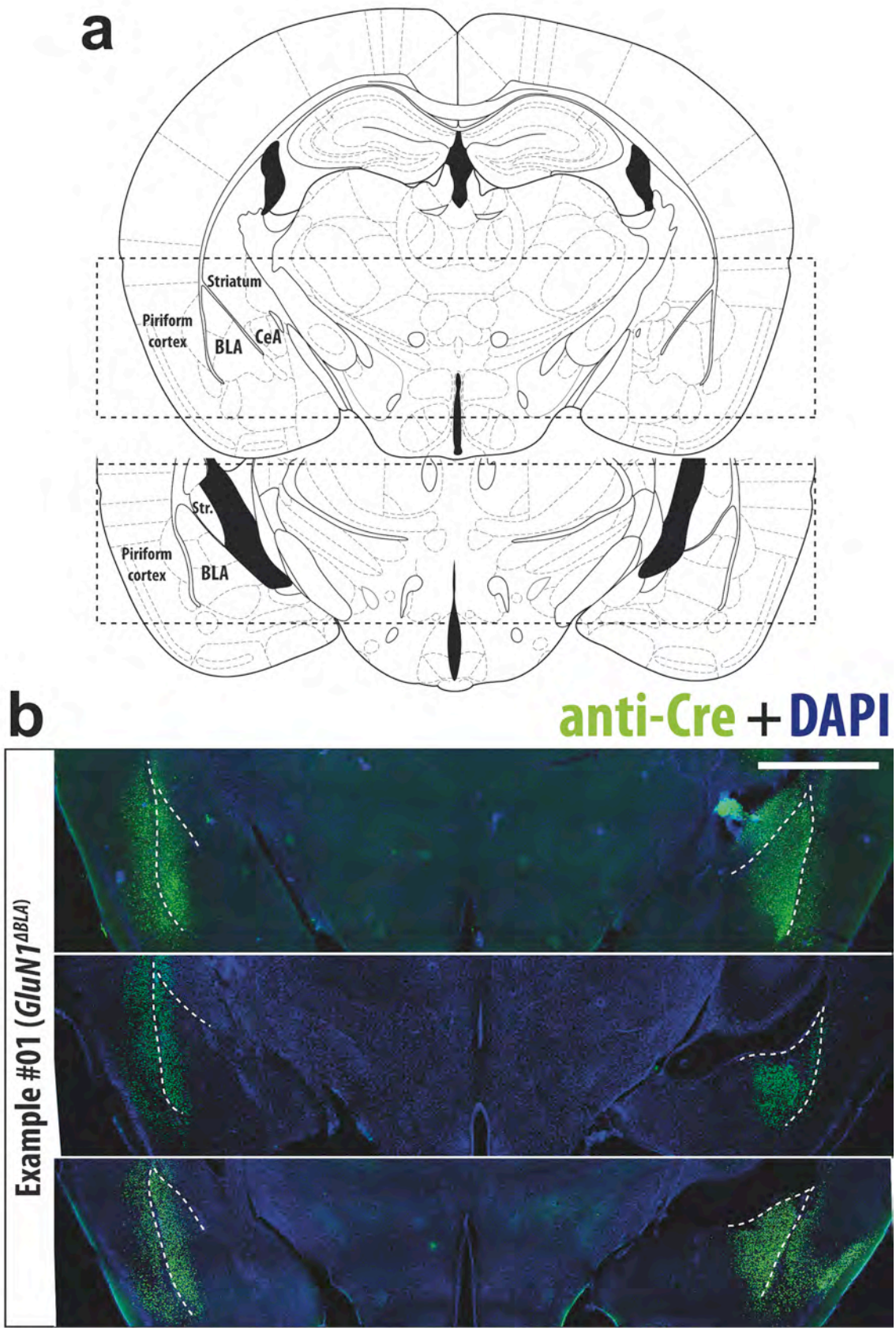
a
Striatum
Piriform cortex
BLA
CeA
Str.
Piriform cortex
BLA
b
anti-Cre + DAPI
Example #01 (GluN1ΔBLA)

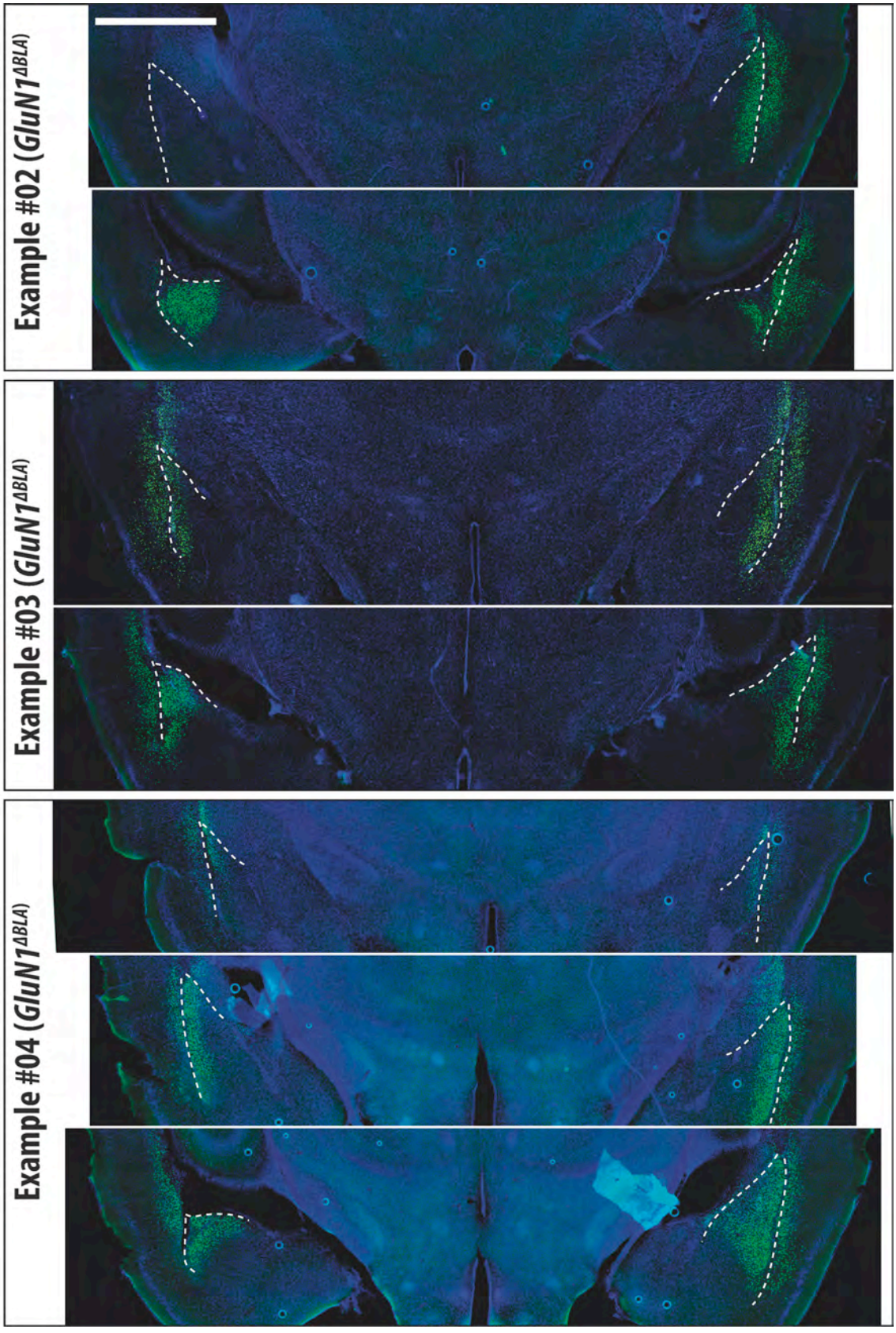
Example #02 (GluN1ΔBLA)
Example #03 (GluN1ΔBLA)
Example #04 (GluN1ΔBLA)

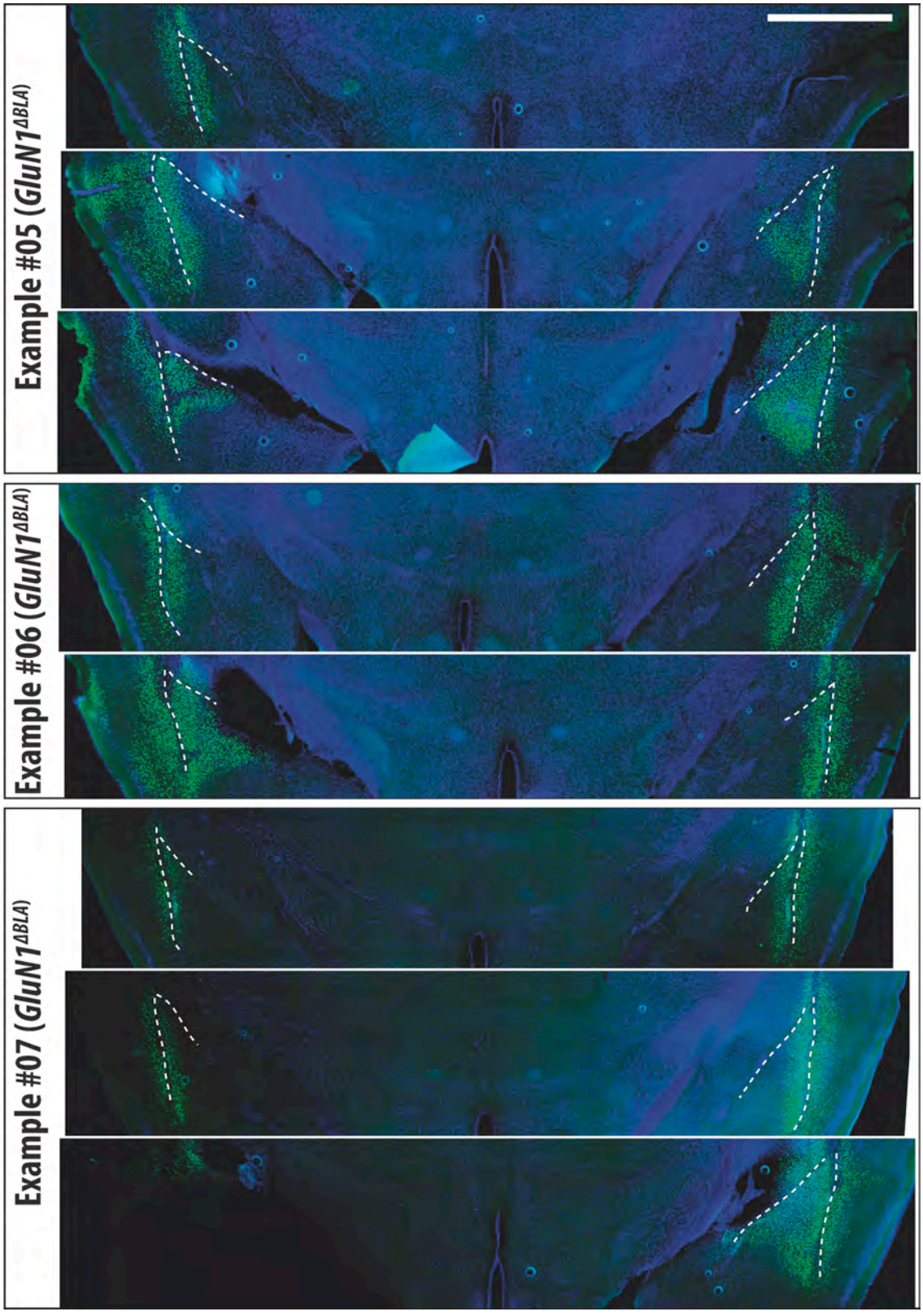
Example #05 (GluN1ΔBLA)
Example #06 (GluN1ΔBLA)
Example #07 (GluN1ΔBLA)

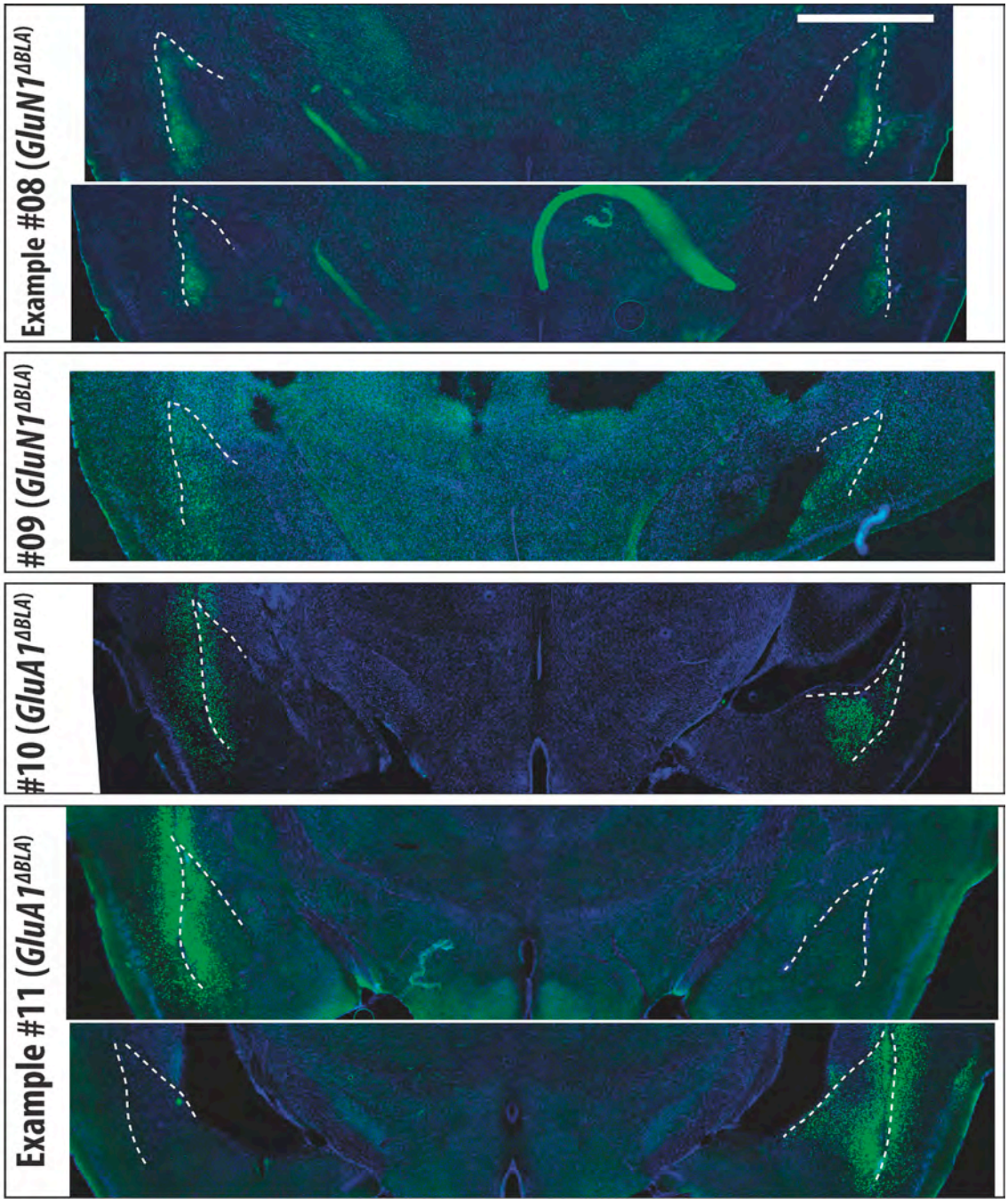
Example #08 (GluN1ΔBLA)
#09 (GluN1ΔBLA)
#10 (GluA1ΔBLA)
Example #11 (GluA1ΔBLA)

9. Bibliography

Abdallah, N.M.-B.B., Fuss, J., Trusel, M., Galsworthy, M.J., Bobsin, K., Colacicco, G., Deacon, R.M.J., Riva, M.A., Kellendonk, C., Sprengel, R., *et al.* (2011). The puzzle box as a simple and efficient behavioral test for exploring impairments of general cognition and executive functions in mouse models of schizophrenia. Experimental Neurology *227*, 42-52.

Alberini, C.M. (2011). The Role of Reconsolidation and the Dynamic Process of Long-Term Memory Formation and Storage. Frontiers in behavioral neuroscience *5*, 1-10.

Alexopoulou, A.N., Couchman, J.R., and Whiteford, J.R. (2008). The CMV early enhancer/chicken beta actin (CAG) promoter can be used to drive transgene expression during the differentiation of murine embryonic stem cells into vascular progenitors. BMC Cell Biol *9*, 2.

Amann, L.C., Halene, T.B., Ehrlichman, R.S., Luminais, S.N., Ma, N., Abel, T., and Siegel, S.J. (2009). Chronic ketamine impairs fear conditioning and produces long-lasting reductions in auditory evoked potentials. Neurobiol Dis *35*, 311-317.

Anderson, W.F. (1998). Human gene therapy. Nature *392*, 25-30.

Armony, J.L., Quirk, G.J., and LeDoux, J.E. (1998). Differential effects of amygdala lesions on early and late plastic components of auditory cortex spike trains during fear conditioning. J Neurosci *18*, 2592-2601.

Atchison, R.W. (1970). The role of herpesviruses in adenovirus-associated virus replication in vitro. Virology *42*, 155-162.

Ausubel, F.M. (2000). Current protocols in molecular biology, Vol 4 (John Wiley & Sons).

Bannerman, D.M., Deacon, R.M.J., Brady, S., Bruce, A., Sprengel, R., Seeburg, P.H., and Rawlins, J.N.P. (2004). A Comparison of GluR-A-Deficient and Wild-Type Mice on a Test Battery Assessing Sensorimotor, Affective, and Cognitive Behaviors. Behavioral Neuroscience *118*, 643-647.

Bauer, E.P., Schafe, G.E., and LeDoux, J.E. (2002). NMDA receptors and L-type voltage-gated calcium channels contribute to long-term potentiation and different components of fear memory formation in the lateral amygdala. J Neurosci *22*, 5239-5249.

Ben Mamou, C., Gamache, K., and Nader, K. (2006). NMDA receptors are critical for unleashing consolidated auditory fear memories. Nat Neurosci *9*, 1237-1239.

Biou, V., Bhattacharyya, S., and Malenka, R. (2008). Endocytosis and recycling of AMPA receptors lacking GluR2/3. Proc Natl Acad Sci USA *105*, 1038-1043.

Bird, A. (2002). DNA methylation patterns and epigenetic memory. Genes Dev *16*, 6-21.

Blanchard, R.J., and Blanchard, D.C. (1969a). Crouching as an index of fear. J Comp Physiol Psychol *67*, 370-375.

Blanchard, R.J., and Blanchard, D.C. (1969b). Passive and active reactions to fear-eliciting stimuli. J Comp Physiol Psychol *68*, 129-135.

Bliss, T.V., and Lomo, T. (1973). Long-lasting potentiation of synaptic transmission in the dentate area of the anaesthetized rabbit following stimulation of the perforant path. J Physiol *232*, 331-356.

Boatman, J.A., and Kim, J.J. (2006). A thalamo-cortico-amygdala pathway mediates auditory fear conditioning in the intact brain. Eur J Neurosci *24*, 894-900.

Bonnet, C., Leheup, B., Béri, M., Philippe, C., Grégoire, M.-J., and Jonveaux, P. (2009). Aberrant GRIA3transcripts with multi-exon duplications in a family with X-linked mental retardation. Am. J. Med. Genet. *149A*, 1280-1289.

Brown, J.S., Kalish, H.I., and Farber, I.E. (1951). Conditioned fear as revealed by magnitude of startle response to an auditory stimulus. J Exp Psychol *41*, 317-328.

Burnashev, N., Monyer, H., Seeburg, P.H., and Sakmann, B. (1992). Divalent ion permeability of AMPA receptor channels is dominated by the edited form of a single subunit. Neuron *8*, 189-198.

Buzsáki, G. (1998). Memory consolidation during sleep: a neurophysiological perspective. J Sleep Res *7 Suppl 1*, 17-23.

Campeau, S., and Davis, M. (1995). Involvement of subcortical and cortical afferents to the lateral nucleus of the amygdala in fear conditioning measured with fear-potentiated startle in rats trained concurrently with auditory and visual conditioned stimuli. J Neurosci *15*, 2312-2327.

Campeau, S., Miserendino, M.J., and Davis, M. (1992). Intra-amygdala infusion of the N-methyl-D-aspartate receptor antagonist AP5 blocks acquisition but not expression of fear-potentiated startle to an auditory conditioned stimulus. Behavioral Neuroscience *106*, 569-574.

Casto, B.C., Armstrong, J.A., Atchison, R.W., and Hammon, W.M. (1967). Studies on the relationship between adeno-associated virus type 1 (AAV-1) and adenoviruses. II. Inhibition of adenovirus plaques by AAV; its nature and specificity. Virology *33*, 452-458.

Cetin, A., Komai, S., Eliava, M., Seeburg, P.H., and Osten, P. (2006). Stereotaxic gene delivery in the rodent brain. Nat Protoc *1*, 3166-3173.

Chiyonobu, T., Hayashi, S., Kobayashi, K., Morimoto, M., Miyanomae, Y., Nishimura, A., Nishimoto, A., Ito, C., Imoto, I., Sugimoto, T.*, et al.* (2007). Partial tandem duplication ofGRIA3 in a male with mental retardation. Am. J. Med. Genet. *143A*, 1448-1455.

Ciron, C., Cressant, A., Roux, F., Raoul, S., Cherel, Y., Hantraye, P., Déglon, N., Schwartz, B., Barkats, M., Heard, J.-M.*, et al.* (2009). Human alpha-iduronidase gene transfer mediated by adeno-associated virus types 1, 2, and 5 in the brain of nonhuman primates: vector diffusion and biodistribution. Hum Gene Ther *20*, 350-360.

Collingridge, G., Olsen, R., Peters, J., and Spedding, M. (2008). A nomenclature for ligand-gated ion channels. Neuropharmacology, 4.

Collins, D.R., and Paré, D. (2000). Differential fear conditioning induces reciprocal changes in the sensory responses of lateral amygdala neurons to the CS(+) and CS(-). Learn Mem *7*, 97-103.

Crabbe, J.C., Wahlsten, D., and Dudek, B.C. (1999). Genetics of mouse behavior: interactions with laboratory environment. Science *284*, 1670-1672.

Cui, Z., Lindl, K.A., Mei, B., Zhang, S., and Tsien, J.Z. (2005). Requirement of NMDA receptor reactivation for consolidation and storage of nondeclarative taste memory revealed by inducible NR1 knockout. Eur J Neurosci *22*, 755-763.

Cui, Z., Wang, H., Tan, Y., Zaia, K.A., Zhang, S., and Tsien, J.Z. (2004). Inducible and reversible NR1 knockout reveals crucial role of the NMDA receptor in preserving remote memories in the brain. Neuron *41*, 781-793.

Dalby, B., Cates, S., Harris, A., Ohki, E.C., Tilkins, M.L., Price, P.J., and Ciccarone, V.C. (2004). Advanced transfection with Lipofectamine 2000 reagent: primary neurons, siRNA, and high-throughput applications. Methods *33*, 95-103.

Davis, M., Falls, W., Campeau, S., and Kim, M. (1993). Fear-potentiated startle: a neural and pharmacological analysis. Behav Brain Res *58*, 175-198.

Davis, M., and Whalen, P.J. (2001). The amygdala: vigilance and emotion. Mol Psychiatry *6*, 13-34.

Dessaud, E., Salaün, D., Gayet, O., Chabbert, M., and deLapeyrière, O. (2006). Identification of lynx2, a novel member of the ly-6/neurotoxin superfamily, expressed in neuronal subpopulations during mouse development. Mol Cell Neurosci *31*, 232-242.

Dudai, Y., and Eisenberg, M. (2004). Rites of passage of the engram: reconsolidation and the lingering consolidation hypothesis. Neuron *44*, 93-100.

Ebbinghaus, H. (1885). Über das Gedächtnis: Untersuchungen zur experimentellen Psychologie (Library Reprints, Inc.).

Egerod, K.L., Holst, B., Petersen, P.S., Hansen, J.B., Mulder, J., Hokfelt, T., and Schwartz, T.W. (2007). GPR39 Splice Variants Versus Antisense Gene LYPD1: Expression and Regulation in Gastrointestinal Tract, Endocrine Pancreas, Liver, and White Adipose Tissue. Mol Endocrinol *21*, 1685-1698.

Fanselow, M.S., and Kim, J.J. (1994). Acquisition of contextual Pavlovian fear conditioning is blocked by application of an NMDA receptor antagonist D,L-2-amino-5-phosphonovaleric acid to the basolateral amygdala. Behavioral Neuroscience *108*, 210-212.

Forrest, D., Yuzaki, M., Soares, H.D., Ng, L., Luk, D.C., Sheng, M., Stewart, C.L., Morgan, J.I., Connor, J.A., and Curran, T. (1994). Targeted disruption of NMDA receptor 1 gene abolishes NMDA response and results in neonatal death. Neuron *13*, 325-338.

Frankland, P.W., and Bontempi, B. (2005). The organization of recent and remote memories. Nat Rev Neurosci *6*, 119-130.

Fuchs, E.C., Zivkovic, A.R., Cunningham, M.O., Middleton, S., Lebeau, F.E.N., Bannerman, D.M., Rozov, A., Whittington, M.A., Traub, R.D., Rawlins, J.N.P., and Monyer, H. (2007). Recruitment of parvalbumin-positive interneurons determines hippocampal function and associated behavior. Neuron *53*, 591-604.

Fukaya, M., Kato, A., Lovett, C., Tonegawa, S., and Watanabe, M. (2003). Retention of NMDA receptor NR2 subunits in the lumen of endoplasmic reticulum in targeted NR1 knockout mice. Proc Natl Acad Sci USA *100*, 4855-4860.

Gais, S., Rasch, B., Wagner, U., and Born, J. (2008). Visual-Procedural Memory Consolidation during Sleep Blocked by Glutamatergic Receptor Antagonists. Journal of Neuroscience *28*, 5513-5518.

Gécz, J., Barnett, S., Liu, J., Hollway, G., Donnelly, A., Eyre, H., Eshkevari, H.S., Baltazar, R., Grunn, A., Nagaraja, R., *et al.* (1999). Characterization of the human glutamate receptor subunit 3 gene (GRIA3), a candidate for bipolar disorder and nonspecific X-linked mental retardation. Genomics *62*, 356-368.

Gewirtz, J.C., and Davis, M. (1997). Second-order fear conditioning prevented by blocking NMDA receptors in amygdala. Nature *388*, 471-474.

Glass, M.J., Hegarty, D.M., Oselkin, M., Quimson, L., South, S.M., Xu, Q., Pickel, V.M., and Inturrisi, C.E. (2008). Conditional deletion of the NMDA-NR1 receptor subunit gene in the central nucleus of the amygdala inhibits naloxone-induced conditioned place aversion in morphine-dependent mice. Exp Neurol *213*, 57-70.

Gong, S., Zheng, C., Doughty, M.L., Losos, K., Didkovsky, N., Schambra, U.B., Nowak, N.J., Joyner, A., Leblanc, G., Hatten, M.E., and Heintz, N. (2003). A gene expression atlas of the central nervous system based on bacterial artificial chromosomes. Nature *425*, 917-925.

Gossen, M., and Bujard, H. (1992). Tight control of gene expression in mammalian cells by tetracycline-responsive promoters. Proc Natl Acad Sci USA *89*, 5547-5551.

Gossen, M., Freundlieb, S., Bender, G., Müller, G., Hillen, W., and Bujard, H. (1995). Transcriptional activation by tetracyclines in mammalian cells. Science *268*, 1766-1769.

Guzmán-Ramos, K., Osorio-Gómez, D., Moreno-Castilla, P., and Bermúdez-Rattoni, F. (2010). Off-line concomitant release of dopamine and glutamate involvement in taste memory consolidation. J Neurochem *114*, 226-236.

Haberman, R.P., and McCown, T.J. (2002). Regulation of gene expression in adeno-associated virus vectors in the brain. Methods *28*, 219-226.

Han, J.-H., Kushner, S.A., Yiu, A.P., Hsiang, H.-L., Buch, T., Waisman, A., Bontempi, B., Neve, R.L., Frankland, P.W., and Josselyn, S.A. (2009). Selective Erasure of a Fear Memory. Science *323*, 1492-1496.

Hecht, B., Müller, G., and Hillen, W. (1993). Noninducible Tet repressor mutations map from the operator binding motif to the C terminus. J Bacteriol *175*, 1206-1210.

Hollmann, M., O'Shea-Greenfield, A., Rogers, S.W., and Heinemann, S. (1989). Cloning by functional expression of a member of the glutamate receptor family. Nature *342*, 643-648.

Huang, Y., and Kandel, E. (1998). Postsynaptic induction and PKA-dependent expression of LTP in the lateral amygdala. Neuron *21*, 169-178.

Hume, R.I., Dingledine, R., and Heinemann, S.F. (1991). Identification of a site in glutamate receptor subunits that controls calcium permeability. Science *253*, 1028-1031.

Humeau, Y., Reisel, D., Johnson, A.W., Borchardt, T., Jensen, V., Gebhardt, C., Bosch, V., Gass, P., Bannerman, D.M., Good, M.A., *et al.* (2007). A pathway-specific function for different AMPA receptor subunits in amygdala long-term potentiation and fear conditioning. J Neurosci *27*, 10947-10956.

Inda, M.C., Muravieva, E.V., and Alberini, C.M. (2011). Memory Retrieval and the Passage of Time: From Reconsolidation and Strengthening to Extinction. Journal of Neuroscience *31*, 1635-1643.

Johnson, J.W., and Ascher, P. (1987). Glycine potentiates the NMDA response in cultured mouse brain neurons. Nature *325*, 529-531.

Kandel, E. (2001). The molecular biology of memory storage: a dialogue between genes and synapses. Science *294*, 1030-1038.

Keinänen, K., Wisden, W., Sommer, B., Werner, P., Herb, A., Verdoorn, T.A., Sakmann, B., and Seeburg, P.H. (1990). A family of AMPA-selective glutamate receptors. Science *249*, 556-560.

Kim, M., Campeau, S., Falls, W.A., and Davis, M. (1993). Infusion of the non-NMDA receptor antagonist CNQX into the amygdala blocks the expression of fear-potentiated startle. Behav Neural Biol *59*, 5-8.

Kim, M., and Davis, M. (1993a). Electrolytic lesions of the amygdala block acquisition and expression of fear-potentiated startle even with extensive training but do not prevent reacquisition. Behav Neurosci *107*, 580-595.

Kim, M., and Davis, M. (1993b). Lack of a temporal gradient of retrograde amnesia in rats with amygdala lesions assessed with the fear-potentiated startle paradigm. Behav Neurosci *107*, 1088-1092.

Klein, R.L., Hamby, M.E., Gong, Y., Hirko, A.C., Wang, S., Hughes, J.A., King, M.A., and Meyer, E.M. (2002). Dose and promoter effects of adeno-associated viral vector for green fluorescent protein expression in the rat brain. Exp Neurol *176*, 66-74.

Kuroda, H., Kutner, R.H., Bazan, N.G., and Reiser, J. (2008). A comparative analysis of constitutive and cell-specific promoters in the adult mouse hippocampus using lentivirus vector-mediated gene transfer. J. Gene Med. *10*, 1163-1175.

Lazic, S.E. (2011). Modeling hippocampal neurogenesis across the lifespan in seven species. Neurobiology of aging.

Lechner, H., and Squire, L. (1999). 100 years of consolidation—remembering Müller and Pilzecker. Learning & Memory.

LeDoux, J. (2003). The emotional brain, fear, and the amygdala. Cell Mol Neurobiol *23*, 727-738.

LeDoux, J.E., Iwata, J., Pearl, D., and Reis, D.J. (1986). Disruption of auditory but not visual learning by destruction of intrinsic neurons in the rat medial geniculate body. Brain Res *371*, 395-399.

Lee, H., and Kim, J.J. (1998). Amygdalar NMDA receptors are critical for new fear learning in previously fear-conditioned rats. J Neurosci *18*, 8444-8454.

Lee, J.L.C., Milton, A.L., and Everitt, B.J. (2006). Reconsolidation and extinction of conditioned fear: inhibition and potentiation. J Neurosci *26*, 10051-10056.

Lemberger, T., Parlato, R., Dassesse, D., Westphal, M., Casanova, E., Turiault, M., Tronche, F., Schiffmann, S.N., and Schütz, G. (2007). Expression of Cre recombinase in dopaminoceptive neurons. BMC neuroscience *8*, 4.

LeWitt, P.A., Rezai, A.R., Leehey, M.A., Ojemann, S.G., Flaherty, A.W., Eskandar, E.N., Kostyk, S.K., Thomas, K., Sarkar, A., Siddiqui, M.S., *et al.* (2011). AAV2-GAD gene therapy for advanced Parkinson's disease: a double-blind, sham-surgery controlled, randomised trial. The Lancet Neurology *10*, 309-319.

Link, E., Edelmann, L., Chou, J.H., Binz, T., Yamasaki, S., Eisel, U., Baumert, M., Südhof, T.C., Niemann, H., and Jahn, R. (1992). Tetanus toxin action: inhibition of neurotransmitter release linked to synaptobrevin proteolysis. Biochem Biophys Res Commun *189*, 1017-1023.

Lu, W., Shi, Y., Jackson, A.C., Bjorgan, K., During, M.J., Sprengel, R., Seeburg, P.H., and Nicoll, R.A. (2009). Subunit Composition of Synaptic AMPA Receptors Revealed by a Single-Cell Genetic Approach. Neuron *62*, 254-268.

Mack, V., Burnashev, N., Kaiser, K.M., Rozov, A., Jensen, V., Hvalby, O., Seeburg, P.H., Sakmann, B., and Sprengel, R. (2001). Conditional restoration of hippocampal synaptic potentiation in Glur-A-deficient mice. Science *292*, 2501-2504.

Malenka, R.C., and Nicoll, R.A. (1999). Long-term potentiation--a decade of progress? Science *285*, 1870-1874.

Mandillo, S., Tucci, V., Hölter, S.M., Meziane, H., Banchaabouchi, M.A., Kallnik, M., Lad, H.V., Nolan, P.M., Ouagazzal, A.-M., Coghill, E.L., *et al.* (2008). Reliability, robustness, and reproducibility in mouse behavioral phenotyping: a cross-laboratory study. Physiological Genomics *34*, 243-255.

Maren, S., Aharonov, G., and Fanselow, M. (1996a). Retrograde abolition of conditional fear after excitotoxic lesions in the basolateral amygdala of rats: absence of a temporal gradient. Behav Neurosci *110*, 718-726.

Maren, S., Aharonov, G., Stote, D.L., and Fanselow, M.S. (1996b). N-methyl-D-aspartate receptors in the basolateral amygdala are required for both acquisition and expression of conditional fear in rats. Behavioral Neuroscience *110*, 1365-1374.

Maren, S., and Fanselow, M. (1995). Synaptic plasticity in the basolateral amygdala induced by hippocampal formation stimulation in vivo. J Neurosci *15*, 7548-7564.

Maren, S., and Quirk, G.J. (2004). Neuronal signalling of fear memory. Nat Rev Neurosci *5*, 844-852.

Matus-Amat, P., Higgins, E.A., Sprunger, D., Wright-Hardesty, K., and Rudy, J.W. (2007). The role of dorsal hippocampus and basolateral amygdala NMDA receptors in the acquisition and retrieval of context and contextual fear memories. Behavioral Neuroscience *121*, 721-731.

Mayford, M., Bach, M.E., Huang, Y.Y., Wang, L., Hawkins, R.D., and Kandel, E.R. (1996). Control of memory formation through regulated expression of a CaMKII transgene. Science *274*, 1678-1683.

Mayford, M., Wang, J., Kandel, E.R., and O'Dell, T.J. (1995). CaMKII regulates the frequency-response function of hippocampal synapses for the production of both LTD and LTP. Cell *81*, 891-904.

McGaugh, J.L. (2000). Memory--a Century of Consolidation. Science *287*, 248-251.

McGee Sanftner, L.H., Rendahl, K.G., Quiroz, D., Coyne, M., Ladner, M., Manning, W.C., and Flannery, J.G. (2001). Recombinant AAV-mediated delivery of a tet-inducible reporter gene to the rat retina. Mol Ther *3*, 688-696.

McHugh, T.J., Jones, M.W., Quinn, J.J., Balthasar, N., Coppari, R., Elmquist, J.K., Lowell, B.B., Fanselow, M.S., Wilson, M.A., and Tonegawa, S. (2007). Dentate gyrus NMDA receptors mediate rapid pattern separation in the hippocampal network. Science *317*, 94-99.

McIlwain, K.L., Merriweather, M.Y., Yuva-Paylor, L.A., and Paylor, R. (2001). The use of behavioral test batteries: effects of training history. Physiol Behav *73*, 705-717.

McKernan, M.G., and Shinnick-Gallagher, P. (1997). Fear conditioning induces a lasting potentiation of synaptic currents in vitro. Nature *390*, 607-611.

McLaughlin, S.K., Collis, P., Hermonat, P.L., and Muzyczka, N. (1988). Adeno-associated virus general transduction vectors: analysis of proviral structures. J Virol *62*, 1963-1973.

Miller, C., and Sweatt, J. (2007). Covalent modification of DNA regulates memory formation. Neuron *53*, 857-869.

Misanin, J.R., Miller, R.R., and Lewis, D.J. (1968). Retrograde amnesia produced by electroconvulsive shock after reactivation of a consolidated memory trace. Science *160*, 554-555.

Miserendino, M., Sananes, C., Melia, K., and Davis, M. (1990). Blocking of acquisition but not expression of conditioned fear-potentiated startle by NMDA antagonists in the amygdala. Nature *345*, 716-718.

Monahan, P.E., and Samulski, R.J. (2000). Adeno-associated virus vectors for gene therapy: more pros than cons? Mol Med Today *6*, 433-440.

Monfils, M., Cowansage, K., Klann, E., and Ledoux, J. (2009). Extinction-Reconsolidation Boundaries: Key to Persistent Attenuation of Fear Memories. Science.

Muzyczka, N. (1992). Use of adeno-associated virus as a general transduction vector for mammalian cells. Curr Top Microbiol Immunol *158*, 97-129.

Myskiw, J.C., Fiorenza, N.G., Izquierdo, L.A., and Izquierdo, I. (2010). Molecular mechanisms in hippocampus and basolateral amygdala but not in parietal or cingulate cortex are involved in extinction of one-trial avoidance learning. Neurobiol Learn Mem *94*, 285-291.

Nader, K., Schafe, G.E., and Le Doux, J.E. (2000). Fear memories require protein synthesis in the amygdala for reconsolidation after retrieval. Nature *406*, 722-726.

Nagai, T., Ibata, K., Park, E.S., Kubota, M., Mikoshiba, K., and Miyawaki, A. (2002). A variant of yellow fluorescent protein with fast and efficient maturation for cell-biological applications. Nat Biotechnol *20*, 87-90.

Nakai, H., Yant, S.R., Storm, T.A., Fuess, S., Meuse, L., and Kay, M.A. (2001). Extrachromosomal recombinant adeno-associated virus vector genomes are primarily responsible for stable liver transduction in vivo. J Virol *75*, 6969-6976.

Nakashiba, T., Young, J.Z., McHugh, T.J., Buhl, D.L., and Tonegawa, S. (2008). Transgenic inhibition of synaptic transmission reveals role of CA3 output in hippocampal learning. Science *319*, 1260-1264.

Niewoehner, B., Single, F.N., Hvalby, Ø., Jensen, V., Meyer zum Alten Borgloh, S., Seeburg, P.H., Rawlins, J.N., Sprengel, R., and Bannerman, D.M. (2007). Impaired spatial working memory but spared spatial reference memory following functional loss of NMDA receptors in the dentate gyrus. Eur J Neurosci *25*, 837-846.

Noordmans, A.J., Song, D.K., Noordmans, C.J., Garrity-Moses, M., During, M.J., Fitzsimons, H.L., Imperiale, M.J., and Boulis, N.M. (2004). Adeno-associated viral glutamate decarboxylase expression in the lateral nucleus of the rat hypothalamus reduces feeding behavior. Gene Ther *11*, 797-804.

Nordeen, S.K. (1988). Luciferase reporter gene vectors for analysis of promoters and enhancers. BioTechniques *6*, 454-458.

Nowak, L., Bregestovski, P., Ascher, P., Herbet, A., and Prochiantz, A. (1984). Magnesium gates glutamate-activated channels in mouse central neurones. Nature *307*, 462-465.

Pare, D., Quirk, G.J., and Ledoux, J.E. (2004). New vistas on amygdala networks in conditioned fear. J Neurophysiol *92*, 1-9.

Pavlov, I.P. (1927). Conditioned reflexes: an investigation of the physiological activity of the cerebral cortex (Oxford University Press: G. Cumberlege).

Paxinos, G., and Franklin, K.B.J. (2001). The mouse brain in stereotaxic coordinates, 2nd edn (San Diego, Calif. London: Academic).

Pedreira, M.E., and Maldonado, H. (2003). Protein synthesis subserves reconsolidation or extinction depending on reminder duration. Neuron *38*, 863-869.

Pedreira, M.E., Pérez-Cuesta, L.M., and Maldonado, H. (2002). Reactivation and reconsolidation of long-term memory in the crab Chasmagnathus: protein synthesis requirement and mediation by NMDA-type glutamatergic receptors. J Neurosci *22*, 8305-8311.

Peel, A.L., and Klein, R.L. (2000). Adeno-associated virus vectors: activity and applications in the CNS. J Neurosci Methods *98*, 95-104.

Phillips, R.G., and LeDoux, J.E. (1992). Differential contribution of amygdala and hippocampus to cued and contextual fear conditioning. Behavioral Neuroscience *106*, 274-285.

Phillips, R.G., and LeDoux, J.E. (1994). Lesions of the dorsal hippocampal formation interfere with background but not foreground contextual fear conditioning. Learn Mem *1*, 34-44.

Pilpel, N., Landeck, N., Klugmann, M., Seeburg, P.H., and Schwarz, M.K. (2009). Rapid, reproducible transduction of select forebrain regions by targeted recombinant virus injection into the neonatal mouse brain. J Neurosci Methods *182*, 55-63.

Pomata, P.E., Belluscio, M.A., Riquelme, L.A., and Murer, M.G. (2008). NMDA receptor gating of information flow through the striatum in vivo. J Neurosci *28*, 13384-13389.

Prusky, G.T., West, P.W., and Douglas, R.M. (2000). Behavioral assessment of visual acuity in mice and rats. Vision Res *40*, 2201-2209.

Quirk, G.J., Armony, J.L., and LeDoux, J.E. (1997). Fear conditioning enhances different temporal components of tone-evoked spike trains in auditory cortex and lateral amygdala. Neuron *19*, 613-624.

Quirk, G.J., Repa, C., and LeDoux, J.E. (1995). Fear conditioning enhances short-latency auditory responses of lateral amygdala neurons: parallel recordings in the freely behaving rat. Neuron *15*, 1029-1039.

Rami, A., Bréhier, A., Thomasset, M., and Rabié, A. (1987). Cholecalcin (28-kDa calcium-binding protein) in the rat hippocampus: development in normal animals and in altered thyroid states. An immunocytochemical study. Dev Biol *124*, 228-238.

Reisel, D., Bannerman, D., Schmitt, W., Deacon, R., Flint, J., Borchardt, T., Seeburg, P., and Rawlins, J. (2002). Spatial memory dissociations in mice lacking GluR1. Nat Neurosci *5*, 868-873.

Repa, J.C., Muller, J., Apergis, J., Desrochers, T.M., Zhou, Y., and LeDoux, J.E. (2001). Two different lateral amygdala cell populations contribute to the initiation and storage of memory. Nat Neurosci *4*, 724-731.

Richardson, W.D., and Westphal, H. (1984). Requirement for either early region 1a or early region 1b adenovirus gene products in the helper effect for adeno-associated virus. J Virol *51*, 404-410.

Rogan, M., Staubli, U., and LeDoux, J. (1997). Fear conditioning induces associative long-term potentiation in the amygdala. Nature *390*, 604-607.

Rogers, S.W., Andrews, P.I., Gahring, L.C., Whisenand, T., Cauley, K., Crain, B., Hughes, T.E., Heinemann, S.F., and McNamara, J.O. (1994). Autoantibodies to glutamate receptor GluR3 in Rasmussen's encephalitis. Science *265*, 648-651.

Romanski, L.M., and LeDoux, J.E. (1992). Equipotentiality of thalamo-amygdala and thalamo-cortico-amygdala circuits in auditory fear conditioning. J Neurosci *12*, 4501-4509.

Rondi-Reig, L., Libbey, M., Eichenbaum, H., and Tonegawa, S. (2001). CA1-specific N-methyl-D-aspartate receptor knockout mice are deficient in solving a nonspatial transverse patterning task. Proc Natl Acad Sci U S A *98*, 3543-3548.

Rondi-Reig, L., Petit, G.H., Tobin, C., Tonegawa, S., Mariani, J., and Berthoz, A. (2006). Impaired sequential egocentric and allocentric memories in forebrain-specific-NMDA receptor knock-out mice during a new task dissociating strategies of navigation. J Neurosci *26*, 4071-4081.

Roozendaal, B., Koolhaas, J.M., and Bohus, B. (1991). Central amygdala lesions affect behavioral and autonomic balance during stress in rats. Physiol Behav *50*, 777-781.

Rumpel, S., LeDoux, J., Zador, A., and Malinow, R. (2005). Postsynaptic receptor trafficking underlying a form of associative learning. Science *308*, 83-88.

Russo, N.J., Kapp, B.S., Holmquist, B.K., and Musty, R.E. (1976). Passive avoidance and amygdala lesions: relationship with pituitary-adrenal system. Physiol Behav *16*, 191-199.

Ryan, M.D., King, A.M., and Thomas, G.P. (1991). Cleavage of foot-and-mouth disease virus polyprotein is mediated by residues located within a 19 amino acid sequence. J Gen Virol *72 (Pt 11)*, 2727-2732.

Sadler, R., Herzig, V., and Schmidt, W.J. (2007). Repeated treatment with the NMDA antagonist MK-801 disrupts reconsolidation of memory for amphetamine-conditioned place preference. Behav Pharmacol *18*, 699-703.

Sambrook, J., and Russell, D.W. (2001). Molecular cloning: a laboratory manual, Vol 2, 3 edn (CSHL Press).

Samulski, R.J., Chang, L.S., and Shenk, T. (1989). Helper-free stocks of recombinant adeno-associated viruses: normal integration does not require viral gene expression. J Virol *63*, 3822-3828.

Sanchis-Segura, C., Borchardt, T., Vengeliene, V., Zghoul, T., Bachteler, D., Gass, P., Sprengel, R., and Spanagel, R. (2006). Involvement of the AMPA receptor GluR-C subunit in alcohol-seeking behavior and relapse. J Neurosci *26*, 1231-1238.

Sanderson, D.J., and Bannerman, D.M. (2010). The role of habituation in hippocampus-dependent spatial working memory tasks: Evidence from GluA1 AMPA receptor subunit knockout mice. Hippocampus, n/a-n/a.

Sanderson, D.J., Good, M.A., Seeburg, P.H., Sprengel, R., Rawlins, J.N., and Bannerman, D.M. (2008). The role of the GluR-A (GluR1) AMPA receptor subunit in learning and memory. Prog Brain Res *169*, 159-178.

Sanderson, D.J., Good, M.A., Skelton, K., Sprengel, R., Seeburg, P.H., Rawlins, J.N.P., and Bannerman, D.M. (2009). Enhanced long-term and impaired short-term spatial memory in GluA1 AMPA receptor subunit knockout mice: Evidence for a dual-process memory model. Learning & Memory *16*, 379-386.

Sara, S.J. (2000a). Retrieval and Reconsolidation: Toward a Neurobiology of Remembering. Learning & Memory *7*, 73-84.

Sara, S.J. (2000b). Strengthening the shaky trace through retrieval. Nat Rev Neurosci *1*, 212-213.

Schiavo, G., Benfenati, F., Poulain, B., Rossetto, O., Polverino de Laureto, P., DasGupta, B.R., and Montecucco, C. (1992). Tetanus and botulinum-B neurotoxins block neurotransmitter release by proteolytic cleavage of synaptobrevin. Nature *359*, 832-835.

Schmitt, W.B., Deacon, R.M., Seeburg, P., Rawlins, J.N., and Bannerman, D.M. (2003). A within-subjects, within-task demonstration of intact spatial reference memory and impaired spatial working memory in glutamate receptor-A-deficient mice. J Neurosci *23*, 3953-3959.

Schmitt, W.B., Sprengel, R., Mack, V., Draft, R.W., Seeburg, P.H., Deacon, R.M., Rawlins, J.N., and Bannerman, D.M. (2005). Restoration of spatial working memory by genetic rescue of GluR-A-deficient mice. Nat Neurosci *8*, 270-272.

Schoch, S., Deák, F., Königstorfer, A., Mozhayeva, M., Sara, Y., Südhof, T.C., and Kavalali, E.T. (2001). SNARE function analyzed in synaptobrevin/VAMP knockout mice. Science *294*, 1117-1122.

Schüler, T., Mesic, I., Madry, C., Bartholomäus, I., and Laube, B. (2008). Formation of NR1/NR2 and NR1/NR3 heterodimers constitutes the initial step in N-methyl-D-aspartate receptor assembly. J Biol Chem *283*, 37-46.

Scoville, W.B., and Milner, B. (1957). Loss of recent memory after bilateral hippocampal lesions. J Neurol Neurosurg Psychiatr *20*, 11-21.

Shevtsova, Z., Malik, J.M.I., Michel, U., Bähr, M., and Kügler, S. (2005). Promoters and serotypes: targeting of adeno-associated virus vectors for gene transfer in the rat central nervous system in vitro and in vivo. Exp Physiol *90*, 53-59.

Shi, S., Hayashi, Y., Esteban, J.A., and Malinow, R. (2001). Subunit-specific rules governing AMPA receptor trafficking to synapses in hippocampal pyramidal neurons. Cell *105*, 331-343.

Shimizu, E., Tang, Y., Rampon, C., and Tsien, J. (2000). NMDA receptor-dependent synaptic reinforcement as a crucial process for memory consolidation. Science *290*, 1170-1174.

Shimshek, D.R., Jensen, V., Celikel, T., Geng, Y., Schupp, B., Bus, T., Mack, V., Marx, V., Hvalby, Ø., Seeburg, P., and Sprengel, R. (2006). Forebrain-specific glutamate receptor B deletion impairs spatial memory but not hippocampal field long-term potentiation. J Neurosci *26*, 8428-8440.

Sigurdsson, T., Doyere, V., Cain, C.K., and LeDoux, J.E. (2007). Long-term potentiation in the amygdala: a cellular mechanism of fear learning and memory. Neuropharmacology *52*, 215-227.

Sin, M., Walker, P.D., Bouhamdan, M., Quinn, J.P., and Bannon, M.J. (2005). Preferential expression of an AAV-2 construct in NOS-positive interneurons following intrastriatal injection. Brain Res Mol Brain Res *141*, 74-82.

Smale, S.T., and Kadonaga, J.T. (2003). The RNA polymerase II core promoter. Annu Rev Biochem *72*, 449-479.

Sobolevsky, A.I., Rosconi, M.P., and Gouaux, E. (2009). X-ray structure, symmetry and mechanism of an AMPA-subtype glutamate receptor. Nature *462*, 745-756.

Song, I., and Huganir, R.L. (2002). Regulation of AMPA receptors during synaptic plasticity. Trends Neurosci *25*, 578-588.

Soriano, P. (1999). Generalized lacZ expression with the ROSA26 Cre reporter strain. Nature Genetics *21*, 70-71.

Steenland, H.W., Kim, S.S., and Zhuo, M. (2008). GluR3 subunit regulates sleep, breathing and seizure generation. Eur J Neurosci *27*, 1166-1173.

Südhof, T.C. (1995). The synaptic vesicle cycle: a cascade of protein-protein interactions. Nature *375*, 645-653.

Sutherland, G.R., and McNaughton, B. (2000). Memory trace reactivation in hippocampal and neocortical neuronal ensembles. Curr Opin Neurobiol *10*, 180-186.

Suzuki, A., Josselyn, S.A., Frankland, P.W., Masushige, S., Silva, A.J., and Kida, S. (2004). Memory reconsolidation and extinction have distinct temporal and biochemical signatures. J Neurosci *24*, 4787-4795.

Swartzwelder, H.S. (1981). Deficits in passive avoidance and fear behavior following bilateral and unilateral amygdala lesions in mice. Physiol Behav *26*, 323-326.

Tang, W., Ehrlich, I., Wolff, S.B.E., Michalski, A.-M., Wolfl, S., Hasan, M.T., Luthi, A., and Sprengel, R. (2009). Faithful Expression of Multiple Proteins via 2A-Peptide Self-Processing: A Versatile and Reliable Method for Manipulating Brain Circuits. Journal of Neuroscience *29*, 8621-8629.

Tekinay, A.B., Nong, Y., Miwa, J.M., Lieberam, I., Ibanez-Tallon, I., Greengard, P., and Heintz, N. (2009). A role for LYNX2 in anxiety-related behavior. Proc Natl Acad Sci U S A *106*, 4477-4482.

Tenenbaum, L., Chtarto, A., Lehtonen, E., Velu, T., Brotchi, J., and Levivier, M. (2004). Recombinant AAV-mediated gene delivery to the central nervous system. J Gene Med *6 Suppl 1*, S212-222.

Torras-Garcia, M., Lelong, J., Tronel, S., and Sara, S.J. (2005). Reconsolidation after remembering an odor-reward association requires NMDA receptors. Learn Mem *12*, 18-22.

Tsien, J.Z., Huerta, P.T., and Tonegawa, S. (1996). The essential role of hippocampal CA1 NMDA receptor-dependent synaptic plasticity in spatial memory. Cell *87*, 1327-1338.

Udenfriend, S., and Kodukula, K. (1995). Prediction of omega site in nascent precursor of glycosylphosphatidylinositol protein. Meth Enzymol *250*, 571-582.

Vazdarjanova, A., and McGaugh, J.L. (1998). Basolateral amygdala is not critical for cognitive memory of contextual fear conditioning. Proc Natl Acad Sci USA *95*, 15003-15007.

Vekovischeva, O.Y., Aitta-Aho, T., Echenko, O., Kankaanpää, A., Seppälä, T., Honkanen, A., Sprengel, R., and Korpi, E.R. (2004). Reduced aggression in AMPA-type glutamate receptor GluR-A subunit-deficient mice. Genes Brain Behav *3*, 253-265.

Vekovischeva, O.Y., Zamanillo, D., Echenko, O., Seppälä, T., Uusi-Oukari, M., Honkanen, A., Seeburg, P.H., Sprengel, R., and Korpi, E.R. (2001). Morphine-induced dependence and sensitization are altered in mice deficient in AMPA-type glutamate receptor-A subunits. J Neurosci *21*, 4451-4459.

Verdoorn, T.A., Burnashev, N., Monyer, H., Seeburg, P.H., and Sakmann, B. (1991). Structural determinants of ion flow through recombinant glutamate receptor channels. Science *252*, 1715-1718.

von der Goltz, C., Vengeliene, V., Bilbao, A., Perreau-Lenz, S., Pawlak, C.R., Kiefer, F., and Spanagel, R. (2009). Cue-induced alcohol-seeking behaviour is reduced by disrupting the reconsolidation of alcohol-related memories. Psychopharmacology (Berl) *205*, 389-397.

von Engelhardt, J., Doganci, B., Jensen, V., Hvalby, Ø., Göngrich, C., Taylor, A., Barkus, C., Sanderson, D.J., Rawlins, J.N.P., Seeburg, P.H., *et al.* (2008). Contribution of hippocampal and extra-hippocampal NR2B-containing NMDA receptors to performance on spatial learning tasks. Neuron *60*, 846-860.

Wagner, A. (1981). SOP: A model of automatic memory processing in animal behavior. In Information processing in animals: Memory mechanisms, N. Spear, Miller, Rr, ed. (Hilsdale, NJ: Lawrence Erlbaum Associates, Inc.), pp. 5-47.

Walker, D.L., and Davis, M. (2002). The role of amygdala glutamate receptors in fear learning, fear-potentiated startle, and extinction. Pharmacol Biochem Behav *71*, 379-392.

Walker, D.L., Ressler, K.J., Lu, K.-T., and Davis, M. (2002). Facilitation of conditioned fear extinction by systemic administration or intra-amygdala infusions of D-cycloserine as assessed with fear-potentiated startle in rats. J Neurosci *22*, 2343-2351.

Wang, S.-H., de Oliveira Alvares, L., and Nader, K. (2009). Cellular and systems mechanisms of memory strength as a constraint on auditory fear reconsolidation. Nat Neurosci *12*, 905-912.

Weiskrantz, L. (1956). Behavioral changes associated with ablation of the amygdaloid complex in monkeys. J Comp Physiol Psychol *49*, 381-391.

Wenthold, R.J., Yokotani, N., Doi, K., and Wada, K. (1992). Immunochemical characterization of the non-NMDA glutamate receptor using subunit-specific antibodies. Evidence for a hetero-oligomeric structure in rat brain. J Biol Chem *267*, 501-507.

Wiedholz, L.M., Owens, W.A., Horton, R.E., Feyder, M., Karlsson, R.M., Hefner, K., Sprengel, R., Celikel, T., Daws, L.C., and Holmes, A. (2008). Mice lacking the AMPA GluR1 receptor exhibit striatal hyperdopaminergia and 'schizophrenia-related' behaviors. Mol Psychiatry *13*, 631-640.

Wiltgen, B.J., Royle, G.A., Gray, E.E., Abdipranoto, A., Thangthaeng, N., Jacobs, N., Saab, F., Tonegawa, S., Heinemann, S.F., O'Dell, T.J., *et al.* (2010). A role for calcium-permeable AMPA receptors in synaptic plasticity and learning. PLoS ONE *5*.

Wittenberg, G.M., and Tsien, J.Z. (2002). An emerging molecular and cellular framework for memory processing by the hippocampus. Trends Neurosci *25*, 501-505.

Wouda, J.A., Diergaarde, L., Riga, D., van Mourik, Y., Schoffelmeer, A.N.M., and De Vries, T.J. (2010). Disruption of Long-Term Alcohol-Related Memory Reconsolidation: Role of β-Adrenoceptors and NMDA Receptors. Frontiers in behavioral neuroscience *4*, 179.

Wu, Y., Arai, A.C., Rumbaugh, G., Srivastava, A.K., Turner, G., Hayashi, T., Suzuki, E., Jiang, Y., Zhang, L., Rodriguez, J., *et al.* (2007). Mutations in ionotropic AMPA receptor 3 alter channel properties and are associated with moderate cognitive impairment in humans. Proc Natl Acad Sci USA *104*, 18163-18168.

Xu, R., Janson, C.G., Mastakov, M., Lawlor, P., Young, D., Mouravlev, A., Fitzsimons, H., Choi, K.L., Ma, H., Dragunow, M., *et al.* (2001). Quantitative comparison of expression with adeno-associated virus (AAV-2) brain-specific gene cassettes. Gene Ther *8*, 1323-1332.

Yamamoto, M., Wada, N., Kitabatake, Y., Watanabe, D., Anzai, M., Yokoyama, M., Teranishi, Y., and Nakanishi, S. (2003). Reversible suppression of glutamatergic neurotransmission of cerebellar granule cells in vivo by genetically manipulated expression of tetanus neurotoxin light chain. J Neurosci *23*, 6759-6767.

Yamamoto, T., Fujimoto, Y., Shimura, T., and Sakai, N. (1995). Conditioned taste aversion in rats with excitotoxic brain lesions. Neurosci Res *22*, 31-49.

Yang, J., Teng, Q., Garrity-Moses, M.E., McClelland, S., Federici, T., Carlton, E., Riley, J., and Boulis, N.M. (2007). Reversible unilateral nigrostriatal pathway inhibition induced through expression of adenovirus-mediated clostridial light chain gene in the substantia nigra. Neuromolecular Med *9*, 276-284.

Yu, C.R., Power, J., Barnea, G., O'Donnell, S., Brown, H.E.V., Osborne, J., Axel, R., and Gogos, J.A. (2004). Spontaneous neural activity is required for the establishment and maintenance of the olfactory sensory map. Neuron *42*, 553-566.

Zamanillo, D., Sprengel, R., Hvalby, O., Jensen, V., Burnashev, N., Rozov, A., Kaiser, K.M., Köster, H.J., Borchardt, T., Worley, P., *et al.* (1999). Importance of AMPA receptors for hippocampal synaptic plasticity but not for spatial learning. Science *284*, 1805-1811.

Zhao, C., Deng, W., and Gage, F. (2008). Mechanisms and functional implications of adult neurogenesis. Cell *132*, 645-660.

Zhou, Y., Won, J., Karlsson, M.G., Zhou, M., Rogerson, T., Balaji, J., Neve, R., Poirazi, P., and Silva, A.J. (2009). CREB regulates excitability and the allocation of memory to subsets of neurons in the amygdala. Nat Neurosci *12*, 1438-1443.

Zhu, P., Aller, M., Baron, U., Cambridge, S., Bausen, M., Herb, J., Sawinski, J., Cetin, A., Osten, P., Nelson, M., *et al.* (2007). Silencing and Un-silencing of Tetracycline-Controlled Genes in Neurons. PLoS ONE *2*, e533.

Zimmerman, J.M., and Maren, S. (2010). NMDA receptor antagonism in the basolateral but not central amygdala blocks the extinction of Pavlovian fear conditioning in rats. Eur J Neurosci *31*, 1664-1670.

Zola-Morgan, S., Squire, L.R., Alvarez-Royo, P., and Clower, R.P. (1991). Independence of memory functions and emotional behavior: separate contributions of the hippocampal formation and the amygdala. Hippocampus *1*, 207-220.

Zolotukhin, S., Byrne, B.J., Mason, E., Zolotukhin, I., Potter, M., Chesnut, K., Summerford, C., Samulski, R.J., and Muzyczka, N. (1999). Recombinant adeno-associated virus purification using novel methods improves infectious titer and yield. Gene Ther *6*, 973-985.